AD_____

Award Number: W81XWH-10-1-0425

TITLE: Improve T Cell Therapy in Neuroblastoma

PRINCIPAL INVESTIGATOR: Gianpietro Dotti, M.D.

CONTRACTING ORGANIZATION: Baylor College of Medicine
Houston, TX 77030

REPORT DATE: July 2013

TYPE OF REPORT: Revised Annual

PREPARED FOR: U.S. Army Medical Research and Materiel Command
Fort Detrick, Maryland 21702-5012

DISTRIBUTION STATEMENT: Approved for Public Release;
Distribution Unlimited

REPORT DOCUMENTATION PAGE

Form Approved
OMB No. 0704-0188

1. REPORT DATE	2. REPORT TYPE	3. DATES COVERED
July 2013	Annual	1 July 2012 - 30 June 2013

4. TITLE AND SUBTITLE

Improve T cell therapy in neuroblastoma

5a. CONTRACT NUMBER

5b. GRANT NUMBER
W81XWH-10-1-0425

5c. PROGRAM ELEMENT NUMBER

6. AUTHOR(S)

Gianpietro Dotti, M.D.

E-Mail: gdotti@bcm.tmc.edu

5d. PROJECT NUMBER

5e. TASK NUMBER

5f. WORK UNIT NUMBER

7. PERFORMING ORGANIZATION NAME(S) AND ADDRESS(ES)

Baylor College of Medicine
One Baylor Plaza
Houston, TX 77030

8. PERFORMING ORGANIZATION REPORT NUMBER

9. SPONSORING / MONITORING AGENCY NAME(S) AND ADDRESS(ES)
U.S. Army Medical Research and Materiel Command
Fort Detrick, Maryland 21702-5012

10. SPONSOR/MONITOR'S ACRONYM(S)

11. SPONSOR/MONITOR'S REPORT NUMBER(S)

12. DISTRIBUTION / AVAILABILITY STATEMENT
Approved for Public Release; Distribution Unlimited

13. SUPPLEMENTARY NOTES

14. ABSTRACT

Neuroblastoma (NB) is the most common malignant extracranial tumor of childhood. Since NB appears susceptible to immunotherapies that include monoclonal antibodies and T-cell immune responses elicited by tumor vaccine, we have combined the beneficial effects of both humoral and cell-mediated components of the anti tumor response. We demonstrated indeed that adoptive transfer of Epstein-Barr-virus (EBV)-specific cytotoxic T lymphocytes (EBV-CTLs) genetically modified to express a chimeric antigen receptor (CAR-GD2) targeting the GD2 antigen expressed by neuroblasts persist in the peripheral blood and induce objective tumor responses (including complete remissions). We will now augment the expansion and survival of CAR-GD2 modified EBV-CTLs by coexpressing the IL-7Rα that restores their capacity to respond to homeostatic IL-7. We will also enhance the capacity of these cells to invade solid tumor masses by expressing heparanase (HPSE) that disrupts the non-cellular stromal elements of NB. Experiments will be conducted in vitro and in vivo in a xenograft mouse model.

15. SUBJECT TERMS
Neuroblastoma, immunotherapy, chiemric antigen receptor, GD2 antigen, heparanase, regulatory T cells, tumor stroma.

16. SECURITY CLASSIFICATION OF:			17. LIMITATION OF ABSTRACT	18. NUMBER OF PAGES	19a. NAME OF RESPONSIBLE PERSON
a. REPORT	b. ABSTRACT	c. THIS PAGE			USAMRMC
U	U	U	UU		19b. TELEPHONE NUMBER *(include area code)*

Table of Contents

INTRODUCTION

In our recent Phase I study we found that the adoptive transfer of Epstein-Barr-virus (EBV)-specific cytotoxic T lymphocytes (EBV-CTLs) genetically modified to express a chimeric antigen receptor (CAR-GD2) targeting the GD2 antigen expressed by neuroblasts, can persist in the peripheral blood for 6 weeks and induce objective tumor responses (including complete remission) or tumor necrosis in 4/8 subjects with refractory/relapsed NB[1]. Although encouraging, this study also revealed that the signal from the transgenic CTLs progressively declined over time in the majority of patients[2;3] suggesting that the anti tumor effects of these cells could be augmented by prolonging the survival and effector function of the transgenic CTLs, for example by restoring their responsiveness to homeostatic cytokines such as IL-7[4] and inducing a robust $CD8^+$ T cell memory response[5]. Our second approach aims to disrupt the non-cellular stromal elements of NB that may impede access to CAR-modified EBV-CTLs. The ability of tumor-specific CTLs to cross tumor blood vessels is crucial for reaching the tumor cells. Leukocyte extravasation is highly dependent upon the degradation of the components of the subendothelial basement membrane (SBM) and the extracellular matrix (ECM) such as heparan sulfate proteoglycans (HSPGs), fibronectin and collagen[6]. Heparanase (HPSE) is the only known mammalian endoglycosidase degrading HSPGs at distinct HS intra-chain sites[7;8]. Although HPSE is expressed in activated $CD4^+$ lymphocytes, neutrophils, monocytes and B lymphocytes[9-11] we have found it to be deficient in cultured T cells and EBV-CTLs.

BODY

In Task 1 we proposed to co-express CAR-GD2 and IL-7Rα in EBV-CTLs to improve their expansion and anti tumor effects in response to IL-7, whilst avoiding the expansion of regulatory T cells (Treg) (time frame months 1-24).

We first optimized the methodology to expand *ex vivo* fully functional regulatory T cells (Tregs) (as assessed in a model of graft versus host disease (GvHD)) that can be used for the experiments *in vitro* and *in vivo* proposed in this task of the proposal. The results of these experiments have been published in manuscript #1 listed in the Reportable Outcome section (Chakraborty R et al. Haematologica. 2013 Apr;98(4):533-7).

Briefly, the methodology we developed to isolate and expand nTregs is graphically summarized in **Figure 1**.

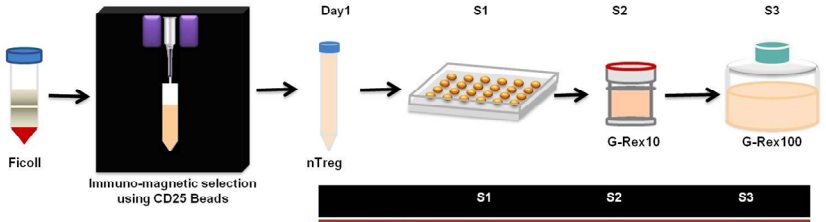

	S1	S2	S3
Time (week)	1	1	1
Temsirolimus (μg/ml)	1	1	1
IL-2 (IU/ml)	n/a	50	50
Treg:Feeders	n/a	1:5	1:5

Figure 1. Schema of the procedure used to select and expand nTregs. *Schematic representation of the procedure used to select the nTregs using magnetic columns (small columns or CliniMACS device) and to expand the nTregs using the G-Rex device.*

Specifically, we reduced the complexity of the selection process of nTregs from the peripheral blood, we isolated putative nTregs exclusively based on their bright expression of the CD25 molecule ($CD25^{Bright}$ cells) without additional selection steps. Starting from $4.5 \times 10^8 \pm 1 \times 10^8$ PBMC (obtained from 50 mL of buffy coat products), we recovered $3 \times 10^6 \pm 1 \times 10^6$ cells. Upon selection these cells consistently coexpressed CD4 and CD25 molecules (95% ± 5%), with limited contamination by $CD8^+$ cells. One day 7 (S1) and day 14 (S2), $2.9 \times 10^6 \pm 0.5 \times 10^5$ and $7.7 \times 10^7 \pm 1.7 \times 10^7$ cells were obtained, respectively. After the third stimulation (day 21, S3), we recovered $1.8 \times 10^9 \pm 7.6 \times 10^7$ cells, corresponding to more than 600 fold expansion (**Fig 2A**). This degree of expansion was significantly higher than that obtained in parallel experiments (5-6 folds) in which isolated nTregs were grown using the same protocol but plated in conventional tissue culture plates (cells at day 21 were $5.3 \times 10^6 \pm 1.6 \times 10^6$ starting from 1×10^6) (**Fig 2B**). The percentage of $CD4^+CD25^+$ cells remained stable over 3 weeks of culture and was 92% ± 5% by day 21, with 69% ± 19% of the cells expressing FoxP3 (**Fig 2C-D**). Expanded nTregs retained their expression of the lymph node homing molecules CD62L and CCR7 (69% ± 4% and 39% ± 3%, respectively), and lacked expression of the IL-7Rα (CD127) (2% ± 1.2%), a known feature of Tregs. Of note, the percentage of FoxP3 expressing cells significantly increased from day 1 to day 21 of culture, and although FoxP3 was not expressed by all the cells by day 21, the *FoxP3* promoter remained consistently unmethylated (**Fig 2E**), indicating the commitment of the expanded cells to the Treg state, despite some of them lacking FoxP3 protein expression.[12] At the end of the culture, contaminating $CD8^+$ T cells were 10% ± 3.7%.

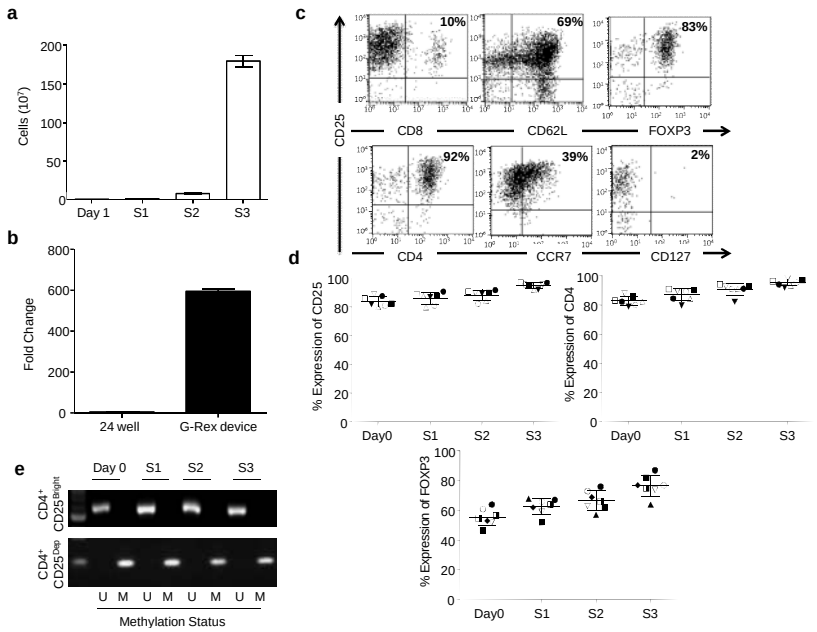

Figure 2. Robust ex vivo expansion of nTregs in the G-Rex device. ***Panel a*** *illustrates the number of nTregs obtained after 1, 2 or 3 (S1, S2 and S3) weeks of culture in the G-Rex device. Data illustrate average and standard deviations (SD) for 7 independent experiments.* ***Panel b*** *compares the fold expansions of nTregs cultured in 24-well plates or in the G-Rex device. Data show mean ± SD of 7 independent experiments.* ***Panel c*** *shows the flow cytometry plots of expanded nTregs on day 21 (S3). The panels illustrate CD4, CD25, CCR7, CD127 and FoxP3 expression for one representative donor.* ***Panel d*** *illustrates the expression of CD25, CD4 and FoxP3 in expanded nTregs after each round of stimulation (S1, S2 and S3). Data summarize the results of 7 independent experiments.* ***Panel e*** *shows the methylation-specific semi-quantitative PCR of the FoxP3 promoter in nTregs obtained after each round of stimulation (S1, S2 and S3).*

Using a CFSE-based suppression assay, we also found that T-cell divisions were suppressed equally well when either freshly isolated nTregs or expanded nTregs (S3) were added to the culture (80% ± 10% and 80% ± 13% suppression, respectively) (p<0.0001). No suppression was observed in the presence of expanded control $CD25^{Depleted}$ cells (12% ± 9% suppression) (**Fig 3A-B**). Importantly, the robust expansion of nTregs achieved in the G-Rex device was obtained without significantly compromising their telomere length (**Fig 3C**). Since by day 21, expanded nTregs contained contaminating $CD8^+$ T cells, we specifically assessed the functionality of these cells, as the infusion of functional $CD8^+$ cells on allogeneic HSCT setting may exacerbate GvHD and thus compromise the protective effects of Tregs. As illustrated in **Fig 3D-E**, T-cell divisions were suppressed equally well when either freshly isolated nTregs, expanded nTregs or selected $CD8^+$ T cells were added to the culture (80% ± 8%, 76% ± 8%, and 66% ± 14% suppression, respectively) (p<0.001), suggesting that contaminating $CD8^+$ cells likely acquired inhibitory properties during the *ex vivo* culture conditions. This inhibitory function of expanded $CD8^+$ T cells was corroborated by the detection of the unmethylated form of the *FoxP3* promoter in these cells (**Fig 3F**).

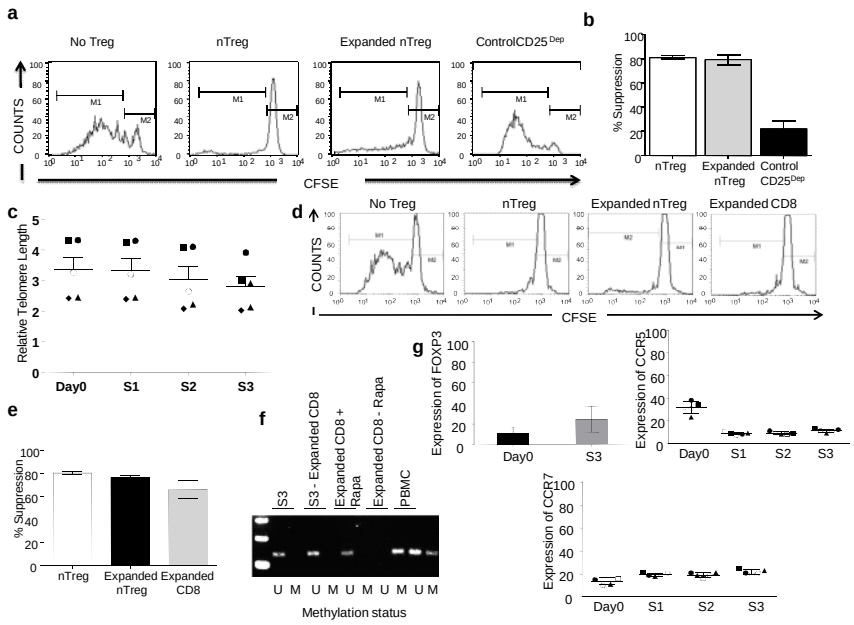

Figure 3. Ex vivo expanded nTregs retain robust suppressive function without undergoing cell senescence. ***Panel a****. The inhibitory activity of freshly isolated nTregs, expanded nTregs (S3), and expanded $CD25^{Depleted}$ cells was assessed by using a CFSE-based suppression assay. Panels illustrate the inhibitory activity of nTregs for a representative experiment.* ***Panel b****. The graph summarizes average and SD of the inhibitory function of nTregs for 7 independent experiments.* ***Panel c****. The graph illustrates the relative telomerase length (RTL) in freshly isolated nTregs (Day 1) and expanded nTregs at S1, S2 and S3. Data show mean ± SD for 7 independent experiments.* ***Panel d****. Contaminating $CD8^+$ cells at day 21 of culture were isolated and analyzed for their suppressive activity and compared to nTregs. Panels illustrate the inhibitory activity for one representative experiment.* ***Panel e****. The graph summarizes average and SD of the inhibitory function of contaminating $CD8^+$ cells and nTregs for 7 independent experiments.* ***Panel f****. Methylation-specific semi-quantitative PCR of FoxP3 promoter in cells obtained at the end of third round of stimulation (S3), nTregs obtained at the end of the third round of stimulation depleted of CD8 (S3-Expanded CD8), the expanded and purified $CD8^+$ population in S3 (Expanded CD8 + Rapa), $CD25^{Depleted}$ population (CD8 –Rapamycin), and PBMC.*

Finally, to investigate if expanded nTregs retained their inhibitory function *in vivo*, we used a xenograft model of lethal GvHD. As illustrated in **Fig 4A**, the weight loss of control mice receiving PBMC and $CD25^{Depleted}$ cells was significantly greater as compared to mice that received PBMC and expanded nTregs (7.2 ± 1.9 g vs.1.9 ± 1 g, respectively) (p = 0.0045). In addition, by day 60, mice receiving expanded nTregs had delayed occurrence or no signs of GvHD (**Fig 4B**), and showed normal size of the spleen as compared to controls (**Fig 4C**). Finally, mice co-infused with expanded nTregs revealed no histopathological lesions compatible with GvHD in their skin, nose, or ear (**Fig 4D**), and showed significantly improved overall survival as compared to control mice (p<0.0003) (**Fig 4E**).

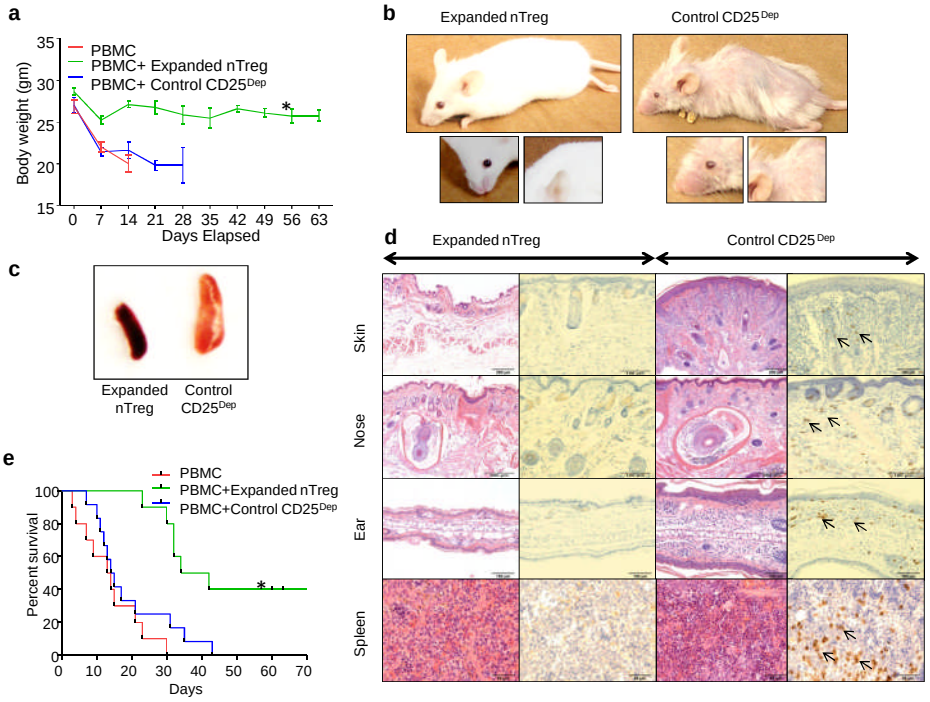

Figure 4. Expanded nTregs control GvHD in a xenogenic mouse model. *Irradiated NSG mice were infused with PBMC either alone or in combination with expanded nTregs (S3) or expanded control* $CD25^{Depeleted}$ *cells at 1:1 ratio.* ***Panel a****. The graph illustrates the measurements of the weight of the NSG mice. Data show mean ± SD of 12 animals for each group (* p = 0.0001).* ***Panel b****. Images show that control mice developed signs of GvHD, such as hair loss and orbital tightening.* ***Panel c****. Spleen enlargements were observed in mice infused with control* $CD25^{Depleted}$ *cells.* ***Panel d****. Representative H&E and immunohistochemistry staining for* $CD8^+$ *T cells in tissue sections obtained from skin, nose, ear, and spleen of treated mice. Control mice showed evidence of chronic dermatitis, with moderate diffuse epithelial hyperplasia, hyperkeratosis and marked multifocal coalescing subcutaneous and dermal mononuclear inflammatory cell infiltrates. Arrows indicate infiltrating* $CD8^+$ *T cells.* ***Panel e****. Kaplan-Meier survival curve comparing NSG mice receiving human PBMC alone or in combination with expanded nTregs or expanded control* $CD25^{Depeleted}$ *cells (12 animals for each group) (*p = 0.0003).*

Our proposed strategy has significant advantages. First, we have minimized the cell purification process to a single immune magnetic selection step based on their CD25 expression, which is sufficient to minimize the presence of $CD8^+CD25^+$ cells in the final Treg products, provided that rapalogs are added to the cultures during the expansion phase of the selected cells. Importantly, we have observed that, in the presence of rapalogs, any "contaminating" $CD8^+CD25^+$ cells persisting at the end of the 21 days of culture show inhibitory properties and methylation of *FoxP3* promoter. This is in accordance with previous observations showing that, in specific culture conditions, $CD8^+$ cells may develop suppressive activity. Second, and most importantly, we have optimized a robust and cost-effective expansion protocol of Tregs. Stimulation of Tregs is obtained with anti-CD3/CD28 mAbs and feeder cells, which are less expensive than coated beads. In addition, cells are easily accommodated, with minimal manipulation, in small gas permeable static culture flasks (G-Rex) that promote efficient gas exchange and availability of nutrients to the cells, while diluting waste products. Remarkably, expanded Tregs had no significant shortening of their telomere lengths, indicating their potential capacity to undergo further divisions *in vivo* after adoptive transfer, and retained inhibitory function after freezing and thawing. This developed methodology allowed us to generate sufficient Tregs to accomplish our specific project. In addition, we have implemented a cost-effective and simplified production of nTregs that will likely facilitate the implementation of clinical trials based on the infusion of these cells to control GvHD after allogeneic HSCT and graft rejection in solid organ transplant recipients, and to treat autoimmune diseases.

Having optimized the methodolody to generate large amount of fully functional Tregs, we then demonstrated that our proposed hypothesis that the genetic manipulation of EBV-CTLs to express CAR-GD2 and IL-7Rα renders these cells resistant to the inhibitory effects of Tregs *in vitro* and *in vivo* in a xenograft neuroblastoma model is correct. The results of these experiments have been summarized in manuscript #2 listed in the Reportable Outcome section (Perna et. Clinical Cancer Research in press).

Briefly, to restore the responsiveness to IL-7 and to redirect the antigen specificity of EBV-CTLs against neuroblastoma, we generated a bicistronic γ-retroviral vector encoding the IL-7Rα and a GD2-specific CAR linked through a 2A (TAV) sequence (SFG.IL-7Rα.2A.CAR-GD2) (**Fig 5A**). EBV-CTLs established from 5 healthy EBV-seropositive donors were transduced with the vector, and the expression of both IL-7Rα and CAR-GD2 was measured by FACS analysis. As shown in **Fig 5B**, both CAR-GD2 and IL-7Rα were stably expressed (64% ± 3% and 34% ± 9%, respectively) in transduced EBV-CTLs, while the expression of the native IL-7Rα on control cells remained negligible (4% ± 1%). To evaluate the functionality of the transgenic IL-7Rα, we measured the phosphorylation of STAT5 in response to either IL-2 or IL-7. In the absence of cytokines, control and IL-7Rα.CAR-GD2$^+$ EBV-CTLs showed negligible phosphorylation of STAT5 (3% ± 2% and 8% ± 4%, respectively). In IL-7Rα.CAR-GD2$^+$ EBV-CTLs, near equal STAT5 phosphorylation of Tyr-694 was detected in response to IL-2 (49% ± 7%) or IL-7 (38% ± 6%, respectively) (p= NS). By contrast, in control cells, STAT5 was phosphorylated in response to IL-2 (63% ± 8%) but not to IL-7 (6% ± 5%) ($p < 0.05$) (**Fig 5C**). The functionality of the transgenic IL-7Rα was further supported by progressive selection of transgenic cells if cultures were supplemented with IL-7. As illustrated in **Fig 5D**, when IL-7Rα.CAR-GD2$^+$ CTLs were stimulated weekly with autologous LCLs and IL-7, the expression of both IL-7Rα and CAR-GD2 progressively increased between the third and sixth antigen-specific stimulation (from 34% ± 9% to 66% ± 5% for IL-7Rα, and from 64% ± 3% to 80% ± 7% for CAR-GD2). By contrast, when CTLs were expanded in the presence of IL-2, no enrichment of either transgenes was observed, since this cytokine equally supports the *ex vivo* growth of transduced and non transduced CTLs (data not shown).

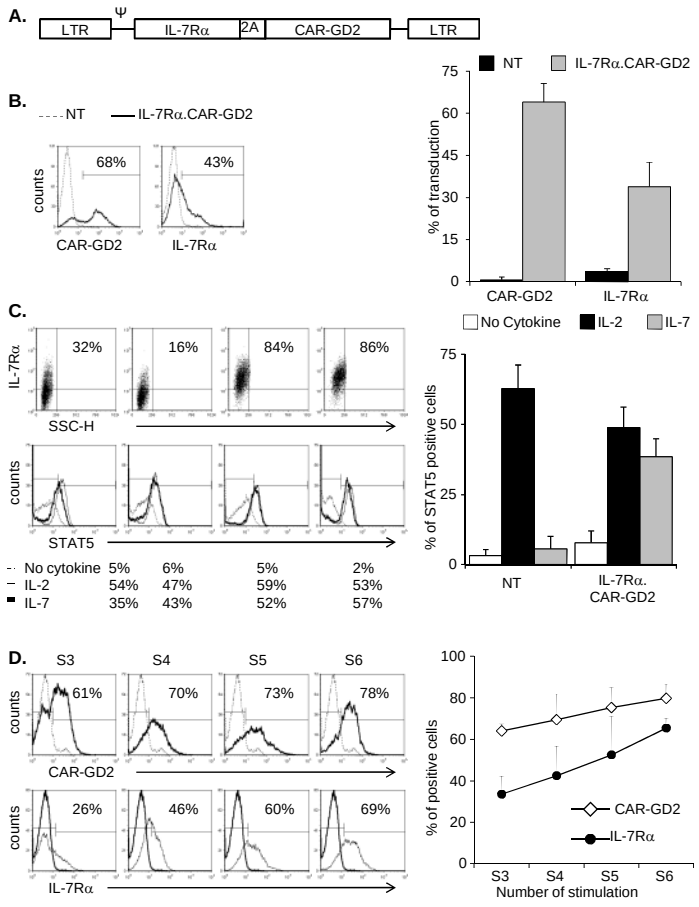

Figure 5. EBV-CTLs are effectively transduced with the bicistronic vector encoding both the IL-7Rα and the CAR-GD2. Panel A *illustrates the schema of the bicistronic γ-retroviral vector encoding the IL-7Rα and GD2-specific CAR linked through a 2A (TAV) sequence.* ***Panel B*** *shows the expression of CAR-GD2 (top histogram) and IL-7Rα (bottom histogram) evaluated by FACS analysis day 7 after transduction. The dotted line indicates control EBV-CTLs while the bold line indicates the transduced EBV-CTLs. The graph represents mean ± SD of 5 donors.* ***Panel C*** *illustrates IL-7Rα expression in four IL-7Rα.CAR-GD2$^+$ EBV-CTLs generated (upper panels) and STAT5 phosphorylation (lower panels) in the absence of cytokines (thin black line), in response to IL-2 (dotted line) or IL-7 (black bold line).* ***Panel D*** *shows the progressive enrichment in cells expressing the two transgenes IL-7Rα and CAR-GD2 when IL-7Rα.CAR-GD2$^+$ EBV-CTLs were expanded in the presence of IL-7. S3, S4, S5 and S6 indicate the transgene expression detected week 3 (S3), week 4 (S4), week 5 (S5) and week 6 (S6), respectively after transduction. Graph represents mean ± SEM of 4 different EBV-CTL lines.*

The enrichment of transgenic T cells following exposure to IL-7 was a consequence of the proliferation of IL-7Rα.CAR-GD2$^+$ EBV-CTLs. As illustrated in **Fig 6A**, CFSE labeled-control and IL-7Rα.CAR-GD2$^+$ EBV-CTLs divided equally well when stimulated with LCLs (ratio 4:1) in the presence of IL-2 (proliferation: 68% ± 6% and 68% ± 4%, respectively). By contrast, in the presence of IL-7, IL-7Rα.CAR-GD2$^+$ but not control EBV-CTLs had significantly greater proliferation: 63% ± 3% vs. 14% ± 1%, respectively ($p<0.001$). The number of EBV-CTLs proliferating in response to EBV-LCLs and IL-7 was generally higher than expected based on the ectopic expression of IL-7Rα. This higher level is likely a consequence of the physiological production of IL-2 by EBV-CTLs in response to their cognate EBV antigens (EBV-LCLs) (data not shown). Finally, exposure of IL-7Rα.CAR-GD2$^+$ EBV-CTLs to IL-7 did not affect their antitumor properties. As shown in **Fig 6B**, when EBV-CTLs were cultured with CHLA-255 cells, only IL-7Rα.CAR-GD2$^+$ cells controlled tumor growth in the presence

of either IL-2 or IL-7 (6% ± 1% and 4% ± 1%, respectively), while tumor cells outgrew in cultures containing control EBV-CTLs irrespective of the cytokine added (43% ± 5% and 57% ± 12%, respectively) (p<0.001).

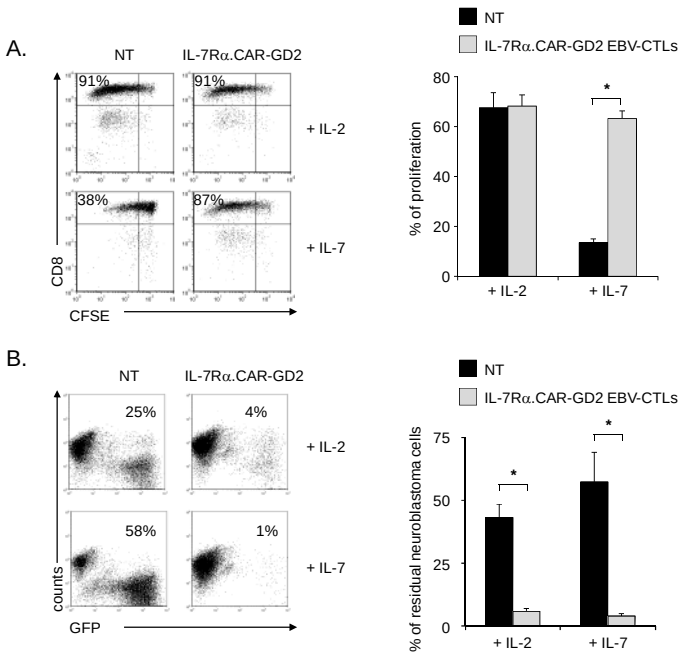

Figure 6. IL-7 supports the proliferation and effector function of IL-7Rα.CAR-GD2$^+$ EBV-CTLs. Panel A *shows a representative CFSE-based proliferation assay of control and IL-7Rα.CAR-GD2$^+$ EBV-CTLs. Control and IL-7Rα.CAR-GD2$^+$ EBV-CTLs were activated in the presence of autologous irradiated LCLs and either IL-2 or IL-7. CFSE dilution was evaluated on day 7 using FACS analysis. The graph represents mean ± SD of 5 independent experiments.* ***Panel B*** *illustrates a representative co-culture experiment in which control and IL-7Rα.CAR-GD2$^+$ EBV-CTLs were co-cultured with CHLA-255 GFP-tagged tumor cells (at ratio 1:2) in the presence of IL-2 or IL-7. Residual tumor cells were enumerated by flow cytometry on day 7 of culture. The graph shows mean ± SD of 5 independent experiments. *p<0.001.*

We then used *ex vivo* expanded CD4$^+$CD25$^+$ Tregs isolated from healthy donors rather than freshly isolated Tregs for the following reasons. First, the experiments required a significant number of Tregs that could not be obtained upon fresh isolation even from buffy coat preparations. Second, circulating Tregs obtained after immunomagnetic selection based on CD4 and CD25 selection are frequently contaminated by CD4$^+$CD25$^+$IL7Rα$^+$ cells that lack regulatory activity, but respond to IL-7 (data not shown)(31). We first confirmed that the nominal Treg population retained their inhibitory properties. As shown in **Fig 7A**, the proliferation of activated PBMCs (80% ± 3% in the presence of control CD4$^+$CD25$^-$ cells) was significantly inhibited in the presence of the expanded Treg population (27% ± 6%) (p< 0.001). We then confirmed that these Tregs, like freshly isolated Tregs(22), lacked expression of IL-7Rα (3% ± 0.4% positive) (**Fig 7B**). As a consequence, STAT5 was only phosphorylated in these Tregs in response to IL-2 (MFI = 75 ± 9) (p<0.001) and not in response to IL-7 (MFI = 23 ± 3) (**Fig 7C**). Finally, a CFSE-based dilution assay showed that Tregs only proliferated after polyclonal activation in the presence of IL-2 and not on exposure to IL-7 (MFI 1439 ± 207 vs 445 ± 68, respectively; p<0.001) (**Fig 7D**).

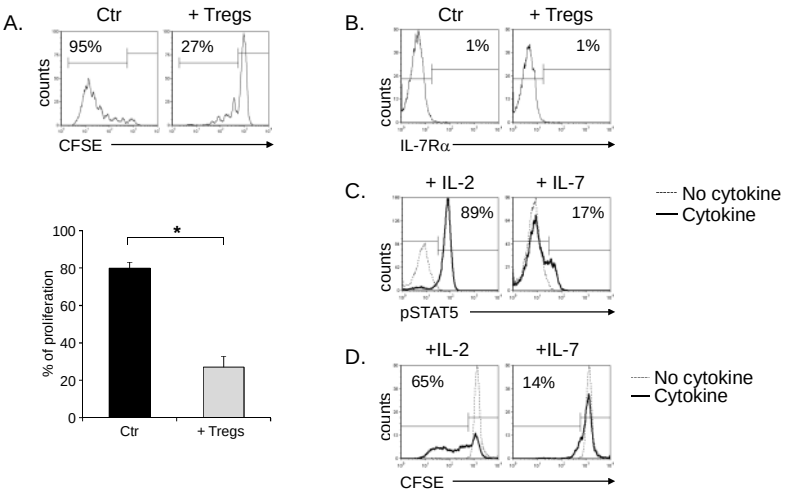

Figure 7. Ex vivo expanded Tregs do not respond to IL-7. Panel A *shows a CFSE-based assay to illustrate the inhibitory activity of ex vivo expanded Tregs. PBMCs labeled with CFSE were activated in the absence (left histograms) or in the presence of Tregs (right histograms) at a ratio of 1:1. CFSE dilution was measured on day 7 of culture by flow cytometry. The graph represents mean ± SEM of 6 independent experiments.* ***Panel B*** *illustrates the expression of IL-7Rα in ex vivo expanded Tregs in a representative experiment. The plot on the left shows the isotype control, while the plot on the right the IL-7Rα profile. * p< 0.001.* ***Panel C*** *shows the phosphorylation of STAT5 in Tregs not stimulated (dotted lines) or stimulated with IL-2 (left panel) or IL-7 (right panel).* ***Panel D*** *illustrates the proliferative response of Tregs exposed to IL-2 or IL-7. Tregs were labeled with CFSE and stimulated in the presence of IL-2 (left panel) or IL-7 (right panel). CFSE dilution was evaluated on day 7 by flow cytometry. The solid and dotted lines represent the CFSE dilution of Tregs stimulated with or without cytokines, respectively.*

Having demonstrated that IL-7 supports the proliferation and function of IL-7Rα.CAR-GD2$^+$ EBV-CTLs, we then investigated whether the beneficial effects of IL-7 were maintained in the presence of functional Tregs. As illustrated in **Fig 8A**, when IL-7Rα.CAR-GD2$^+$ EBV-CTLs were cultured with CHLA-255 cells (effector:target

ratio of 1:2) they significantly controlled the growth of these tumor cells by day 7 of culture in the presence of either IL-2 or IL-7 (residual cells were 6% ± 1% and 4% ± 1%, respectively). By contrast, when expanded Tregs were added to the co-culture (ratio CTLs:Tregs 1:1), the antitumor activity of IL-7Rα.CAR-GD2$^+$ EBV-CTLs was significantly inhibited in the presence of IL-2 but not of IL-7 (residual cells in culture: 14% ± 3% vs. 7% ± 2%, respectively; p<0.05). In addition, IL-7 also supported the proliferation of IL7Rα.CAR-GD2$^+$ EBV-CTLs in the presence of Tregs upon physiological costimulation with autologous LCLs. As the CFSE dilution assay shows in **Fig 8B**, the proliferation of IL-7Rα.CAR-GD2$^+$ EBV-CTLs in response to IL-2 (68% ± 4%) was significantly compromised in the presence of Tregs (to 34% ± 6%, p<0.01). In contrast, when IL-7 was added to the culture, IL-7Rα.CAR-GD2$^+$ EBV-CTLs divided well even in the presence of Tregs (proliferation was 63% ± 3% without Tregs and 56% ± 2% in the presence of Tregs). The CFSE dilution of IL-7Rα.CAR-GD2$^+$ EBV-CTLs co-cultured with Tregs was significantly increased in the presence of IL-7 as compared to IL-2 (p=0.005).

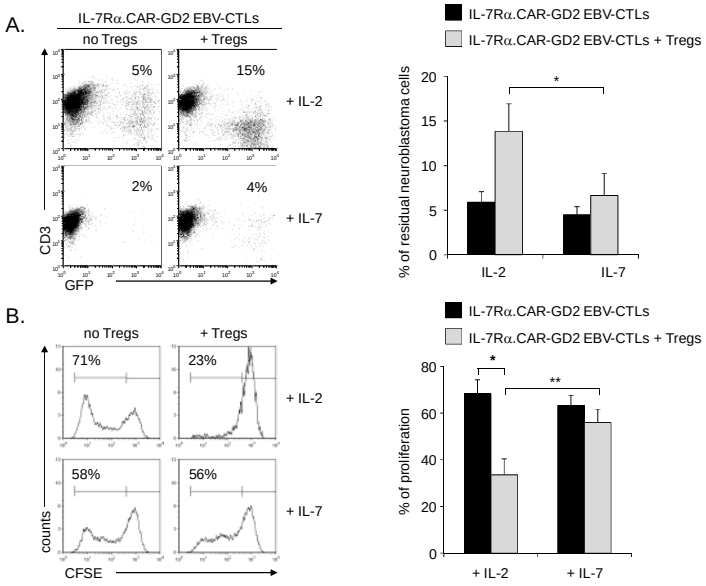

Figure 8. IL-7, unlike IL-2, supports in vitro the proliferation and function of IL-7Rα.CAR-GD2$^+$ EBV-CTLs in the presence of Tregs. Panel A. *IL-7Rα.CAR-GD2$^+$ EBV-CTLs were co-cultured with CHLA-255 GFP-tagged cells (ratio 1:2) in the presence of IL-2 or IL-7, with or without Tregs. The percentage of residual tumor cells was measured by flow cytometry on day 7 of culture. The plots on the left show a representative experiment, while the graph on the right summarizes mean ± SD of 5 independent experiments.* ***Panel B****. IL-7Rα.CAR-GD2$^+$ EBV-CTLs were labeled with CFSE and activated with autologous LCLs in the presence of IL-2 (upper plots) or IL-7 (lower plots) with or without Tregs. CFSE dilution was measured at day 7 of culture by flow cytometry. The plots on the left show a representative experiment, while the graph represents mean ± SD of 5 independent experiments. * p<0.01; ** p=0.005*

To assess the *in vivo* capacity of IL-7 to support the antitumor activity of IL-7Rα.CAR-GD2$^+$ EBV-CTLs, we used NSG mice engrafted i.p. with the FFLuc$^+$ cell line CHLA-255. As shown in **Fig 9,** control mice that received only tumor cells or control CTLs showed a rapid increase of the bioluminescence signal (2.3 x 10^8 ± 3 x 10^7 photons) and were sacrificed by day 18. Mice infused with IL-7Rα.CAR-GD2$^+$ EBV-CTLs and IL-2 had superior tumor control (1.6 x10^8 ± 2 x 10^7 photons at day 34), but this effect was abrogated when Tregs were co-infused (2.4 x 10^8 ± 4 x 10^7 photons at day 34, p<0.05). In contrast, mice infused with IL-7Rα.CAR-GD2$^+$ EBV-CTLs and IL-7 controlled tumor growth equally well in the absence (1.2 x 10^8 ± 3 x 10^7 photons) or in presence of Tregs (1.3 x 10^8 ± 6 x 10^6 photons) at day 34.

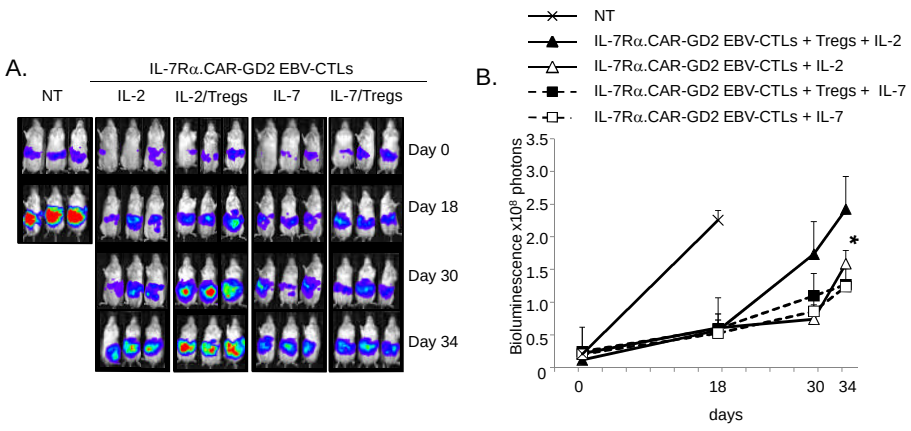

Figure 9. IL-7, but not IL-2, supports in vivo anti-tumor activity of IL-7Rα.CAR-GD2$^+$ EBV-CTLs in the presence of Tregs. *NSG mice engrafted i.p. with CHLA-255 cells tagged with FFLuc were infused with IL-7Rα.CAR-GD2$^+$ EBV-CTLs and received IL-2 ± Tregs or IL-7 ± Tregs. Tumor growth was monitored using an in vivo imaging system (Xenogen – IVIS imaging system). A group of mice received control EBV-CTLs or tumor cells only (Control).* ***Panel A*** *shows the images of different groups of mice.* ***Panel B*** *illustrates the mean ± SD of photons for 8 mice/group in two independent experiments. * p<0.05.*

As a conclusion of this work, we developed a strategy that selectively promotes the *in vivo* expansion of CAR-redirected CTLs without favoring the proliferation and function of Tregs that may limit long-term persistence and activity of the infused effector cells and thereby compromise antitumor efficacy. Here we demonstrate that

CAR-redirected EBV-CTLs engineered to regain responsiveness to IL-7 by restoring their expression of IL-7Rα, proliferate in response to a combination of native TCR receptor and IL-7 stimulation without favoring the expansion and function of Tregs. As a consequence, we observed an increase in their CAR-mediated anti-neuroblastoma activity, even in the presence of Tregs.

Task 2. To evaluate the contribution of IL-7Rα ligation and co-stimulation from viral-infected target cells on the development of long-lived memory CAR-GD2-mofied EBV-CTLs in a humanized SCID mouse model previously engrafted with human hematopoietic stem cells (time frame months 12-48).

To develop this task we have generated artificial antigen presenting cells (aAPCs) to express CD40L and OX40L efficiently boost in vitro virus specific CTLs. Briefly, in order to develop a cellular vaccine to reactivate pp65-specific T cells, we generated aAPCs by engineering K562 to express either CD40L or OX40L or pp65/eGFP or the combinations CD40L/pp65 and OX40L/pp65. Single cell clones were used for the experiments. The expression of CD40L, OX40L and pp65 were assessed by FACS analysis (**Fig 10A**) and by western blotting (**Fig 10B**), respectively. To verify if apoptotic bodies derived from irradiated aAPCs can be taken up by monocytes, we stained monocytes and aAPCs with red and green fluorescent cell linker for phagocytic cell labeling, respectively. During the coculture we observed that monocytes can indeed capture apoptotic bodies from irradiated aAPCs (**Fig 10C**). We observed that CD40L expression on aAPCs effectively induces maturation of professional APCs. Indeed, when isolated monocytes were cocultured with aAPCs, we found rapid up-regulation of CD80, CD83, CD11c and HLA-DR on monocytes 24 hours after stimulation (**Fig 10D**). The capacity of aAPCs to elicit pp65-specific T cells was assessed in experiments in which PBMC collected from CMV seropositive donors were cocultured with irradiated aAPCs. As shown in **Fig 10E**, after 10 - 12 days of culture, aAPCs expressing pp65 reactivated CMV-specific T cells as demonstrated by the increased frequencies of IFNγ spot forming units (SFU). In this set of experiments, we decided to leave out the K562/OX40L/pp65 because they did not show capacity to induce maturation of professional APC or promote uptake of apoptotic bodies. Although inferior to the PBMC loaded with pp65 peptides (INFγ SFU 789 ± 130), aAPCs expressing pp65 were effective in reactivating CMV-specific T cells (INFγ SFU 83 ± 25 vs. 292 ± 56, 502 ± 104, 477 ± 91 for K562, K562/pp65, K562/CD40L/pp65, K562/CD40L/OX40L/pp65 respectively; p<0.001). The addition of CD40L significantly increased the boosting of CMV-specific T cells (INFγ SFU 292 ± 56 vs. 502 ± 104 for K562/pp65 and K562/CD40L/pp65, respectively; p=0.034). The combination CD40L/OX40L was similar to CD40L alone (INFγ SFU 292 ± 56 vs. 477 ± 91 for K562/pp65 vs. K562/CD40L/OX40L/pp65, respectively p=0.021). As expected control PBMC and PBMC stimulated either with wild type K562 or K562/CD40L or K562/OX40L did not stimulate CMV-specific responses (INFγ SFU 111 ± 22, 83 ± 25, 96 ± 27 and 92 ± 19). In all cases an irrelevant peptide was used as a negative control, and in all cases the IFNγ reactivity was negligible (< 30 SFU/10^5 cells). Phenotypic analysis of expanded cells by day 10 – 12 of culture showed a significant difference in natural killer (NK, $CD3^-CD56^+$) cells in presence of CD40L/pp65 (31% ± 13%) and CD40L/OX40L/pp65 (31% ± 14%) aAPCs compared to aAPC encoded for pp65 alone (47% ± 15%) p=0.014.

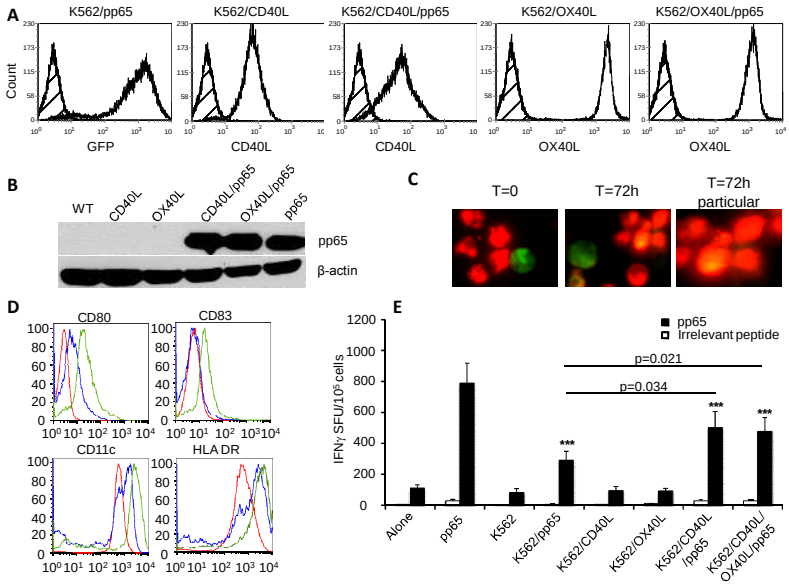

Figure 10. pp65-aAPCs are able to reactivate in vitro CMV-specific T cells from seropositive PBMC. Panel A. *Rappresentative FACS plots of the expression of eGFP and the costimulation molecules on K562 transduced cells.* ***Panel B****. Western blotting showing the expression of pp65 in the different aAPCs.* ***Panel C.*** *Uptake of apoptotic bodies derived from aAPCs by monocytes. Monocytes labeled with PKH26 red fluorescent cell linker compound were cocultured (5:1 ratio) with irradiated K562/Cd40L/OX40L/pp65 labeled with PKH2 green fluorescent cell linker compound.* ***Panel D.*** *Representative FACS plot of expression of CD80, CD83, CD11c and HLA DR by monocytes after 72h of stimulation with irradiated K562/pp65 (in blue) and K562/CD40L/OX40L/pp65 (in green). The red line represents the expression of the marker before stimulation.* ***Panel E.*** *shows the frequency of reactivated specific T cells from 11 CMV seropositive donors against CMV (pp65)*

using IFNγ ELIspot; the graft represents the mean ± SEM SFC/10^5 input cells. Controls were stimulated with an irrelevant pepmix.

Having generated functional aAPCs we then demonstrated that these cells can boost *in vivo* virus specific CTLs. Briefly, having demonstrated *in vitro* the functional activity of the aAPCs, we then assessed their capacity to boost *in vivo* CMV-specific T-cell responses. NOG/SCID/$\gamma_c^{-/-}$ mice were coinfused with PBMC obtained from CMV seropositive donors and aAPCs. Mice were then vaccinated 3 times with irradiated aAPCs *in vivo*, and immune responses elicited were measured 7 days after the last vaccinations (**Fig 11A**). In the majority of cases, mice infused with aAPCs encoding pp65 irrespective of the presence of CD40L and OX40L showed larger spleens than mice infused with control aAPCs expressing CD40L/OX40L but lacking pp65 (data not shown). However, as illustrated in **Fig 11B**, at the time of the analysis we found that aAPCs expressing either CD40L or OX40L increases the engraftment of human $CD45^+$ cells (28% ± 4% and 31% ± 6%, for CD40L/OX40L and CD40L/OX40L/pp65, respectively). A lower percentage of CD45 engraftment was observed compared to CD40L/OX40L and CD40L/OX40L/pp65: in CD40L/pp65 (20% ± 6%, p=NS) and pp65 alone (p=0.014 and p=0.033, respectively). Immunophenotype of $CD45^+$ cells isolated from the spleens has shown a significant difference in the percentage of $CD4^+$ T cells (p=0.017) in the condition in which the aAPCs express both costimulatory molecules and pp65 alone; similar engraftment of CD8+, NK and CD19+ was observed in all experimental group (**Fig 11C**). In sharp contrast, vaccination with aAPCs expressing CD40L/OX40L/pp65 strongly influenced the frequency of CMV-specific T-cell precursors. As shown in **Fig 11D**, although T cells recovered from the spleens of mice coinfused with aAPCs showed detectable CMV-specific precursors in all experimental conditions, the combination *in vivo* of K562/CD40L/pp65 and K562/OX40L/pp65 showed the highest elicitation of CMV-specific T-cell precursors (101 ± 21 IFNγ SFU/10^5 cells) compared to the combination of K562/CD40L and K562/OX40L (28 ± 6 IFNγ SFU/10^5 cells) (p<0.001) and pp65 alone (53 ± 22 IFNγ SFU/10^5 cells) (p=0.048).

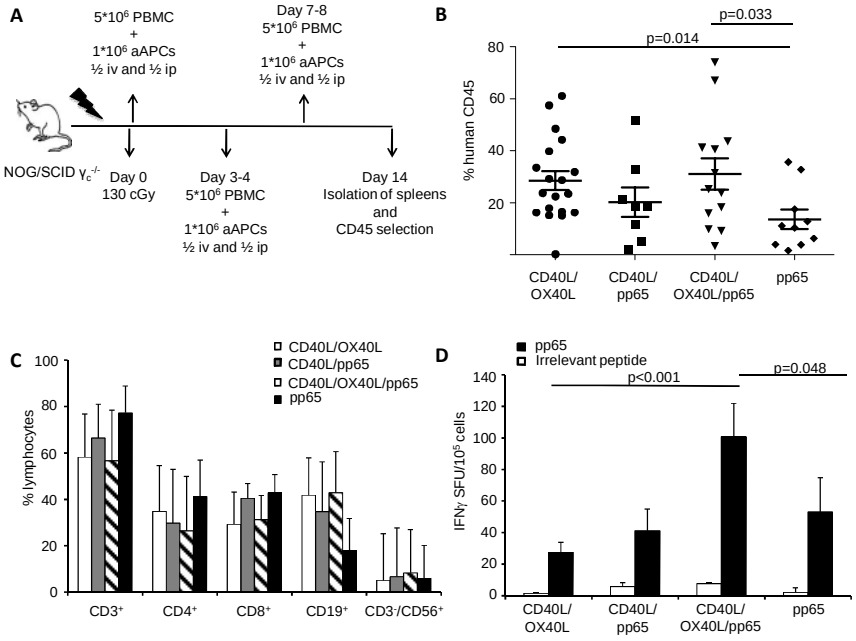

Figure 11. Boosting in vivo of CMV specific T cells by K562/CD40L/OX40L/pp65. ***Panel A*** *shows a schematic representation of xenograft mouse model.* ***Panel B****. shows the percentage of CD45 engraftment collected from the spleens after boosting in vivo with different aAPCs for at least of 8 mice per group.* ***Panel C****. The graft shows the mean ± standard deviation of different lymphocytes subsets.* ***Panel D****. shows the frequency of reactivated specific T cells from CD45 engrafted cells against CMV (pp65) using IFNγ ELIspot; the graft represents the mean ± SEM SFC/10^5 input cells. Controls were stimulated with an irrelevant pepmix.*

Since the aAPCs are boosting virus specific CTLs *in vivo* we then evaluated if virus specific CTL redirected with a CAR targeting the GD2 antigen expressed by neuroblasts can also be boosted. Briefly, we generated CAR-GD2 redirected CMV CTLs which were stimulated with aAPCs in presence of autologous PBMC to test the capacity of aAPCs to boost CAR T cells. In this set of experiments, we evaluated if CD40L/OX40L/pp65 aAPCs, which have showed better capacity to stimulate CMV responses, retained this ability also with CAR redirected CMV CTLs. We performed the experiments using CD40L/OX40L. Based on the previous data we decide to do not test the K562/pp65 because they do not show similar or better capacity of reactivation of CMV specific T cells in seropositive donors. In **Fig 12A**, CAR redirected CMV CTLs stimulated with CD40L/OX40L/pp65 aAPCs showed significant enrichment of pp65 frequency (1397 ± 212 SFU/10^5 cells) compared to CD40L/OX40L aAPCs stimulation (749 ± 146) (p=0.004). The analysis of CAR responses by IFNγ ELISpot showed that CD40L/OX40L/pp65 aAPCs are able to boost significantly better also the CAR T cells 2819 ± 452 SFU/10^5 cells compared to using CD40L/OX40L aAPCs (1610 ± 267 SFU/10^5 cells, p=0.002). The phenotypes of these cells indicated that the pp65 and CAR enrichments observed by ELISpot analysis after using CD40L/OX40L/pp65 aAPCs correlated

with higher CAR expression, in terms of percentage of expression or mean of fluorescence intensity (MFI), and pp65 tetramer staining **(Fig 12B)**. We then tested if after boosting the CAR redirected CMV-CTLs maintained activity versus specific targets. We performed a standard ^{51}Cr-release assay, and we observed that CAR redirected CMV-CTLs retained effector function against GD2$^+$ and pp65 pulsing target cells; in particular specifically lysed was observed in GD2$^+$ CHLA-255 cells (55% ± 17% and 63 ± 14% CD40L/OX40L and CD40L/OX40L/pp65 stimulated cells respectively) and pp65 pulsed PHAB (31% ± 7% and 59 ± 3% CD40L/OX40L and CD40L/OX40L/pp65 stimulated cells respectively). All CTLs showed negligible activity against the GD2$^-$ target cell line Raji (16% ± 8% and 11 ± 3% CD40L/OX40L and CD40L/OX40L/pp65 stimulated cells respectively) and irrelevant peptide pulsed PHAB (2% ± 1% and 3 ± 1% CD40L/OX40L and CD40L/OX40L/pp65 stimulated cells respectively) (**Fig 11C**). As expected, non transduced CMV CTLs lysed none of these targets except the pp65 pulsed PHAB (50% ± 9% and 48 ± 17% CD40L/OX40L and CD40L/OX40L/pp65 stimulated cells respectively). The antitumor activity and the activation of CAR-redirected CMV CTL were confirmed also by increase of frequencies of IFNγ in ELISpot and in co-culture. For the ELIspot, we plated T cells and tumor, CHLA 255 (GD2$^+$) and Raji (GD2$^-$) at ratio 1:1. The analysis after 24 hours showed higher IFNγ secretion in presence of GD2$^+$ target (295 ± 81 and 421 ± 21 SFU/10^5 cells for CD40L/OX40L and CD40L/OX40L/pp65 stimulated cells respectively) compared to GD2$^-$ Raji cells (75 ± 341 and 96 ± 18 SFU/10^5 cells for CD40L/OX40L and CD40L/OX40L/pp65 stimulated cells respectively) (**Fig 12D**).

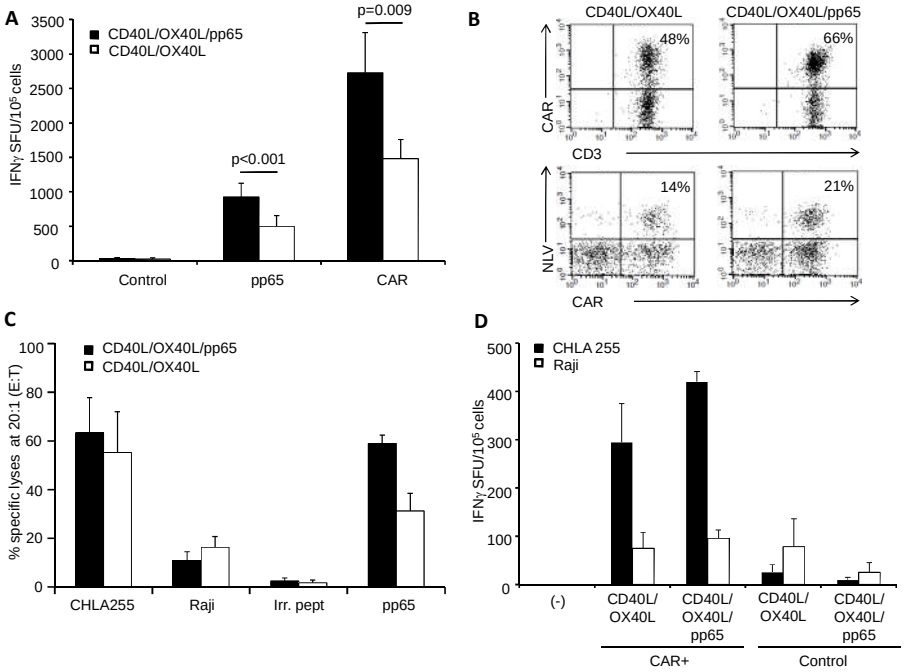

Figure 12. CAR redirected CMV CTL can be boosted in vitro by aAPCs encoding for pp65, CD40L and OX40L. ***Panel A*** *shows the frequency of reactivated specific T cells after boosting the CAR-GD2 redirected CMV specific CTL in vitro by aAPCs encoding for CD40L/OX40L (white bars) and CD40L/OX40L/pp65 (black bars). The frequency against pp65-CMV, irrelevant peptide and CAR was IFNγ ELIspot assay. Data summarize means ± SE of 9 independent experiments.* ***Panel B*** *shows dot plot a representative donor analysis of expression of CAR and CMV tetramer after stimulation in vitro by aAPCs.* ***Panel C*** *shows cytotoxic activity of CD40L/OX40L (white bars) and CD40L/OX40L/pp65 (black bars) assessed by ^{51}Cr-release assay at a 20:1 effector:target ratio. CHLA-255 (GD2$^+$), Raji (GD2$^-$) and PHA blasts pulsed with pp65 or with irrelevant peptide (irr. pept) were used as target cells. Data summarize mean ± SD of 4 independent experiments.* ***Panel D.*** *shows the IFNγ Elispot analysis of CAR-GD2 redirected CMV specific CTL stimulated with different aAPCs in co-culture with GD2$^+$ Tumor (CHLA 255) and GD2$^-$ tumor cells (Raji) at ratio 1:1 effetor:target. Data summarize mean ± SD of 3 independent experiments.*

We will continue this project to demonstrate that this approach can be used to boost CAR-redirected CTLs *in vivo* in a xenograft model of neuroblastoma and whether the addition of IL-7Ra may further enhance the effects of this vaccine *in vivo*.

Task 3: To co-express CAR-GD2 and HPSE in EBV-CTLs and determine the consequent modulation of NB tissue infiltration and killing (time frame 1-48).

We first demonstrated that HPSE is defective in *ex vivo* expanded T cells, but it can be restored by retroviral gene transfer and this improves T-cell invasive capacity. Briefly, we first assessed whether *ex vivo* expanded T cells were defective in their capacity to degrade ECM. Using a Matrigel^{TM}-based cell invasion assay, we compared freshly isolated resting T cells (FI-T) (comprising naive, effector-memory and central-memory T cells), briefly activated T cells (BA-T) exposed for 24 hours to OKT3/CD28 cross-linking antibodies (Abs), long term *ex vivo* expanded T cells (LTE-T) activated and cultured *ex vivo* for 12-14 days and consisting of central-memory and effector-memory T cells, and freshly isolated monocytes. Monocytes isolated from 5 different healthy donors showed the highest capacity to degrade ECM (63% ± 23%) (**Fig 13A**). Consistent with previously reported data in rodents[12], BA-T showed enhanced invasion of ECM as compared to FI-T (34% ±

8% versus 23% ± 8%, respectively; p= 0.05). Conversely, LTE-T had a significantly reduced ability to degrade ECM (8% ± 6%) as compared to both BA-T (p= 0.01) and FI-T (p= 0.022) (**Fig 13A**). Next to dissect the mechanism(s) responsible for this observation we evaluated the expression and function of HPSE in each cell population. In accordance with the cell invasion assay, monocytes and both $CD4^+$ and $CD8^+$ cells from FI-T and BA-T retained the expression of the active form of HPSE (50KDa) as assessed by western blotting while LTE-T lost expression of the enzyme by day 2 of culture, then remaining consistently negative during the culture period (**Fig 13B**). Furthermore, HPSE was not re-expressed even when LTE-T were rested and then reactivated using OKT3/CD28 Abs on day 14 of culture. The lack of HPSE expression by LTE-T was confirmed by immunofluorescence studies (**Fig 13C**). The 65kDa precursor form of HPSE was not consistently detected in all samples analysed. However, in selected samples where the latent and active forms of HPSE could be simultaneously detected, we found a clear transition from latent to active form in both central-memory ($CD45RO^+CD62L^+$) and effector-memory ($CD45RO^+CD62L^-$) T-cell subsets isolated from PBMC after stimulation with OKT3/CD28 Abs (data not shown). The absence of the HPSE protein in LTE-T was paralleled by the down-regulation of the specific mRNA, as assessed by quantitative RT-PCR. As shown in **Fig 13D,** HPSE-specific mRNA decreased immediately after activation in both $CD4^+$ and $CD8^+$ T cells compared to $CD14^+$ cells ($p<0.005$ and $p<0.031$, respectively) and remained low over the following 14 days of culture. Re-activation of LTE-T on day 14 of culture with OKT3/CD28 Abs did not restore HPSE mRNA expression in neither subset. The lack of cellular HSPE in LTE-T was also confirmed by the absence of enzymatic activity in the culture supernatant. As shown in **Fig 13E**, HPSE enzymatic activity was detected in supernatants collected within the first 72 hours after activation of FI-T which can be attributed to its accumulation in the culture media. However, HPSE enzymatic activity returned to background levels 72 hours later (from 0.34 ± 0.2 U/ml and 0.45 ± 0.27 U/ml, for $CD4^+$ and $CD8^+$ respectively, to 0.22 ± 0.06 U/ml) (**Fig 13E**).

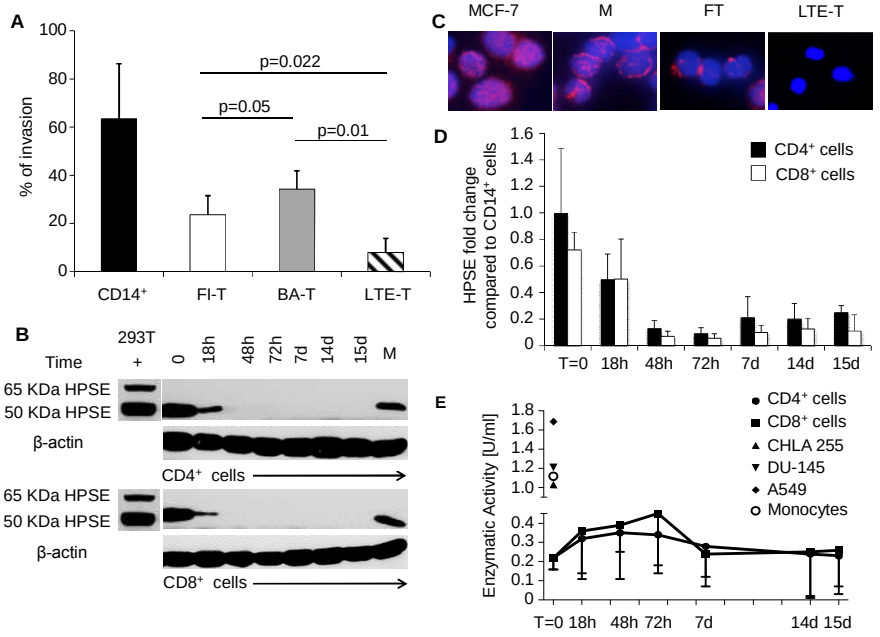

Figure 13. Ex vivo expanded T cells show reduced invasion of ECM due to loss of the HPSE. Panel A. *ECM invasion assay of monocytes ($CD14^+$ cells, black bar), freshly isolated T lymphocytes (FI-T) (white bar), briefly activated T cells (BA-T) (grey bar) and long term ex vivo expanded T cells (LTE-T) (striped bar). Data summarize means ± standard deviation (SD) of 5 independent experiments.* ***Panel B****. Western blotting showing the expression of HPSE in monocytes, FI-T, BA-T and LTE-T $CD4^+$ and $CD8^+$ at different time points. β-actin staining was used to ensure equal loading of the samples. Data are from 4 donors. At day 14 of LTE-T were reactivated using OKT3/CD28 Ab and then analysed on day 15. Wild type or human HPSE transfected 293T cells were used as negative and positive controls, respectively. M = monocytes.* ***Panel C****. Representative immunofluorescence staining for HPSE in MCF-7, monocytes, FI-T and LTE-T. Nuclei are stained with DAPI and shown in blue, while HPSE is stained with red-fluorescent dye (Alexa Fluor 555). Magnification is 20X.* ***Panel D****. Quantitative RT-PCR of HPSE in FI-T, BA-T and LTE-T $CD4^+$ (black bars) and $CD8^+$ (white bars). Fold change in gene expression was calculated with respect to monocytes. Data summarize means ± SD of 4 independent experiments. At day 14 of culture, T cells were reactivated using OKT3/CD28 Ab, and then analysed on day 15.* ***Panel E****. HPSE enzymatic activity was assessed in supernatants collected from FI-T, BA-T and LTE-T $CD4^+$ (circle) and $CD8^+$ (square). At day 4 and 14 of culture, LTE-T were collected, washed and re-suspended in fresh media. On day 14, LTE-T were reactivated using OKT3/CD28 Ab, and analysed on day 15. For the starting time point (T=0) value we used non-activated T cells rested for 48-72 hours in media. The tumor cell lines CHLA-255, A549 and DU-145, known to release HPSE, were used as positive controls to estimate assay sensitivity. Monocyte lysates of $CD14^+$ cells pooled from 4 different donors were also used as a positive control.*

To explore the mechanism(s) that are involved in HPSE down-regulation in LTE-T, we focused our attention on p53 that has been previously described to be downregulated in tumor cells that over-express HPSE[13]. We measured p53 mRNA expression in activated T cells and found that, in contrast with HPSE mRNA, p53 mRNA

increases in both $CD4^+$ and $CD8^+$ T cells upon activation (**Fig 14A**). This effect was associated with upregulation of the corresponding p53 protein subunits (**Fig 14B**). In order to demonstrate a direct link between p53 upregulation and HPSE downregulation, we evaluated whether p53 binds to the HPSE promoter. Chromatin immunoprecipitation (ChIP) showed that p53 binds indeed to the HPSE promoter in LTE-T (**Fig 14C**). To further demonstrate that this event is not simply observed in T cells cultured *ex vivo* but it physiologically occurs during the transition from naïve ($CD45RA^+$) to antigen-experienced T cells ($CD45RO^+$), we repeated the ChIP in freshly isolated $CD45RA^+$ T cells before and after TCR cross linking. As shown in **Fig 14D**, $CD45RA^+$ cells only show the p53 binding to HPSE promoter 72 hours after TCR cross linking that dictates their transition from naïve to antigen-experienced T cells.

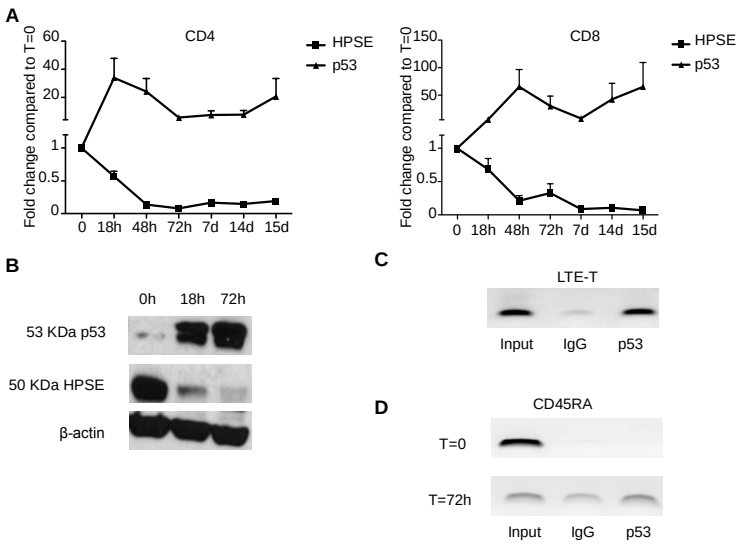

Figure 14. p53 down regulates HPSE gene expression by binding to HPSE promoter. Panel A. *Quantitative RT-PCR of HPSE and p53 in FI-T, BA-T and LTE-T $CD4^+$ (left) and $CD8^+$ (right). Fold change in gene expression was calculated respect to FI-T (T=0). Data summarize means ± SD of 3 independent experiments. At day 14 of culture, T cells were reactivated using OKT3/CD28 Ab, and then analysed on day 15.* ***Panel B.*** *Western blotting showing the expression of HPSE and p53 in FI-T, BA-T and LTE-T $CD3^+$. β-actin staining was used to ensure equal loading of the samples.* ***Panel C and D.*** *ChIP analysis was performed in LTE-T and $CD45RA^+$ cells before and after TCR cross linking to demonstrate that p53 binds to HPSE promoter.*

Having found that LTE-T down-regulate the expression of HPSE, thereby loosing their capability to degrade ECM, we hypothesized that HPSE re-expression in LTE-T through retroviral gene transfer would restore their invasion capability. As illustrated in **Fig 15A**, LTE-T from 9 different healthy donors were successfully transduced with a retroviral vector encoding both HPSE and eGFP. Subsequent flow cytometry analyses showed that 51% ± 18% of the $CD3^+$ cells stably expressing GFP also expressed HPSE as assessed by Western blotting (**Fig 15B**). As demonstrated in functional assays, HPSE(I)eGFP$^+$ LTE-T better degrade ECM (48% ± 19%) than control LTE-T (29% ± 18%; p= 0.025) (**Fig 15C**). This difference was further strengthened when transduced T cells were enriched for HPSE expression based upon GFP positivity (>90%) and before being tested by the Matrigel^{TM} cell invasion assay (69% ± 19%, p< 0.001). The addition of the HPSE-inhibitor, Heparin H1 confirmed that the restored invasion properties of HPSE(I)eGFP$^+$ LTE-T were HPSE-specific, as the invasion of GFP-sorted LTE-T was significantly reduced from 74% ± 14% to 29% ± 9% (p< 0.01) (**Fig 15D**).

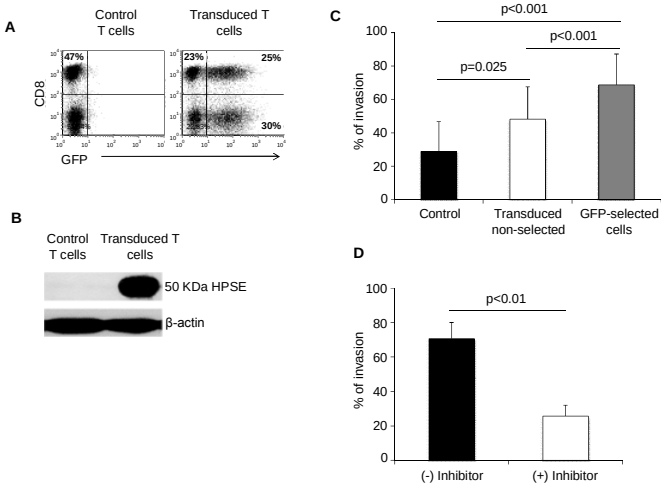

Figure 15. Activated T cells modified to express HPSE reacquire the capacity to degrade ECM. *After activation with OKT2/CD28 Abs, T cells were transduced with a retroviral vector encoding HPSE and eGFP (SFG.HPSE(I)eGFP).* ***Panel A.*** *Dot plots illustrate the GFP expression of both $CD4^+$ and $CD8^+$ T cells at day 12 of culture in one of 9 representative donors.* ***Panel B.*** *Western blotting analysis showing the expression of HPSE in control and transduced T cells at day 12 of culture, in one representative donor. β-actin staining was used to ensure equal loading of the samples.* ***Panel C.*** *ECM invasion assay of control and SFG.HPSE(I)eGFP$^+$ LTE-T, with or without selection for GFP expression. Data summarize mean ± SD of 9 independent experiments.* ***Panel D.*** *ECM invasion assay of HPSE-transduced LTE-T in the presence or in the absence of the inhibitor, heparin H1. Data summarize mean ± SD of 4 independent experiments.*

We have then generated a bicistronic vector that functionally encodes both HPSE and CAR-GD2 that targets neuroblastoma. We found that T cells genetically modified with this novel vector show enhanced invasion.

Briefly, because the expression of HPSE in LTE-T restores their capacity to degrade ECM, we assessed whether this property leading to an improved cell invasion could be coupled with an antitumor specificity. We used neuroblastoma (NB) as a cancer model since we can target this solid tumor with a CAR specific for the NB-associated antigen GD2[14]. LTE-T from 5 healthy donors were transduced with retroviral vectors encoding either the CAR alone or both HPSE and CAR (CAR(I)HPSE). On day 14 of culture, CAR expression was 71% ± 14% and 56% ± 6% when CAR and CAR(I)HPSE vectors were used, respectively (**Fig 16A**). CAR molecules were expressed by both $CD4^+$ and $CD8^+$ T cells (39% ± 19% and 60% ± 18% for CAR^+ T cells; and 38% ± 13% and 61% ± 13% for $CAR(I)HPSE^+$ T cells). HPSE was consistently detected by Western blotting (**Fig 16B**) in T cells transduced with the CAR(I)HPSE vector. Importantly both genes were functional. When tested in a standard ^{51}Cr-release assay, both CAR^+ and $CAR(I)HPSE^+$ LTE-T lysed the $GD2^+$ target LAN-1 (71% ± 22% and 41% ± 16%, respectively, at a 20:1 E:T ratio) and CHLA-255 (76% ± 7% and 55% ± 13%, respectively). In contrast, CAR^+ and $CAR(I)HPSE^+$ LTE-T showed negligible activity against the $GD2^-$ target Raji (8% ± 3% and 2% ± 2%, respectively) (**Fig 16C**). As expected, control LTE-T lysed none of these targets. The antitumor activity of CAR-modified T cells was associated with a preserved Th1 cytokine profile as these cells retained release of IFNγ (927 ± 328 and 527 ± 320 pg/ml/10^6 cells for CAR^+ and $CAR(I)HPSE^+$ LTE-T, respectively) and IL-2 (83 ± 6 and 61 ± 27 pg/ml/10^6 cells CAR^+ and $CAR(I)HPSE^+$ LTE-T, respectively) in response to the antigen (**Fig 16D**). In sharp contrast to their comparable cytotoxic function, only $CAR(I)HPSE^+$ LTE-T degraded ECM significantly well (66% ± 1%) as compared to CAR^+ LTE-T or control LTE-T (13% ± 9% and 16% ± 10%, respectively) (p= 0.004 and p< 0.001).

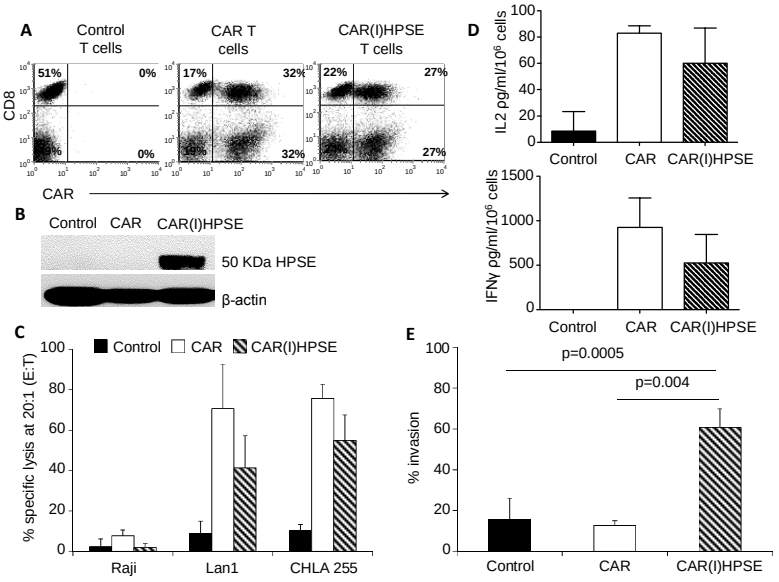

Figure 16. HPSE and GD2-specific CAR co-expressed by T lymphocytes retain anti-GD2 specificity and have enhanced capacity to degrade ECM. *Activated T cells were transduced with retroviral vectors encoding either the GD2-specific CAR alone (SGF.CAR) or both the GD2-specific CAR and HPSE (SFG.CAR(I)HPSE).* ***Panel A.*** *Flow cytometry analysis to detect CAR expression by control T cells and T cells transduced with either CAR or CAR(I)HPSE vectors. Plots are representative of 5 independent experiments.* ***Panel B*** *illustrates the expression of HPSE by western blotting in control and LTE-T transduced with CAR or CAR(I)HPSE vectors. β-actin staining is shown to demonstrate equal loading of samples. Data representative of 5 donors.* ***Panel C.*** *Cytotoxic activity of control (black bars), CAR^+ (white bars) and CAR^+HPSE^+ (striped bars) LTE-T assessed by ^{51}Cr-release assay at a 20:1 effector:target ratio. LAN-1 and CHLA-255 ($GD2^+$), and Raji ($GD2^-$) were used as target cells. Data summarize mean ± SD of 4 independent experiments.* ***Panel D.*** *LTE-T transduced with either CAR or CAR(I)HPSE vectors release both IL-2 and IFNγ in response to $GD2^+$ tumor cells. Data summarize mean ± SD of 4 independent experiments.* ***Panel E.*** *Invasion of ECM by control, CAR^+ and CAR^+HPSE^+ LTE-T. Data summarize mean ± SD of 5 independent experiments.*

To dissect whether the expression of HPSE provided a selective advantage to CAR^+ T cells, we used a more complex antitumor system *ex vivo* and we studied anti-NB activity in the presence of ECM for T cells to degrade in order to reach their tumor targets. Accordingly, we plated LTE-T and tumor cells in a Matrigel invasion assay and measured the capacity of T cells to degrade ECM and then eliminate CHLA-255 or LAN-1 tumor cells expressing GFP (for flow cytometry quantification). As illustrated in **Fig 17A,B**, after 3 days of culture, both CAR^+ and $CAR(I)HPSE^+$ LTE-T eliminated LAN-1 and CHLA-255 tumor cells equally well in the absence of ECM (less than <3% residual GFP^+ cells), as compared to control LTE-T (31% ± 6% and 42% ± 10% residual GFP^+ cells, respectively). By contrast, in the presence of ECM, $CAR(I)HPSE^+$ LTE-T eliminated all but 16% ± 8% and 19% ± 1% of LAN-1 and CHLA-255 cells, respectively compared to residual 37% ± 12% and 52% ± 9% in the presence of CAR^+ LTE-T (p= 0.001). Control LTE-T did not show antitumor activity in any condition (residual LAN-1 and CHAL-255 45% ± 9% and 68% ± 3%, respectively), as expected.

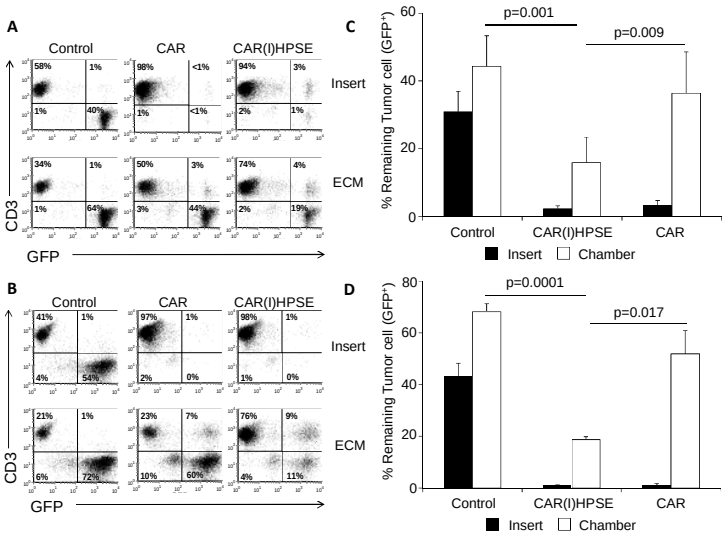

Figure 17. T cells co-expressing HPSE and GD2-CAR have enhanced antitumor activity in the presence of ECM. *Control and LTE-T transduced with retroviral vectors encoding either CAR or CAR(I)HPSE were plated in the upper part of ECM assay and evaluated for their capacity to eliminate LAN-1/GFP$^+$ or CHLA-225/GFP$^+$ cells plated in the lower chamber of the invasion assay. After 24 hours, inserts and chambers were removed, and at day 3 of culture, invading cells were collected and stained with anti-CD3 antibody to identify T cells; GFP-expression by the tumor cells allowed these to be assessed by flow cytometry after treatment/invasion to measure antitumor activity. The same assay containing only the insert (black bars) was used to evaluate the antitumor effects of transduced T cells in the absence of ECM.* ***Panel A*** *and* ***B*** *illustrate representative dot plots of the flow cytometry analysis for culture in the presence of LAN-1 and CHLA-225, respectively.* ***Panel C*** *and* ***D*** *summarize mean ± SE of 5 independent experiments.*

We finally have demonstrated that coexpression of HPSE and CAR-GD2 in T cells promotes better anti-tumor activity in two xenograft models of neuroblastoma. These results have been summarized in manuscript # 4 (Caruana et al, submitted for publication). Briefly, to validate our findings *in vivo*, we established two xenograft models of NB by implanting NOG/SCID/$\gamma_c^{-/-}$ mice intraperitoneally (i.p.) with either CHLA-255 or LAN-1 in the presence of Matrigel^{TM} to allow the formation of complex and structured tumors. We utilized the i.p. route to minimize confounding variables related to tumor homing, a known issue in NB tumor models[15]. After 10 days, mice received i.p. either control LTE-T, CAR$^+$ or CAR(I)HPSE$^+$ LTE-T. As shown in **Fig 18A**, mice implanted with CHLA-255 and treated with CAR(I)HPSE$^+$ LTE-T had a significantly improved survival by day 40 as compared to mice treated with control LTE-T ($p< 0.001$) or CAR$^+$ LTE-T ($p< 0.007$). Furthermore, when surviving mice at day 40 from each treatment group were euthanized, and assessed for the presence of macroscopic tumors, we found that only 2 of 7 (29%) mice alive and infused with CAR$^+$ LTE-T were tumor free. Conversely, 8 of 17 (47%) mice alive and infused with CAR(I)HPSE$^+$ LTE-T had no evidence of tumor. In another set of experiments, mice were euthanized on day 12-14 after T-cell infusion to measure T-cell infiltration at the tumor site. The tumors of mice infused with CAR(I)HPSE$^+$ LTE-T had greater infiltration of T cells (4.6% ± 2.4%), compared to tumors collected from mice treated with control (0.6% ± 0.5; p=0.029) or CAR$^+$ LTE-T (0.1% ± 0.1; p=0.043) (**Fig 18B**). Similar results were obtained in mice engrafted with the NB LAN-1 cell line (**Fig 18C**).

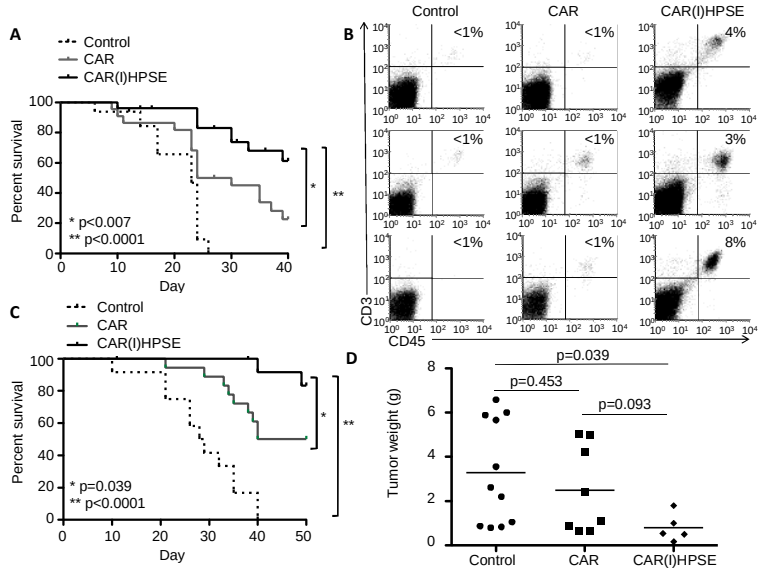

Figure 18. CAR-GD2$^+$HPSE$^+$ LTE-T cells show enhanced tumor infiltration in vivo and improved overall survival in two xenogenic mouse model. ***Panel A.*** *Kaplan-Meier analysis of mice engrafted with the tumor cell line CHLA-255 and treated with control (dotted line), CAR$^+$ (grey line) and CAR(I)HPSE$^+$ LTE-T (black line). Data summarize the results of 64 mice (16 infused with control T cells, 22 with CAR$^+$ and 26 with CAR(I)HPSE$^+$ LTE-L).* ***Panel B****. Flow cytometry analysis of CD3$^+$ cells detected within the tumor samples. Dot plots are representative of 3 mice per group.* ***Panel C.*** *Kaplan-Meier analysis of mice engrafted with the tumor cell line LAN-1 and treated with control (dotted line), CAR$^+$ (grey line) and CAR(I)HPSE$^+$ LTE-T (black line). Data summarize the results of 44 mice (12 infused with control T cells, 18 with CAR$^+$ and 14 with CAR(I)HPSE$^+$ LTE-L).* ***Panel D****. Weight of the tumors collected from mice euthanized.*

Mice infused with CAR(I)HPSE$^+$ LTE-T had a significantly improved survival as compared to mice treated with control LTE-T ($p<0.0001$) or CAR$^+$ LTE-T ($p<0.039$) at day 50. Tumors collected from euthanized mice also showed a reduction in weight when mice were infused with CAR(I)HPSE$^+$ LTE-T as compared to control (0.8 g ± 0.6 g vs. 3.3 g ± 2.4 g) ($p=0.039$), and a trend when compared to mice infused with CAR$^+$ LTE-T (0.8 g ± 0.6 g vs. 2.5 g ± 2 g) ($p=0.093$) (**Fig 18D**).

Since NB cell lines require Matrigel^{TM} to engraft when infused i.p. to form complex and structured tumors, we also validated the relevance of our proposed approach in promoting T-cell infiltration of the tumor by intrarenally implanting CHLA-255 cells labeled with Firefly luciferase in NOG/SCID/$\gamma_c^{-/-}$ mice, since this orthotopic approach develops solid tumors without the use of Matrigel[16]. Tumor sections from mice infused with CAR(I)HPSE$^+$ LTE-T showed enhanced infiltration of T cells within the tumor compared with CAR$^+$ LTE-T (173 ± 32 and 357 ± 72 CD3$^+$ for CAR$^+$ and CAR(I)HPSE$^+$ LTE-T, respectively; $p=0.028$) (**Fig 19A,B,C**). The long-term observation of the infused mice also showed improved survival of mice infused with CAR(I)HPSE$^+$ LTE-T by day 50 ($p<0.005$) (**Fig 19D**).

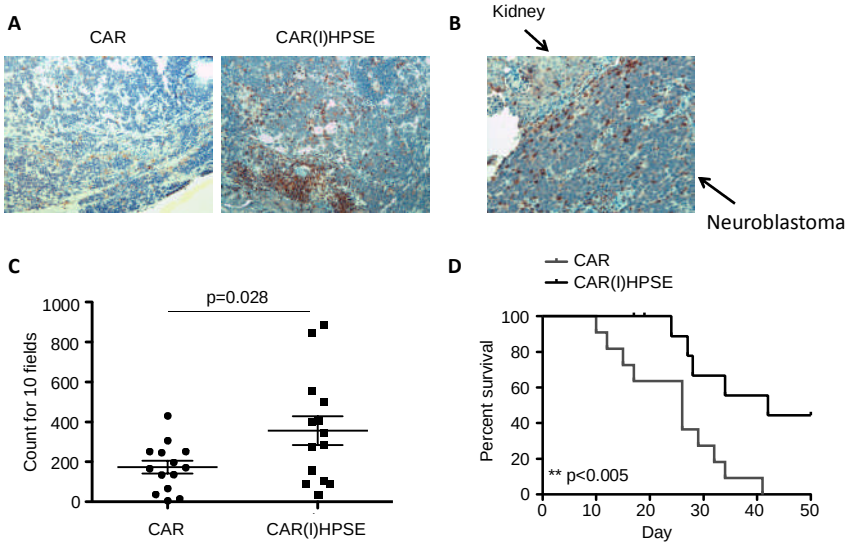

Figure 19. Enhanced tumor infiltration by CAR-GD2$^+$HPSE$^+$ LTE-T cells in orthotopic xenogenic mouse model. Panel A. *Immunohistochemistry staining of tumors implanted in the kidney illustrates enhanced tumor infiltration of CD3$^+$ cells in mice infused with CAR-GD2$^+$HPSE$^+$ LTE-T cells as compared to mice infused with CAR-GD2$^+$ LTE-T. 10X magnification.* ***Panel B.*** *shows 20X magnification of CAR-GD2$^+$HPSE$^+$ treated mouse.* ***Panel C.*** *Infiltration was measured as count of human CD3$^+$ cells in 10 random fields per section.* ***Panel D.*** *Kaplan-Meier analysis of mice engrafted within the kidney with the CHLA255 cell line and then infused either with CAR$^+$ (grey line) and CAR(I)HPSE$^+$ LTE-T (black line). Data summarize the results of 22 mice (11 infused with CAR$^+$ and 11 with CAR(I)HPSE$^+$ LTE-L).*

Our data show for the first time that the *ex vivo* culture required to generate tumor-specific T cells for treatment of cancer patients impairs their physiologic production of HPSE, a key enzyme for the degradation of the HSPGs present in ECM and cell surface. Lack of HPSE limits tumor-directed T-cell invasion through the stroma impeding efficient access to the cancer cells. While expression of HPSE by gene transfer restores the capacity of CAR-redirected T cells to degrade HPSGs of the tumor stroma enhancing their antitumor effects in a neuroblastoma model. This manuscript is almost ready for submission (Caruana et all).

KEY RESEARCH ACCOMPLISHMENTS

- We optimized the methodology to expand *ex vivo* fully functional regulatory T cells (Tregs) (as assessed in a model of graft versus host disease (GvHD)) that can be used for the experiments *in vitro* and *in vivo* proposed in this task of the proposal. The results of these experiments have been published in manuscript #1 listed in the Reportable Outcome section (Chakraborty R et al. Haematologica. 2013 Apr;98(4):533-7).
- We formally demonstrated that our proposed hypothesis that the genetic manipulation of EBV-CTLs to express CAR-GD2 and IL-7Rα renders these cells resistant to the inhibitory effects of Tregs *in vitro* and *in vivo* in a xenograft neuroblastoma model is correct. The results of these experiments have been summarized in manuscript #2 listed in the Reportable Outcome section (Perna et. Clinical Cancer Research in press).
- We have generated artificial antigen presenting cells (aAPCs) that express pp65, CD40L and OX40L efficiently boost *in vitro* virus specific CTLs.
- We have demonstrated that these engineered aAPCs boost *in vivo* virus specific CTLs in a xenograft model.

- We have demonstrated that engineered aAPCs boost *in vitro* virus specific CTL redirected with a CAR that targets the GD2 antigen expressed by neuroblasts.
- We have demonstrated that HPSE is defective in *ex vivo* expanded T cells, but it can be restored by retroviral gene transfer and this improves T-cell invasive capacity.
- We found that HPSE down regulation in activated T cells is mediated by p53.
- We have generated a bicistronic vectors that functionally encodes both HPSE and CAR-GD2 that targets neuroblastoma. We found that T cells genetically modified with this novel vector show enhanced invasion of the cellular matrix.
- We demonstrated that T cells coexpressing HPSE and CAR-GD2 promote better anti-tumor activity in two xenograft models of neuroblastoma. These results have been summarized in manuscript # 4 (Caruana et al, manuscript in preparation).

REPORTABLE OUTCOMES

1 Chakraborty R, Mahendravada A, Perna SK, Rooney CM, Heslop HE, Vera JF, Savoldo B, Dotti G. Robust and cost effective expansion of human regulatory T cells highly functional in a xenograft model of graft versus host disease. Haematologica. 2013 Apr;98(4):533-7.

2 Perna S, Pagliara D, Mahendravada A, Liu H, Brenner M, Savoldo B and Dotti G.Interleukin-7 mediates selective expansion of tumor-redirected cytotoxic T lymphocytes without enhancement of regulatory T-cell inhibition. Clinical Cancer Research in press.

3 Arber C, Abhyankar H, Heslop H, Brenner MK, **Dotti G**, Savoldo B. The immunogenicity of virus-derived 2A sequences in immunocompetent individuals. Gene Therapy2013 Sep;20(9):958-62.

4 Caruana I, Savoldo B, Hoyos V, Weber G, Marchetti D and Dotti G. Restoring deficient expression of heparanase in tumor-specific T lymphocytes enhances their anti-tumor effects. Manuscript in prparation.

CONCLUSIONS

From Task 1 we have demonstrated that our proposed approach to modulate the IL-7/IL-7Rα receptor axis in EBV-CTLs redirected with a CAR that targets the GD2 antigen expressed by neuroblastoma promotes the expansion of these cells in response to IL-7 without favoring the expansion of Tregs. This is highly relevant since this strategy will support better expansion of these cells in patients with neuroblastoma without promoting Tregs that are particularly abundant in these patients and significantly contribute in blocking immune responses.

From Task 2 we have generated artificial antigen presenting cells aAPCs that can boost virus-specific CTLs expressing a CAR GD2 specific. We will continue to validate these aAPCs in a xenograft model of neuroblastoma. If the experiments are successful, this represents another relevant strategy that can be added to the one described in Task 1 to promote the survival on CAR-redirected CTLs in patients with neuroblastoma.

From task 3 we have discovered a major deficiency of T cells used for adoptive immunotherapy. These cells lack the expression of a key enzyme – HPSE – that drives their infiltration of the stroma of solid tumors. We also demonstrate that this defect can be repaired enhancing the capacity of these cells to eliminate neuroblastoma cells in a relevant xenogenic mouse model. This approach may also play a crucial role in improving the clinical efficacy of CAR-redirected CTLs.

Reference List

1. Pule MA, Savoldo B, Myers GD et al. Virus-specific T cells engineered to coexpress tumor-specific receptors: persistence and antitumor activity in individuals with neuroblastoma. Nat.Med. 2008;14:1264-1270.

2. Pule MA, Savoldo B, Myers GD et al. Virus-specific T cells engineered to coexpress tumor-specific receptors: persistence and antitumor activity in individuals with neuroblastoma. Nat.Med. 2008;14:1264-1270.

3. Louis CU, Savoldo B, Dotti G et al. Antitumor activity and long-term fate of chimeric antigen receptor-positive T cells in patients with neuroblastoma. Blood 2011;118:6050-6056.

4. Vera J, Savoldo B, Vigouroux S et al. T lymphocytes redirected against the kappa light chain of human immunoglobulin efficiently kill mature B lymphocyte-derived malignant cells. Blood 2006;108:3890-3897.

5. Buentke E, Mathiot A, Tolaini M et al. Do CD8 effector cells need IL-7R expression to become resting memory cells? Blood 2006;108:1949-1956.

6. Parish CR. The role of heparan sulphate in inflammation. Nat.Rev.Immunol. 2006;6:633-643.

7. Parish CR. The role of heparan sulphate in inflammation. Nat.Rev.Immunol. 2006;6:633-643.

8. Edovitsky E, Elkin M, Zcharia E, Peretz T, Vlodavsky I. Heparanase gene silencing, tumor invasiveness, angiogenesis, and metastasis. J.Natl.Cancer Inst. 2004;96:1219-1230.

9. Parish CR. The role of heparan sulphate in inflammation. Nat.Rev.Immunol. 2006;6:633-643.

10. de Mestre AM, Staykova MA, Hornby JR, Willenborg DO, Hulett MD. Expression of the heparan sulfate-degrading enzyme heparanase is induced in infiltrating CD4+ T cells in experimental autoimmune encephalomyelitis and regulated at the level of transcription by early growth response gene 1. J.Leukoc.Biol. 2007;82:1289-1300.

11. de Mestre AM, Soe-Htwe T, Sutcliffe EL et al. Regulation of mouse Heparanase gene expression in T lymphocytes and tumor cells. Immunol.Cell Biol. 2007;85:205-214.

12. de Mestre AM, Staykova MA, Hornby JR, Willenborg DO, Hulett MD. Expression of the heparan sulfate-degrading enzyme heparanase is induced in infiltrating CD4+ T cells in experimental autoimmune encephalomyelitis and regulated at the level of transcription by early growth response gene 1. J.Leukoc.Biol. 2007;82:1289-1300.

13. Baraz L, Haupt Y, Elkin M, Peretz T, Vlodavsky I. Tumor suppressor p53 regulates heparanase gene expression. Oncogene 2006;25:3939-3947.

14. Pule MA, Straathof KC, Dotti G et al. A chimeric T cell antigen receptor that augments cytokine release and supports clonal expansion of primary human T cells. Mol.Ther. 2005;12:933-941.

15. Craddock JA, Lu A, Bear A et al. Enhanced tumor trafficking of GD2 chimeric antigen receptor T cells by expression of the chemokine receptor CCR2b. J.Immunother. 2010;33:780-788.

16. Patterson DM, Shohet JM, Kim ES. Preclinical models of pediatric solid tumors (neuroblastoma) and their use in drug discovery. Curr.Protoc.Pharmacol. 2011;Chapter 14:Unit.

Robust and cost effective expansion of human regulatory T cells highly functional in a xenograft model of graft-*versus*-host disease

Rikhia Chakraborty,[1] Aruna Mahendravada,[1] Serena K. Perna,[1] Cliona M. Rooney,[1,2,3] Helen E. Heslop,[1,2,4] Juan F. Vera,[1,4] Barbara Savoldo,[1,2] and Gianpietro Dotti[1,3,4]

[1]Center for Cell and Gene Therapy and Departments of [2]Pediatrics, [3]Immunology, and [4]Medicine, Baylor College of Medicine, Methodist Hospital and Texas Children's Hospital, Houston, USA

ABSTRACT

The low frequency of naturally occurring regulatory T cells (nTregs) in peripheral blood and the suboptimal protocols available for their *ex vivo* expansion limit the development of clinical trials based on the adoptive transfer of these cells. We have, therefore, generated a simplified, robust and cost-effective platform for the large-scale expansion of nTregs using a gas permeable static culture flask (G-Rex) in compliance with Good Manufacturing Practice. More than 10^9 putative Tregs co-expressing CD25 and CD4 molecules (92±5%) and FoxP3 (69±19%) were obtained within 21 days of culture. Expanded Tregs showed potent regulatory activity *in vitro* (80±13% inhibition of $CD8^+$ cell division) and *in vivo* (suppression or delay of graft-*versus*-host disease in a xenograft mouse model) indicating that the cost-effective and simplified production of nTregs we propose will facilitate the implementation of clinical trials based on their adoptive transfer.

Introduction

Regulatory T cells (Tregs) are implicated in controling graft-*versus*-host disease (GvHD) post allogeneic hematopoietic stem cell transplantation (HSCT)[1] prompting the quest for novel therapies based on their adoptive transfer.

Initial studies to prevent or treat GvHD[2,3] were based on the infusion of freshly isolated naturally occurring Tregs (nTregs) circulating in peripheral blood.[4] Even though these studies established the overall safety of Treg-based therapies, they also clearly indicated that the low numbers of Tregs collected from the peripheral blood are inadequate for controlling GvHD.[5] Given these limitations, protocols aimed at effectively selecting and expanding *ex vivo* fully functional nTregs in compliance with Good Manufacturing Practice (GMP) are badly needed.

Here we describe a simplified and cost-effective methodology that consistently and reproducibly expands nTregs that retain potent inhibitory function both *in vitro* and *in vivo*.

Design and Methods

Isolation of nTregs and culture conditions

Buffy coats were obtained from healthy volunteer donors (Gulf Coast Regional Blood Center, Houston, TX, USA) (IRB H-7634). Putative nTregs ($CD4^+CD25^{Bright}$) were enriched from peripheral blood mononuclear cells (PBMC) using positive selection, after labeling cells with a minimal amount of CD25-specific microbeads (2 μL/10^7 cells; Miltenyi Biotec Inc., Auburn, CA, USA).[2,6] Immediately after selection (Day 1), $CD25^{Bright}$ cells (10^6 cells/mL) were resuspended in complete medium, consisting of RPMI1640 (Hyclone, Logan, UT, USA), 10% AB-human serum (Valley Biomedical, Winchester, VA, USA), 2 mM L-glutamine (BioWhittaker Inc., Walkersville, MD, USA), penicillin-streptomycin (BioWhittaker), and β-mercaptoethanol (50 μM) (Invitrogen, Carlsbad, CA, USA) and then activated with anti-CD3 (OKT3, Orthoclone, Cilag Ag Int., Zug, Switzerland) (1 μg/mL) and anti-CD28 monoclonal antibodies (mAb) (1 μg/mL)[6] (BD Biosciences PharMingen, San Diego, CA, USA) in the presence of temsirolimus (LC Laboratories, Woburn, MA, USA) at a final concentration of 100 nM.[7] On Day 7 (S1), cells were harvested, washed, counted and seeded in a G-Rex10[8] (Wilson Wolf Manufacturing, Saint Paul, MN, USA) (*http://www.wilsonwolf.com/*) and supplemented with soluble OKT3 (1 μg/mL), CD28 mAb (1 μg/mL), rIL-2 (50 IU/mL)[6] (Proleukin; Chiron, Emeryville, CA, USA), temsirolimus (100 nM) and irradiated (40 Gy) allogeneic feeders obtained from at least two pooled CMV-seronegative donors meeting testing requirements for whole blood donation (1:5 Treg:feeders ratio). On Day 14 (S2), cells were seeded in the G-Rex100[8] and supplemented with the same reagents used in S1. On Day 21 (S3), cells were harvested, counted and used for functional experiments. CD25 depleted cells ($CD25^{Dep}$) expanded in parallel without temsirolimus were used as control cells. To further validate our approach for clinical use, putative nTregs were isolated using the CliniMACS device. Briefly, PBMC were labeled with clinical grade CD25-specific microbeads (18 μL buffer and 2 μL of beads for 1 x 10^7 cells). After incubation and washes, cell selection was then started according to E-cell System software version 3.2. At the end of the selection, cells were expanded as described for small-scale experiments. On Days 14 (S2) and 21 (S3), aliquots of expanded Tregs were cryopreserved in dimethyl sulfoxide (DMSO) according to standard procedure and stored in liquid nitrogen.

Results and Discussion

Naturally occurring Tregs undergo robust ex vivo expansion in the G-Rex device

The methodology to isolate and expand nTregs is graphically summarized in the *Online Supplementary Figure S1*. To reduce the complexity of the process of selection from the peripheral blood, we isolated putative nTregs exclusively based on their bright expression of the CD25 molecule

 doi:10.3324/haematol.2012.076430
The online version of this article has a Supplementary Appendix.
Manuscript received on August 24, 2012. Manuscript accepted on November 13, 2012.
Correspondence: gdotti@bcm.edu

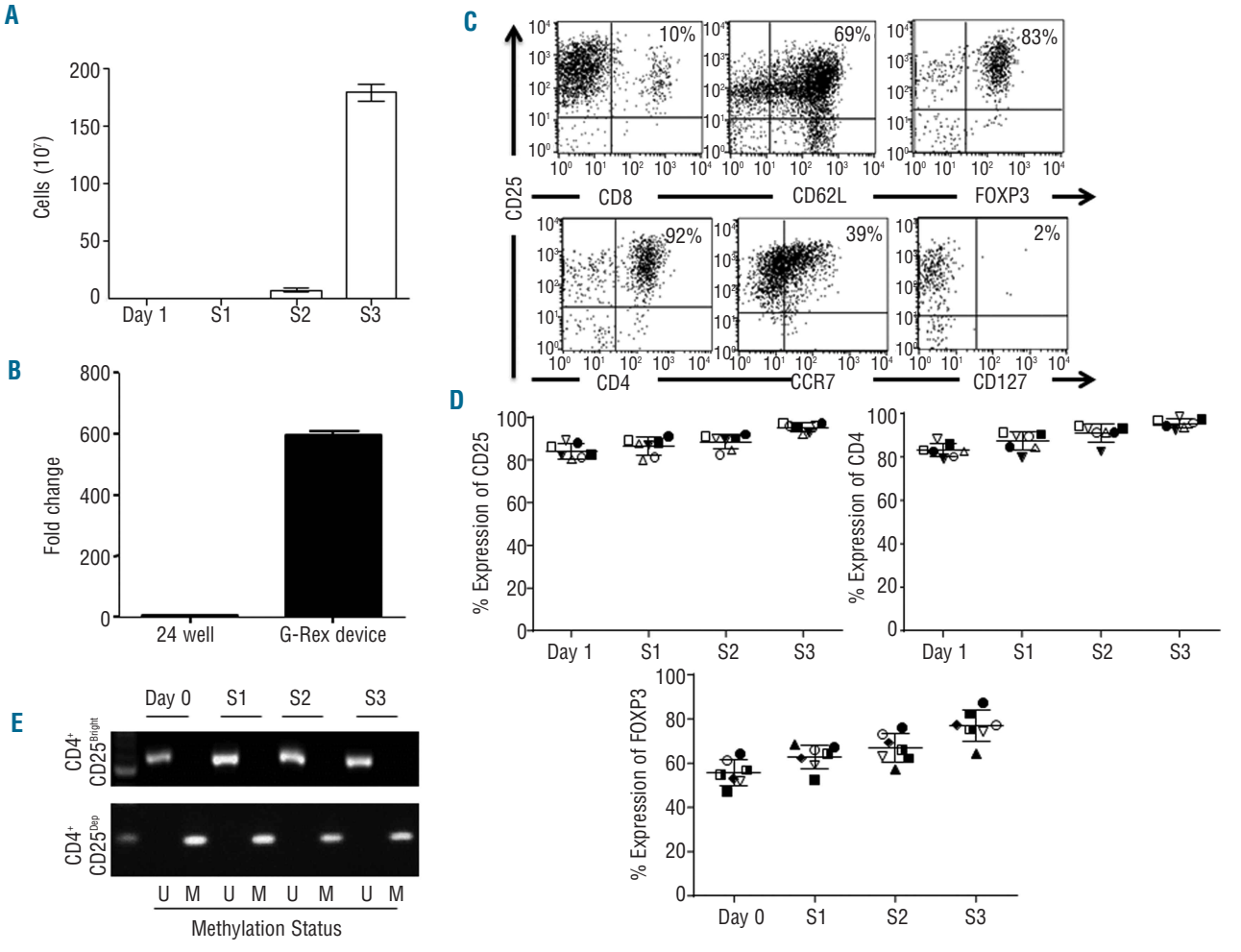

Figure 1. Robust *ex vivo* expansion of nTregs in the G-Rex device. (A) illustrates the number of nTregs obtained after 1, 2 or 3 (S1, S2 and S3) weeks of culture in the G-Rex device. Data illustrate average and standard deviations (SD) for 7 independent experiments. (B) Compares the fold expansions of nTregs cultured in 24-well plates or in the G-Rex device. Data show mean ± SD of 7 independent experiments. (C) Shows the flow cytometry plots of expanded nTregs on Day 21 (S3). The panels illustrate CD4, CD25, CCR7, CD127 and FoxP3 expression for one representative donor. (D) Illustrates the expression of CD25, CD4 and FoxP3 in expanded nTregs after each round of stimulation (S1, S2 and S3). Data summarize the results of 7 independent experiments. (E) Shows the methylation-specific semi-quantitative PCR of the *FoxP3* promoter in nTregs and control $CD25^{Dep}$ cells obtained after each round of stimulation (S1, S2 and S3).

($CD25^{Bright}$ cells) without additional selection steps. Starting from $4.5x10^8 \pm 1x10^8$ PBMC (obtained from 50 mL of buffy coat products), we recovered $3x10^6 \pm 1x10^6$ cells. Upon selection, these cells consistently co-expressed CD4 and CD25 molecules (95%±5%), with limited contamination by $CD8^+$ cells. On Day 7 (S1) and Day 14 (S2), $2.9x10^6 \pm 0.5x10^5$ and $7.7x10^7 \pm 1.7x10^7$ cells were obtained, respectively. After the third stimulation (Day 21, S3), we recovered $1.8x10^9 \pm 7.6x10^7$ cells, corresponding to an over 600-fold expansion (Figure 1A). This degree of expansion was significantly higher than that obtained in parallel experiments (5-6 fold) in which isolated nTregs were grown using the same protocol but plated in conventional 24-well tissue culture plates (cells at Day 21 were $5.3x10^6 \pm 1.6x10^6$ starting from $1x10^6$) (Figure 1B). The percentage of $CD4^+CD25^+$ cells remained stable over three weeks of culture and was 92±5% by Day 21, with 69±19% of the cells expressing FoxP3 (Figure 1C and D). Expanded nTregs retained their expression of the lymph node homing molecules CD62L and CCR7 (69±4% and 39±3%, respectively), and lacked expression of the IL-7Rα (CD127) (2±1.2%), a known feature of Tregs.[9] Of note, the percentage of $FoxP3^+$ cells significantly increased from Day 1 to Day 21 of culture. *FoxP3* promoter remained consistently unmethylated indicating the commitment of the expanded cells to the Treg state, despite some of them lacking FoxP3 protein expression by Day 21 of culture (Figure 1E).[10] In contrast, the *FoxP3* promoter of cultured $CD25^{Dep}$ control cells remained consistently methylated (Figure 1E). The phenotypic analysis of $CD25^{Dep}$ cells after three stimulations (S3) showed that CD4, CD25, FoxP3, CCR5 and CCR7 were expressed by 55±21%, 7±6.5%, 12±11%, 9±7%, and 11±5% of the cells, respectively.

Ex vivo *expanded nTregs maintain robust suppressive activity without undergoing senescence*

Using a CFSE-based suppression assay, we found equal suppression of T-cell divisions by either freshly isolated

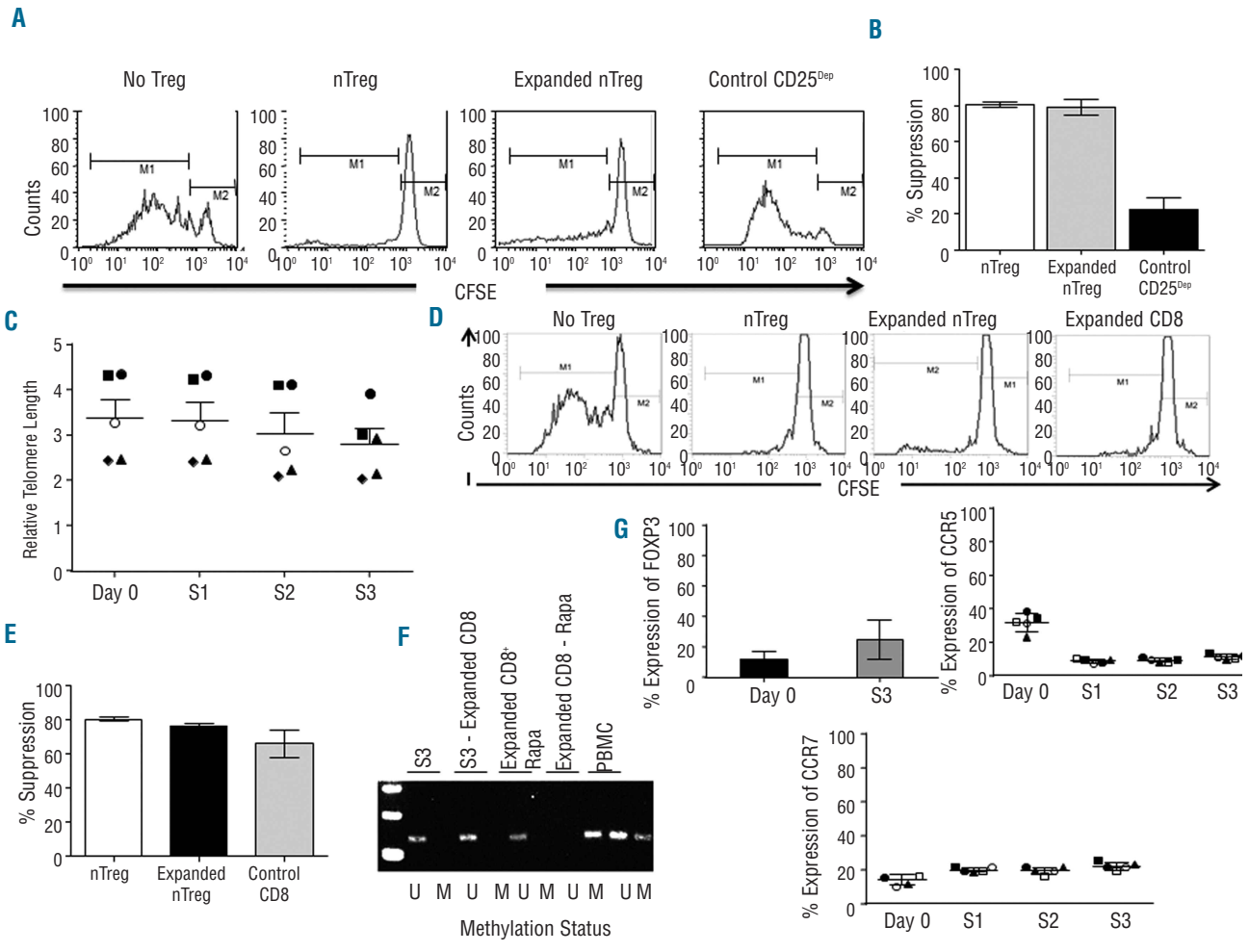

Figure 2. ***Ex vivo*** **expanded nTregs retain robust suppressive function without undergoing cell senescence. (A) The inhibitory activity of freshly isolated nTregs, expanded nTregs (S3), and expanded CD25^{Dep} cells was assessed using a CFSE-based suppression assay. Panels illustrate the inhibitory activity of nTregs for a representative experiment. (B) The graph summarizes average and SD of the inhibitory function of nTregs for 7 independent experiments. (C) The graph illustrates the relative telomerase length (RTL) in freshly isolated nTregs (Day 1) and expanded nTregs at S1, S2 and S3. Data show mean ± SD for 7 independent experiments. (D) Contaminating CD8$^+$ cells at Day 21 of culture were isolated and analyzed for their suppressive activity and compared to nTregs. Panels illustrate the inhibitory activity for one representative experiment. (E) The graph summarizes average and SD of the inhibitory function of contaminating CD8$^+$ cells and nTregs for 7 independent experiments. (F) Methylation-specific semi-quantitative PCR of *FoxP3* promoter in cells obtained at the end of third round of stimulation (S3), nTregs obtained at the end of the third round of stimulation depleted of CD8 (S3-Expanded CD8), the expanded and purified CD8$^+$ cells in S3 (Expanded CD8 + Rapa), CD25^{Dep} population (CD8–Rapamycin), and PBMC. (G) Illustrates the expression of *FoxP3* (after three stimulation, S3), and of CCR7 and CCR5 (after each stimulation, S1, S2, and S3) in the contaminating CD8$^+$ cells. Data summarize the results of 5 independent experiments.**

nTregs or expanded nTregs (S3) (80±10% and 80±13% suppression, respectively) (P<0.0001). No suppression was observed in the presence of expanded control CD25^{Dep} cells (12±9% suppression) (Figure 2A and B). Importantly, the robust expansion of nTregs achieved in the G-Rex device was obtained without significantly compromising their telomere length. In freshly isolated nTregs (Day 1) and expanded nTregs at S1, S2 and S3, relative telomerase length (RTL) was 3.4±0.96%, 3±0.98%, 3±0.99%, 2.8±1.8%, respectively (Figure 2C), suggesting that, in addition to cell divisions, a significant preservation of cell viability contributes to the large number of cells expanded in the G-Rex device. Since by Day 21, expanded nTregs contained contaminating CD8$^+$ cells (10±3.7%), we specifically assessed the functionality of these cells, as the infusion of functional CD8$^+$ cells in the allogeneic HSCT setting may exacerbate GvHD and thus compromise the protective effects of Tregs. As illustrated in Figure 2D and E, T-cell divisions were suppressed equally well when either freshly isolated nTregs, expanded nTregs or selected CD8$^+$ cells were added to the culture (80±8%, 76±8%, and 66±14% suppression, respectively) (P<0.001), suggesting that contaminating CD8$^+$ cells likely acquired inhibitory properties during the *ex vivo* culture conditions. This inhibitory function of expanded CD8$^+$ cells was corroborated by the detection of the unmethylated form of the *FoxP3* promoter in these cells (Figure 2F). Even if we cannot exclude that some of the contaminating CD8$^+$ cells have effector function, experiments in which the suppression assays were performed using different ratios of CD8$^+$ cells and T-effector cells showed that

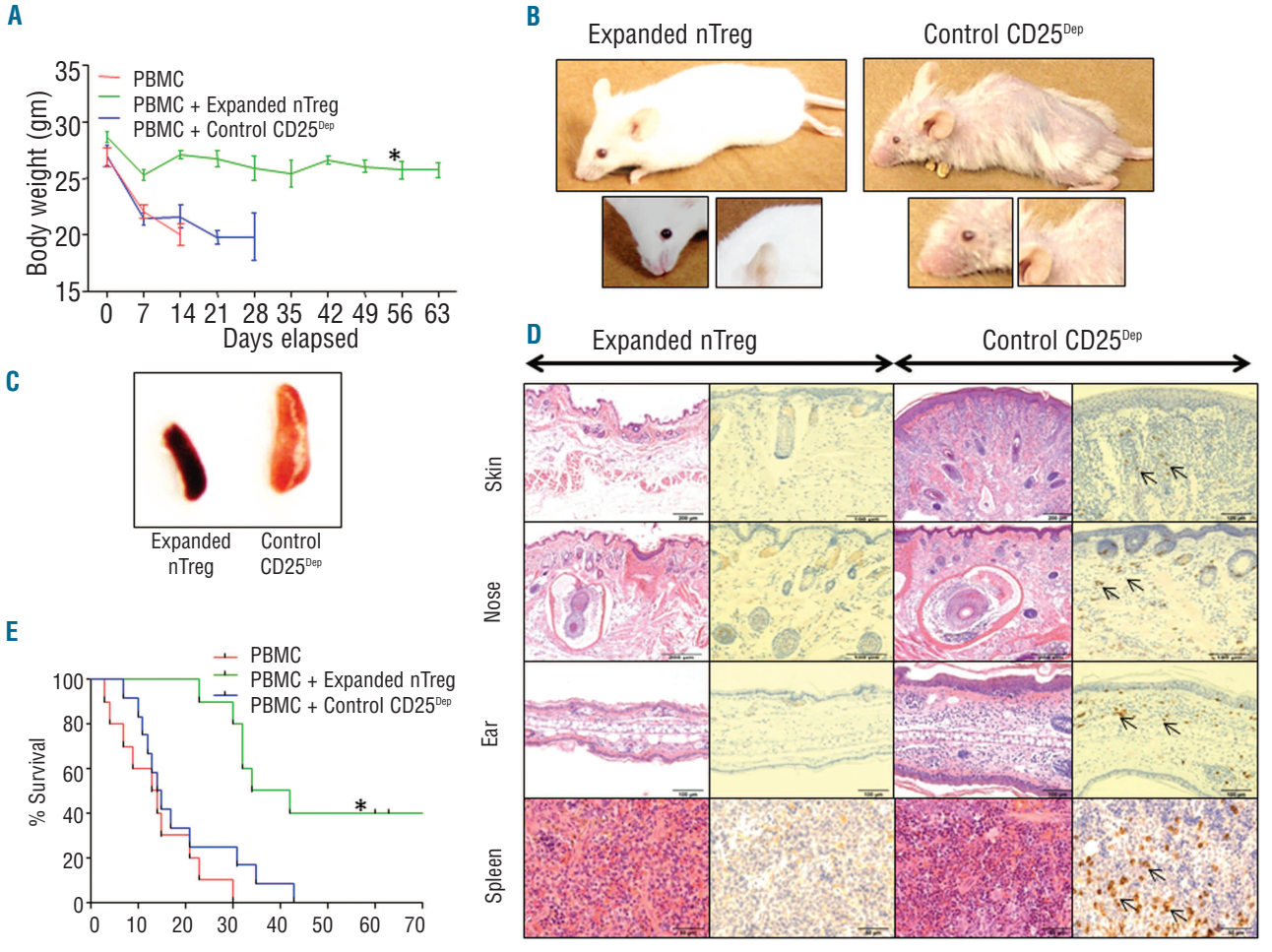

Figure 3. Expanded nTregs control GvHD in a xenogeneic mouse model. Irradiated NSG mice were infused with PBMC either alone or in combination with expanded nTregs (S3) or expanded control CD25^{Dep} cells at 1:1 ratio. (A) The graph illustrates the measurements of the weight of the NSG mice. Data show mean ± SD of 12 animals for each group (*P=0.0001). (B) Images show that control mice developed signs of GvHD, such as hair loss and orbital tightening. (C) Spleen enlargements were observed in mice infused with control CD25^{Dep} cells. (D) Representative H&E and immunohistochemistry staining for CD8^{+} cells in tissue sections obtained from skin, nose, ear, and spleen of treated mice. Control mice showed evidence of chronic dermatitis, with moderate diffuse epithelial hyperplasia, hyperkeratosis and marked multifocal coalescing subcutaneous and dermal mononuclear inflammatory cell infiltrates. Arrows indicate infiltrating CD8^{+} cells. (E) Kaplan-Meier survival curve comparing NSG mice receiving human PBMC alone or in combination with expanded nTregs or expanded control CD25^{Dep} cells (12 animals for each group) (*P=0.0003).

their overall inhibitory function was significantly retained at 1:10 dilution (*Online Supplementary Figure S2*). The phenotypic analysis of these CD8^{+} cells showed that 25±13% of them expressed FoxP3 and 11±1.6% and 22±2.3% expressed CCR5 and CCR7, respectively (Figure 2G).

Expanded nTregs control GvHD in a xenogeneic mouse model

To investigate whether expanded nTregs retained their inhibitory function *in vivo*, we used a xenograft model of lethal GvHD.[11] As illustrated in Figure 3A, the weight loss of control mice receiving PBMC and CD25^{Dep} cells was significantly greater as compared to mice that received PBMC and expanded nTregs (7.2±1.9 g *vs.* 1.9±1 g, respectively) (P=0.0045). In addition, by Day 60, mice receiving expanded nTregs had delayed occurrence or no signs of GvHD (Figure 3B), and showed normal sized spleen as compared to controls (Figure 3C). Finally, mice co-infused with expanded nTregs revealed no histopathological lesions compatible with GvHD in their skin, nose, or ear (Figure 3D), and showed significantly improved overall survival as compared to control mice (P<0.0003) (Figure 3E). As illustrated in the *Online Supplementary Figure S3A*, Tregs co-infused with PBMC did not abrogate the engraftment of PBMC, suggesting that in this model Tregs inhibit the expansion of T cells that cause the occurrence of GvHD. Finally, as previously demonstrated by others,[12] nTregs expanded in the presence of rapamycin did not produce IL-17 (*Online Supplementary Figure S3B*).

nTregs selected and expanded using the CliniMACS and G-Rex devices, respectively, maintain potent in vitro and in vivo suppressive function

To make our methodology GMP compliant, we adapted the selection using the CliniMACS system. CD25^{Bright} cells ($2.3x10^{6}$ ± $0.7x10^{6}$) were positively selected from PBMC ($4.6x10^{8}$ ± $0.7x10^{8}$) of 3 buffy coats, using clinical grade anti-CD25 microbeads and expanded as described in the

small scale experiments, resulting in $1.3x10^9$±$3x10^7$ cells by Day 21 of culture (S3) (*Online Supplementary Figure S4A*) (547-fold expansion). These cells consistently co-expressed CD4, CD25 (97±2%) and FoxP3 (82±4%) (*Online Supplementary Figure S4B* and *C*), while the contaminating $CD8^+$ cells were less than 1.2±1%. The expanded Tregs suppressed T-cell divisions *in vitro* (80±10% and 78±5% suppression for expanded and freshly isolated Tregs, respectively) (*Online Supplementary Figure S4D*), and maintained robust *in vivo* suppressive activity improving the overall survival of mice (P=0.0046) (*Online Supplementary Figure S4E*). Finally, because the infusion of freshly cultured Tregs is frequently impractical for clinical applications and a cryopreservation step is usually required for quality control tests, we evaluated whether expanded nTregs retained their functionality following cryopreservation and storage in liquid nitrogen. Expanded Tregs cryopreserved after Day 14 (FS2) or Day 21 (FS3) retained their suppressive activity both *in vitro* (*Online Supplementary Figure S5A*) and *in vivo* (*Online Supplementary Figure S5B*).

Our proposed strategy has significant advantages compared to other protocols.[13,14] First, we have minimized the cell purification process to a single immune magnetic selection step based on their CD25 expression, which is sufficient to minimize the contamination by $CD8^+CD25^+$ cells in the final Treg products, provided that rapalogs are added to the cultures during the expansion phase. Importantly, we have observed that, in the presence of rapalogs, 'contaminating' $CD8^+CD25^+$ cells persisting at the end of the 21 days of culture show inhibitory properties and methylation of *FoxP3* promoter. This is in accordance with previous observations showing that, in specific culture conditions, $CD8^+$ cells may develop suppressive activity.[10,15] Second, and most importantly, we have optimized a robust and cost-effective expansion protocol of Tregs. Stimulation of Tregs is obtained with anti-CD3/CD28 mAbs, now available as clinical grade reagents (Miltenyi Biotec Inc.), and feeder cells that meet GMP requirements.[16,17] In addition, cells are easily accommodated, with minimal manipulation, in small gas permeable static culture flasks (G-Rex) that promote efficient gas exchange and availability of nutrients to the cells, while diluting waste products.

Remarkably, expanded Tregs had no significant shortening of their telomere lengths, indicating their potential capacity to undergo further divisions *in vivo* after adoptive transfer, and retained inhibitory function after freezing and thawing. These are important manufacturing aspects to be considered in clinical protocols of adoptive T-cell therapy as quality control tests of the produced cells are usually required. Hence, the cost-effective and simplified production of nTregs we propose will likely facilitate the implementation of clinical trials based on the infusion of these cells to control GvHD after allogeneic HSCT and graft rejection in solid organ transplant recipients, and to treat autoimmune diseases.

Acknowledgments

The authors would like to thank Dr. Roger Price for pathological evaluations, Dr. Cecilia Ljungberg for assistance with immunohistochemistry, and Reshma Kulkarni for the phenotypic analyses.

Funding

This work was supported in part by R01 CA142636 National Institutes of Health-NCI, W81XWH-10-10425 Department of Defense, Technology/Therapeutic Development Award and PACT (Production Assistance for Cell Therapy (PACT) NIH-NHLBI N01-HB-10-03.

Authorship and Disclosures

Information on authorship, contributions, and financial and other disclosures was provided by the authors and is available with the online version of this article at www.haematologica.org.

References

1. Zorn E, Kim HT, Lee SJ, et al. Reduced frequency of FOXP3+ CD4+CD25+ regulatory T cells in patients with chronic graft-versus-host disease. Blood. 2005;106(8):2903-11.
2. Wang X, Lu L, Jiang S. Regulatory T cells: customizing for the clinic. Sci Transl Med. 2011;3(83):83ps19.
3. Leslie M. Immunology. Regulatory T cells get their chance to shine. Science. 2011; 332(6033):1020-1.
4. Di Ianni M, Falzetti F, Carotti A, et al. Tregs prevent GVHD and promote immune reconstitution in HLA-haploidentical transplantation. Blood. 2011;117(14):3921-8.
5. Hippen KL, Riley JL, June CH, Blazar BR. Clinical perspectives for regulatory T cells in transplantation tolerance. Semin Immunol. 2011;23(6):462-8.
6. Chakraborty R, Rooney C, Dotti G, Savoldo B. Changes in chemokine receptor expression of regulatory T cells after ex vivo culture. J Immunother. 2012;35(4):329-36.
7. Battaglia M, Stabilini A, Roncarolo MG. Rapamycin selectively expands CD4+ CD25+FoxP3+ regulatory T cells. Blood. 2005;105(12):4743-8.
8. Vera JF, Brenner LJ, Gerdemann U, et al. Accelerated production of antigen-specific T cells for preclinical and clinical applications using gas-permeable rapid expansion cultureware (G-Rex). J Immunother. 2010; 33(3):305-15.
9. Liu W, Putnam AL, Xu-Yu Z, et al. CD127 expression inversely correlates with FoxP3 and suppressive function of human CD4+ T reg cells. J Exp Med. 2006;203(7):1701-11.
10. Miyao T, Floess S, Setoguchi R, et al. Plasticity of Foxp3(+) T cells reflects promiscuous Foxp3 expression in conventional T cells but not reprogramming of regulatory T cells. Immunity. 2012;36(2):262-75.
11. van Rijn RS, Simonetti ER, Hagenbeek A, et al. A new xenograft model for graft-versus-host disease by intravenous transfer of human peripheral blood mononuclear cells in RAG2-/- gammac-/- double-mutant mice. Blood. 2003;102(7):2522-31.
12. Tresoldi E, Dell'Albani I, Stabilini A, et al. Stability of human rapamycin-expanded CD4+CD25+ T regulatory cells. Haematologica. 2011;96(9):1357-65.
13. Baecher-Allan C, Hafler DA. Suppressor T cells in human diseases. J Exp Med. 2004; 200(3):273-6.
14. Hippen KL, Merkel SC, Schirm DK, et al. Massive ex vivo expansion of human natural regulatory T cells (T(regs)) with minimal loss of in vivo functional activity. Sci Transl Med. 2011;3(83):83ra41.
15. Zheng SG, Wang JH, Koss MN, Quismorio F Jr, Gray JD, Horwitz DA. CD4+ and CD8+ regulatory T cells generated ex vivo with IL-2 and TGF-β suppress a stimulatory graft-versus-host disease with a lupus-like syndrome. J Immunol. 2004;172(3): 1531-9.
16. Dudley ME, Wunderlich JR, Shelton TE, Even J, Rosenberg SA. Generation of tumor-infiltrating lymphocyte cultures for use in adoptive transfer therapy for melanoma patients. J Immunother. 2003; 26(4):332-42.
17. Smith CA, Ng CY, Heslop HE, et al. Production of genetically modified Epstein-Barr virus-specific cytotoxic T cells for adoptive transfer to patients at high risk of EBV-associated lymphoproleferative disease. J Hematother. 1995;4(2):73-9.

Cancer Therapy: Preclinical

Clinical Cancer Research

Interleukin-7 Mediates Selective Expansion of Tumor-redirected CTLs without Enhancement of Regulatory T-cell Inhibition

Serena K. Perna[1], Daria Pagliara[1], Aruna Mahendravada[1], Hao Liu[1], Malcolm Brenner[1,2,4], Barbara Savoldo[1,2], and Gianpietro Dotti[1,3,4]

Abstract

Purpose: The antitumor activity of chimeric antigen receptor (CAR)–redirected CTLs should be enhanced if it were possible to increase their proliferation and function after adoptive transfer without concomitantly increasing the proliferation and function of regulatory T cells (Treg). Here, we explored whether the lack of IL-7Rα in Tregs can be exploited by the targeted manipulation of the interleukin-7 (IL-7) cytokine–cytokine receptor axis in CAR-engrafted Epstein–Barr Virus–specific CTLs (EBV-CTLs) to selectively augment their growth and antitumor activity even in the presence of Tregs.

Experimental Design: We generated a bicistronic retroviral vector encoding a GD2-specific CAR and the IL-7Rα subunit, expressed the genes in EBV-CTLs, and assessed their capacity to control tumor growth in the presence of Tregs *in vitro* and *in vivo* when exposed to either interleukin-2 (IL-2) or IL-7 in a neuroblastoma xenograft.

Results: We found that IL-7, in sharp contrast with IL-2, supports the proliferation and antitumor activity of IL-7Rα.CAR-GD2$^+$ EBV-CTLs both *in vitro* and *in vivo* even in the presence of fully functional Tregs.

Conclusions: IL-7 selectively favors the survival, proliferation, and effector function of IL-7Rα-transgenic/CAR-redirected EBV-CTLs in the presence of Tregs both *in vitro* and *in vivo*. Thus, IL-7 can have a significant impact in sustaining expansion and persistence of adoptively CAR-redirected CTLs. *Clin Cancer Res; 1–9. ©2013 AACR.*

Introduction

The expression of chimeric antigen receptors (CAR) in T lymphocytes to redirect their antigen specificity has significantly expanded the clinical application of adoptive T-cell immunotherapies against a variety of human malignancies (1, 2). CAR molecules are chimeric proteins, in which a single chain antibody-binding site is fused with the signaling domain CD3ζ that activates T lymphocytes upon binding to the tumor antigen (3). However, in this form, CAR molecules do not provide adequate costimulation to T cells (1, 4, 5). To overcome this limitation, CARs can be expressed by CTLs whose native receptors are specific for virus latency proteins such as those derived from the Epstein–Barr Virus–specific CTLs (EBV-CTLs; refs. 6, 7). These virus-specific CTLs can receive physiologic costimulation from professional antigen presenting cells processing latent viral antigens and kill tumor cells through their CAR (6, 7). Although this approach can produce complete and sustained antitumor responses, for example in some patients with neuroblastoma, in most recipients, CAR-engrafted EBV-CTLs have limited *in vivo* survival and fail to consistently eradicate disease (8, 9). It is likely that the combination of host/tumor associated inhibitory factors and insufficient *in vivo* immunostimulation limit the expansion and persistence of these cells (10).

Regulatory T cells (Treg) play a significant role in impairing the antitumor effects of tumor-specific CTLs (11). Tregs are frequently increased in the peripheral blood and in tumor biopsies of patients with cancer (12–17) and their presence often correlates with poor clinical outcome (15). Thus, the development of strategies aimed at eliminating Tregs or at selectively favoring the expansion of antitumor CTLs may significantly contribute in enhancing the engraftment and antitumor effects of adoptively transferred CTLs. To date, most efforts to increase *in vivo* immunostimulation of adoptively transferred T cells have focused on administration of interleukin (IL)-2 (18). Although this cytokine is a potent T-cell growth factor, it is not selective for effector T-cell subsets and can also enhance the growth and inhibitory activity of Tregs (19).

Authors' Affiliations: [1]Center for Cell and Gene Therapy, and Departments of [2]Pediatrics, [3]Immunology, and [4]Medicine, Baylor College of Medicine, Methodist Hospital and Texas Children's Hospital, Houston, Texas

Corresponding Author: Gianpietro Dotti, Center for Cell and Gene Therapy, Baylor College of Medicine, 6621 Fannin St. MC 3-3320, Houston, TX 77030, Phone: 832-824-6891; Fax: 832-825-4732; E-mail: gdotti@bcm.edu

doi: 10.1158/1078-0432.CCR-13-1016

Translational Relevance

Adoptive transfer of virus-specific CTLs expressing a chimeric antigen receptor (CAR) represents a promising therapy for patients with cancer. However, the *in vivo* expansion of these cells remains suboptimal so that new strategies are required to selectively expand them without favoring the concomitant proliferation and function of regulatory T cells (Treg) that are often abundant in patients with cancer. Our study provides preclinical data, indicating that the manipulation of the interleukin (IL)-7 cytokine–cytokine receptor axis in CAR-engrafted Epstein–Barr Virus–specific CTLs (EBV-CTLs) can be used to selectively expand the CTLs while avoiding the inhibitory effects of Tregs, which would otherwise be enhanced by use of the more broadly acting T-cell growth factor IL-2.

One means by which T lymphocytes can be selectively expanded is by using IL-7, a γ-chain cytokine that promotes homeostatic expansion of naïve and memory T cells but has no activity on Tregs, which lack the IL-7Rα (the private chain of the IL-7 receptor; refs. 20–23). Administration of recombinant IL-7 was well tolerated in early-phase clinical trials, and expanded naive and central-memory T-cell subsets but not Tregs (20, 21). Unfortunately, under physiologic conditions, IL-7 cannot support the *in vivo* expansion of adoptively transferred CAR-redirected CTLs as this is an effector-memory T-cell subset that, like Tregs, also lacks IL-7Rα (24).

Here, we developed models *in vitro* and *in vivo* to demonstrate that human Tregs clearly inhibit the antitumor effects of CAR-redirected EBV-CTLs. We also show that selective modulation of the IL-7 cytokine–cytokine receptor axis in CAR-engrafted EBV-CTLs augments their antitumor effects *in vivo* in the presence of Tregs. This strategy should safely enhance the persistence and survival of adoptively transferred CAR-redirected virus-specific CTLs in patients with cancer.

Materials and Methods

Plasmid construction, retrovirus production, and tumor cell lines

The full-length human IL-7R-α linked through the 2A (TAV) sequence to the CAR-GD2 encoding the CD28 endodomain (25) was cloned into the SFG retroviral vector to generate the bicistronic vector SFG.IL-7Rα.CAR-GD2. The retroviral vectors encoding eGFP and Firefly Luciferase (FFLuc) were previously described (26). Retroviral supernatant was prepared using transient transfection of 293T cells (26). The neuroblastoma cell line CHLA-255 (ref. 27; kindly provided by Dr. Leonid Metelitsa) was derived from a patient, and we verified that this line retains the surface expression of the target antigen GD2.

Generation and transduction of EBV-CTLs

EBV-transformed lymphoblastoid cells (LCL) and EBV-CTLs were prepared using peripheral blood mononuclear cells (PBMC), obtained from healthy donors as previously described (28). EBV-CTLs were transduced with retroviral supernatant after three stimulations with autologous LCLs, as previously described (8), and then maintained in culture by weekly stimulation with LCLs and recombinant IL-2 (50 IU/mL) or IL-7 (2.5 ng/mL; PeproTech).

Expansion of Tregs

To obtain significant numbers of cells for the *in vitro* and *in vivo* experiments, Tregs were isolated and expanded as previously described (29). Briefly, $CD25^{bright}$ T cells were purified from PBMCs by positive selection using immunomagnetic selection in the presence of nonsaturating concentrations (2 μL/1 × 10^7 PBMCs) of anti-human CD25 magnetic beads (Miltenyi Biotech). On day 0, the purified $CD25^+$ T cells were activated in 24-well plates coated with OKT3 (1 μg/mL) and anti-CD28 antibody (BD Pharmingen; 1 μg/mL) in RPMI 1640 in the presence of rapamycin (Sigma) at a final concentration of 100 nmol/L. On days 7 and 14, cells were restimulated with OKT3/CD28 antibodies, irradiated feeder cells, rapamycin, and IL-2 (50 IU/mL) in small bioreactors (G-REX; ref. 29). At the end of the 3-week culture (day 21), cells were used for *in vitro* and *in vivo* experiments. The cell fraction obtained from buffy coats after the selection of $CD25^{bright}$ T cells was further enriched for $CD4^+$ cells which were then used as negative control in parallel culture experiments, in which we evaluated the immunosuppressive activity of Tregs (29, 30).

Immunophenotyping

Cells were stained with fluorescein isothiocyanate (FITC)-, phycoerythrin (PE)-, peridinin-chlorophyll-protein complex (PerCP)-, or allophycocyanin (APC)-conjugated monoclonal antibodies (mAb). We used CD3, CD4, CD8, CD25, and CD127 (IL-7Rα specific) from Becton Dickinson (BD Bioscience) and FoxP3 from eBioscience Inc. CAR-GD2 expression by transduced EBV-CTLs was detected using the specific anti-idiotype antibody 1A7, followed by staining with the secondary antibody RAM-IgG1-PE (Becton Dickinson; ref. 8). STAT5 phosphorylation in Tregs and EBV-CTLs was assessed after cytokine stimulation for 15 minutes using the anti-phospho-STAT5 (Y694) mAb-Alexa Fluor 647 Conjugate (BD Phosflow Reagents). Cells were analyzed using a BD FACSCalibur system equipped with the filter set for quadruple fluorescence signals and the CellQuest software (BD Biosciences). For each sample, we analyzed a minimum of 10,000 events.

Carboxyfluorescein diacetate succinimidyl ester–based assays

Proliferation of Tregs or EBV-CTLs or activated PBMC was assessed by carboxyfluorescein diacetate succinimidyl ester (CFSE) dilution. Briefly, EBV-CTLs were labeled with 1.5 μmol/L CFSE (Invitrogen) and activated with LCLs (ratio 4:1) with or without IL-2 (12.5 IU/mL) or IL-7 (10 ng/mL). CFSE dilution was measured by flow cytometry after 7 days of culture. A similar protocol was used to evaluate the proliferation of CFSE-labeled Tregs post activation with

OKT3, irradiated feeders, and IL-2 or IL-7. To evaluate the suppressive activity of Tregs, CFSE-labeled EBV-CTLs were stimulated with LCLs (ratio 4:1) in the presence of Tregs or control $CD4^+CD25^-$ cells (ratio, 1:1; ref. 30), and of IL-2 (12.5 IU/mL) or IL-7 (10 ng/mL). Similarly, PBMC depleted of $CD25^{bright}$ cells were stained with CFSE and activated in the presence of irradiated allogeneic feeders (ratio 2:1) and OKT3 (500 ng/mL; refs. 29, 30). After 7 days, cells were stained with CD8-APC and CD4-PerCP, analyzed by fluorescence-activated cell sorting (FACS) and cell division assessed by CFSE dilution.

Evaluation of antitumor activity

EBV-CTLs were cultured in the presence of the neuroblastoma cell line (CHLA-255) genetically modified to stably express GFP in the presence or in the absence of Tregs (at the EBV-CTLs:CHLA-255:Treg ratio of 1:2:1) and of IL-2 (12.5 IU/mL) or IL-7 (5 ng/mL). After 7 days, cells were collected, stained with CD3 to identify T cells, and analyzed by FACS. GFP was used to quantify residual tumor cells in culture.

Xenogenic mouse model

To assess the antitumor effect of EBV-CTLs *in vivo* in the presence of Tregs, we used the xenograft mouse model and an *in vivo* imaging system as previously described (7, 24). Mouse experiments were performed in accordance with Baylor College of Medicine's Animal Husbandry guidelines. Briefly, 8- to 10-week-old NSG mice were engrafted intraperitoneally with the CHLA-255 cells (1×10^6 cells per mouse) genetically modified with FFluc to monitor tumor growth using the IVIS bioluminescence system (Xenogen IVIS 200 Biophotonic Imaging System). The intraperitoneal model was selected to minimize confounding issues due to suboptimal cell biodistribution and simultaneous colocalization at the tumor site of CAR-modified EBV-CTLs and Tregs. When the signal (measured as p/sec/cm^2/sr) was consistently increasing, usually by day 7 to 10, mice received intraperitoneal EBV-CTLs (10×10^6 T cells per mouse) with or without Tregs (10×10^6 T cells per mouse; two infusions 1-week apart). IL-2 (500 IU/mouse) or IL-7 (200 ng/mouse) were administered intraperitoneally three times a week.

Statistical analysis

All *in vitro* data were summarized by means and SEM. For the bioluminescent experiments, intensity signals were log-transformed and summarized using mean ± SD at baseline and multiple subsequent time points for each group of mice. Changes in intensity of signal from baseline at each time point were calculated and compared using paired *t* tests or Wilcoxon signed-ranks test. When the *P* value was less than 0.05, a mean difference was accepted as statistically significant. For the bioluminescence experiments, intensity signals were log-transformed and summarized using mean and SDs at baseline and multiple subsequent time points for each group of mice. The response profiles over time were analyzed by the generalized estimating equations method for repeated measurements.

Results

Functional IL-7Rα and CAR-GD2 can be coexpressed in EBV-CTLs

To restore the responsiveness to IL-7 and to redirect the antigen specificity of EBV-CTLs against neuroblastoma, we generated a bicistronic γ-retroviral vector encoding the IL-7Rα and a GD2-specific CAR linked through a 2A (TAV) sequence (SFG.IL-7Rα.2A.CAR-GD2; Fig. 1A). EBV-CTLs established from 5 healthy EBV-seropositive donors were transduced with the vector, and the expression of both IL-7Rα and CAR-GD2 was measured by FACS analysis. As shown in Figure 1B, both CAR-GD2 and IL-7Rα were stably expressed (64% ± 3% and 34% ± 9%, respectively) in transduced EBV-CTLs, whereas the expression of the native IL-7Rα on control cells remained negligible (4% ± 1%).

To evaluate the functionality of the transgenic IL-7Rα, we measured the phosphorylation of STAT5 in response to either IL-2 or IL-7. In the absence of cytokines, control, and IL-7Rα.CAR-GD2$^+$ EBV-CTLs showed negligible phosphorylation of STAT5 (3% ± 2% and 8% ± 4%, respectively). In IL-7Rα.CAR-GD2$^+$ EBV-CTLs, near equal STAT5 phosphorylation of Tyr-694 was detected in response to IL-2 (49% ± 7%) or IL-7 (38% ± 6%, respectively; P = NS). In contrast, in control cells, STAT5 was phosphorylated in response to IL-2 (63% ± 8%) but not to IL-7 (6% ± 5%; $P < 0.05$; Fig. 1C). The levels of IL-7Rα–dependent STAT5 phosphorylation in IL-7Rα.CAR-GD2$^+$ EBV-CTLs exposed to IL-7 were very similar to the amount observed in T lymphocytes physiologically expressing the IL-7Rα and exposed to IL-7 (Supplementary Fig. S1A). The functionality of the transgenic IL-7Rα was further supported by progressive selection of transgenic cells if cultures were supplemented with IL-7. As illustrated in Figure 1D (and Supplementary Fig. S1B), when IL-7Rα.CAR-GD2$^+$ CTLs were stimulated weekly with autologous LCLs and IL-7, the expression of both IL-7Rα and CAR-GD2 progressively increased between the third and sixth antigen-specific stimulation (from 34% ± 9% to 66% ± 5% for IL-7Rα, and from 64% ± 3% to 80% ± 7% for CAR-GD2). In contrast, when CTLs were expanded in the presence of IL-2, no enrichment of either transgenes was observed, as this cytokine equally supports the *ex vivo* growth of transduced and non transduced CTLs (data not shown).

The enrichment of transgenic T cells following exposure to IL-7 was a consequence of the proliferation of IL-7Rα.CAR-GD2$^+$ EBV-CTLs. As illustrated in Figure 2A, CFSE labeled-control and IL-7Rα.CAR-GD2$^+$ EBV-CTLs divided equally well when stimulated with LCLs (ratio 4:1) in the presence of IL-2 (proliferation, 68% ± 6% and 68% ± 4%, respectively). In contrast, in the presence of IL-7, IL-7Rα.CAR-GD2$^+$ but not control EBV-CTLs had significantly greater proliferation, 63% ± 3% versus 14% ± 1%, respectively ($P < 0.001$). The number of EBV-CTLs proliferating in response to EBV-LCLs and IL-7 was generally higher than expected based on the ectopic expression of IL-7Rα. This higher level is likely a consequence of the physiologic production of IL-2 by EBV-CTLs in response to their cognate EBV antigens (EBV-LCLs; Supplementary Fig. S2). Finally,

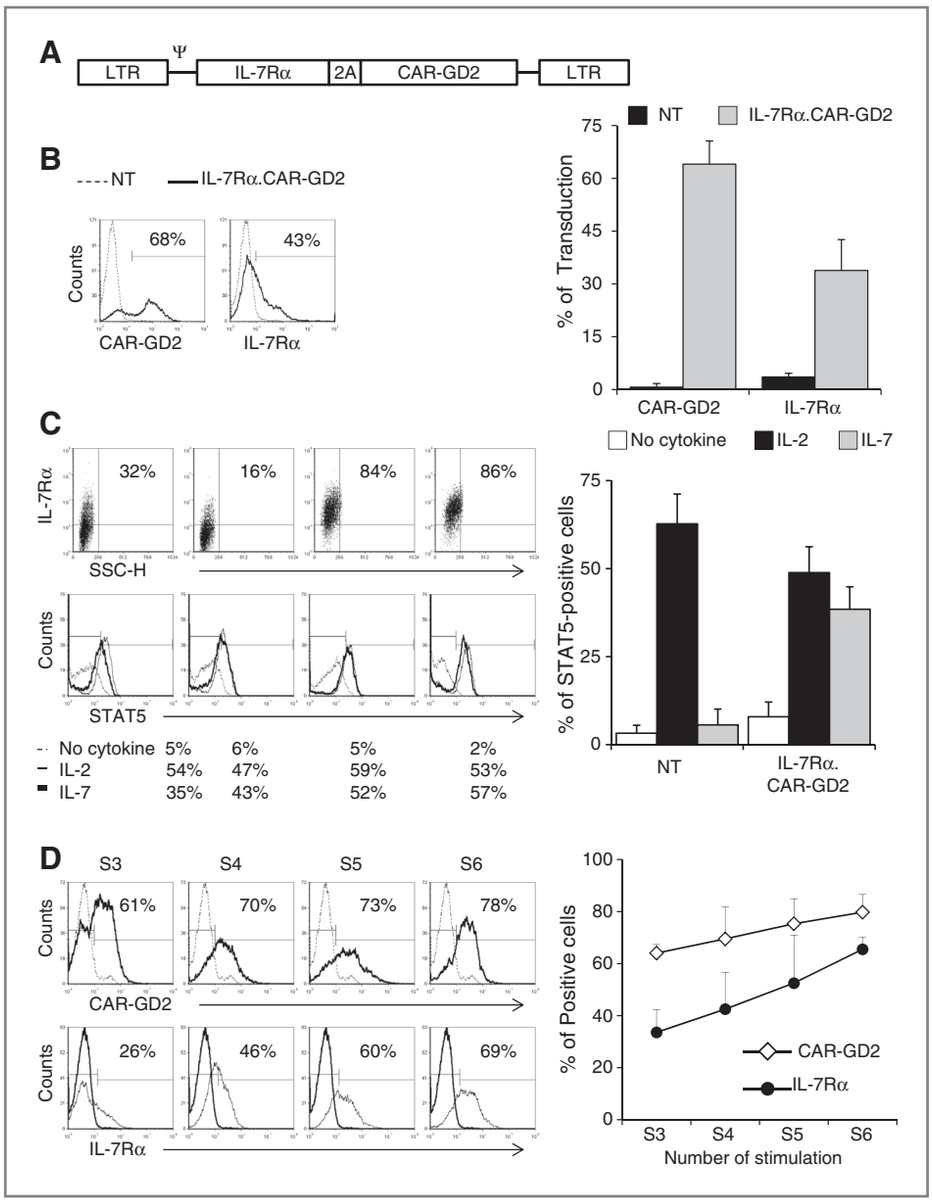

Figure 1. EBV-CTLs are effectively transduced with the bicistronic vector encoding both the IL-7Rα and the CAR-GD2. A, schema of the bicistronic γ-retroviral vector encoding the IL-7Rα and GD2-specific CAR linked through a 2A (TAV) sequence. B, expression of CAR-GD2 (top) and IL-7Rα (bottom) evaluated by FACS analysis day 7 after transduction. The dotted line indicates control EBV-CTLs and the bold line indicates the transduced EBV-CTLs. The graph represents mean ± SD of 5 donors. C, IL-7Rα expression in four IL-7Rα.CAR-GD2$^+$ EBV-CTLs generated (top) and STAT5 phosphorylation (bottom) in the absence of cytokines (thin black line), in response to IL-2 (dotted line), or IL-7 (black bold line). D, progressive enrichment in cells expressing the two transgenes IL-7Rα and CAR-GD2 when IL-7Rα.CAR-GD2$^+$ EBV-CTLs were expanded in the presence of IL-7. S3, S4, S5, and S6 indicate the transgene expression detected week 3 (S3), week 4 (S4), week 5 (S5), and week 6 (S6), respectively after transduction. Graph represents mean ± SEM of four different EBV-CTL lines.

exposure of IL-7Rα.CAR-GD2$^+$ EBV-CTLs to IL-7 did not affect their antitumor properties. As shown in Figure 2B, when EBV-CTLs were cultured with CHLA-255 cells, only IL-7Rα.CAR-GD2$^+$ cells controlled tumor growth in the presence of either IL-2 or IL-7 (6% ± 1% and 4% ± 1%, respectively), whereas tumor cells outgrew in cultures containing control EBV-CTLs irrespective of the cytokine added (43% ± 5% and 57% ± 12%, respectively; $P < 0.001$).

Ex vivo expanded Tregs do not respond to IL-7

We used *ex vivo* expanded CD4$^+$CD25$^+$ Tregs isolated from healthy donors rather than freshly isolated Tregs for the following reasons. First, the experiments required a significant number of Tregs that could not be obtained upon fresh isolation even from buffy coat preparations. Second, circulating Tregs obtained after immunomagnetic selection on the basis of CD4 and CD25 ~~selection~~ are frequently contaminated by CD4$^+$CD25$^+$IL7Rα$^+$ cells that lack regulatory activity, but respond to IL-7 (data not shown; ref. 31). We first confirmed that the nominal Treg population retained their inhibitory properties. As shown in Figure 3A, the proliferation of activated PBMCs (80% ± 3% in the presence of control CD4$^+$CD25$^-$ cells) was significantly inhibited in the presence of the expanded Treg population (27% ± 6%; $P < 0.001$). We then confirmed that these Tregs, like freshly isolated Tregs (22), lacked expression of IL-7Rα (3% ± 0.4% positive; Fig. 3B). As a consequence, STAT5 was only phosphorylated in these Tregs in response to IL-2 (MFI = 75 ± 9; $P < 0.001$) and not in response to IL-7 (MFI = 23 ± 3; Fig. 3C). Finally, a CFSE-

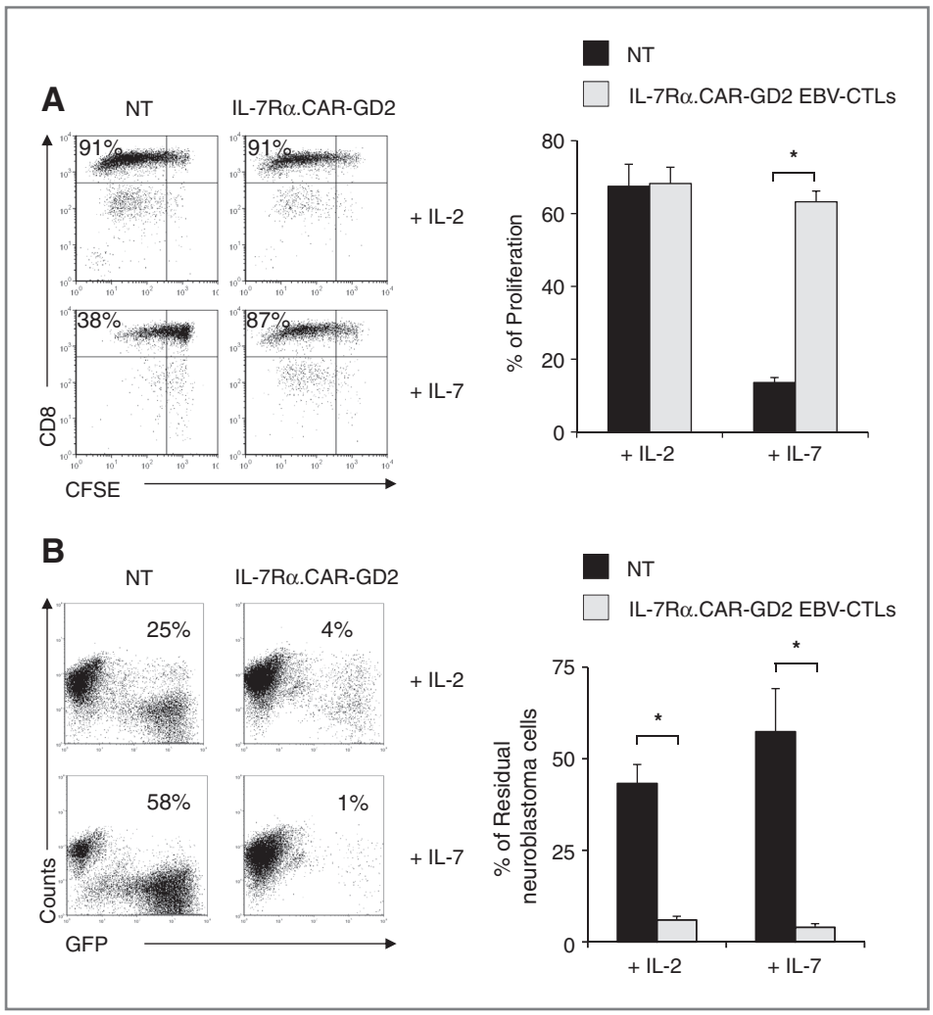

Figure 2. IL-7 supports the proliferation and effector function of IL-7Rα.CAR-GD2$^+$ EBV-CTLs. A, representative CFSE-based proliferation assay of control and IL-7Rα.CAR-GD2$^+$ EBV-CTLs. Control and IL-7Rα.CAR-GD2$^+$ EBV-CTLs were activated in the presence of autologous irradiated LCLs and either IL-2 or IL-7. CFSE dilution was evaluated on day 7 using FACS analysis. The graph represents mean ± SD of five independent experiments. B, representative coculture experiment in which control and IL-7Rα.CAR-GD2$^+$ EBV-CTLs were cocultured with CHLA-255 GFP-tagged tumor cells (at ratio 1:2) in the presence of IL-2 or IL-7. Residual tumor cells were enumerated by flow cytometry on day 7 of culture. The graph shows mean ± SD of five independent experiments. *, $P < 0.001$.

based dilution assay showed that Tregs only proliferated after polyclonal activation in the presence of IL-2 and not on exposure to IL-7 (MFI 1439 ± 207 vs. 445 ± 68, respectively; $P < 0.001$; Fig. 3D).

IL-7 supports the proliferation and effector function of IL-7Rα.CAR-GD2$^+$ EBV-CTLs in the presence of Tregs

Having demonstrated that IL-7 supports the proliferation and function of IL-7Rα.CAR-GD2$^+$ EBV-CTLs, we then investigated whether the beneficial effects of IL-7 were maintained in the presence of functional Tregs. As illustrated in Figure 4A, when IL-7Rα.CAR-GD2$^+$ EBV-CTLs were cultured with CHLA-255 cells (effector:target ratio of 1:2) they significantly controlled the growth of these tumor cells by day 7 of culture in the presence of either IL-2 or IL-7 (residual cells were 6% ± 1% and 4% ± 1%, respectively). In contrast, when expanded Tregs were added to the coculture (ratio CTLs:Tregs 1:1), the antitumor activity of IL-7Rα.CAR-GD2$^+$ EBV-CTLs was significantly inhibited in the presence of IL-2 but not of IL-7 (residual cells in culture, 14% ± 3% vs. 7% ± 2%, respectively; $P < 0.05$). In addition, IL-7 also supported the proliferation of IL7Rα.CAR-GD2$^+$ EBV-CTLs in the presence of Tregs upon physiologic costimulation with autologous LCLs. As the CFSE dilution assay shows in Figure 4B, the proliferation of IL-7Rα.CAR-GD2$^+$ EBV-CTLs in response to IL-2 (68% ± 4%) was significantly compromised in the presence of Tregs (to 34% ± 6%; $P < 0.01$). In contrast, when IL-7 was added to the culture, IL-7Rα.CAR-GD2$^+$ EBV-CTLs divided well even in the presence of Tregs (proliferation was 63% ± 3% without Tregs and 56% ± 2% in the presence of Tregs). The CFSE dilution of IL-7Rα.CAR-GD2$^+$ EBV-CTLs cocultured with Tregs was significantly increased in the presence of IL-7 as compared with IL-2 ($P = 0.005$).

IL-7 supports the *in vivo* antitumor activity of IL-7Rα.CAR-GD2 EBV-CTLs even in the presence of Tregs

To assess the *in vivo* capacity of IL-7 to support the antitumor activity of IL-7Rα.CAR-GD2$^+$ EBV-CTLs, we used NSG mice engrafted intraperitoneally with the FFLuc$^+$ cell line CHLA-255. As shown in Figure 5, control mice that received only tumor cells or control CTLs showed a rapid

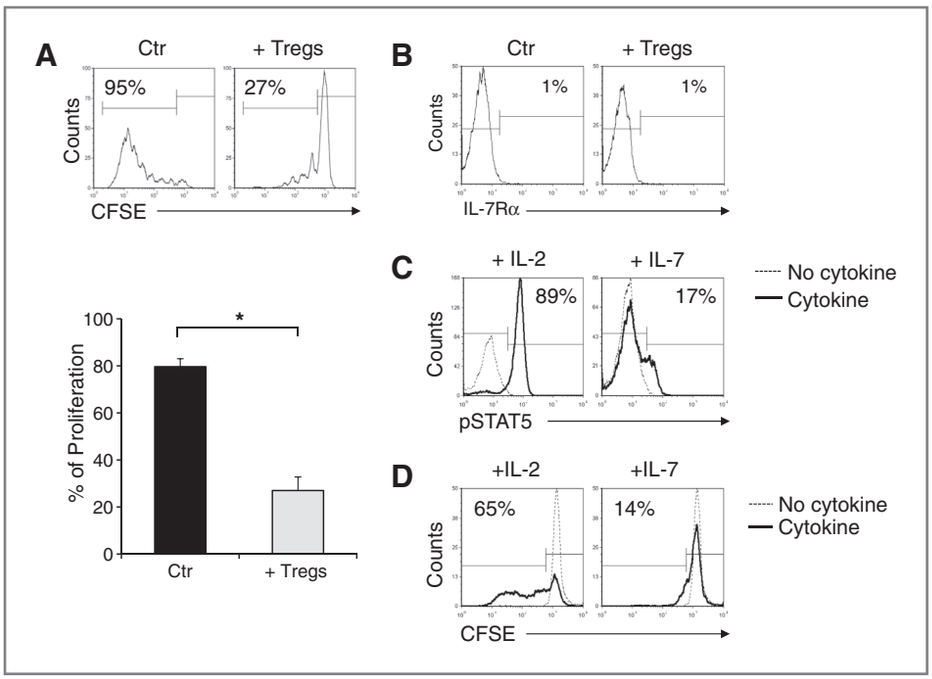

Figure 3. *Ex vivo* expanded Tregs do not respond to IL-7. A, CFSE-based assay to illustrate the inhibitory activity of *ex vivo* expanded Tregs. PBMCs labeled with CFSE were activated in the absence (left) or in the presence of Tregs (right) at a ratio of 1:1. CFSE dilution was measured on day 7 of culture by flow cytometry. The graph represents mean ± SEM of six independent experiments. B, expression of IL-7Rα in *ex vivo* expanded Tregs in a representative experiment. The plot on the left shows the isotype control, whereas the plot on the right shows the IL-7Rα profile. *, $P < 0.001$. C, phosphorylation of STAT5 in Tregs not stimulated (dotted lines) or stimulated with IL-2 (left) or IL-7 (right). D, proliferative response of Tregs exposed to IL-2 or IL-7. Tregs were labeled with CFSE and stimulated in the presence of IL-2 (left) or IL-7 (right). CFSE dilution was evaluated on day 7 by flow cytometry. The solid and dotted lines represent the CFSE dilution of Tregs stimulated with or without cytokines, respectively.

increase of the bioluminescence signal ($2.3 \times 10^8 \pm 3 \times 10^7$ photons) and were sacrificed by day 18. Mice infused with IL-7Rα.CAR-GD2$^+$ EBV-CTLs and IL-2 had superior tumor control ($1.6 \times 10^8 \pm 2 \times 10^7$ photons at day 34), but this effect was abrogated when Tregs were coinfused ($2.4 \times 10^8 \pm 4 \times 10^7$ photons at day 34; $P < 0.05$). In contrast, mice infused with IL-7Rα.CAR-GD2$^+$ EBV-CTLs and IL-7 controlled tumor growth equally well in the absence ($1.2 \times 10^8 \pm 3 \times 10^7$ photons) or in presence of Tregs ($1.3 \times 10^8 \pm 6 \times 10^6$ photons) at day 34.

Discussion

The adoptive transfer of CAR-redirected EBV-CTLs safely induces tumor regression in patients with neuroblastoma and the approach is potentially applicable to other human malignancies (8, 9). To further improve the clinical benefits of this approach, we developed a strategy that selectively promotes the *in vivo* expansion of CAR-redirected CTLs without favoring the proliferation and function of Tregs that may limit long-term persistence and activity of the infused effector cells and thereby compromise antitumor efficacy. Here, we demonstrate that CAR-redirected EBV-CTLs engineered to regain responsiveness to IL-7 by restoring their expression of IL-7Rα proliferate in response to a combination of native TCR receptor and IL-7 stimulation without favoring the expansion and function of Tregs. As a consequence, we observed an increase in their CAR-mediated antineuroblastoma activity, even in the presence of Tregs.

Successful clinical outcome following adoptive transfer of tumor-specific T cells strongly correlates with the *in vivo* survival and proliferation of these cells (18, 32, 33). In addition to the intrinsic properties of T lymphocytes, such as central-memory versus effector-memory versus naïve phenotype that directly dictate the self-maintenance capacity of tumor-specific T cells (34), several tumor-associated mechanisms are also pivotal in determining the consequences of administering tumor-specific T cells (10, 35). Tregs in particular are abundant in the tumor microenvironment and are a major factor in impairing T-cell function. Hence, strategies that selectively increase persistence and expansion of adoptively transferred T cells or that eliminate the influence of this cell subset should be as relevant for T-cell therapies as they have proved to be for cancer-vaccine trials (36).

The administration of recombinant cytokines or the use of cytokine-engineered T cells (30, 37, 38) that selectively support T-cell growth without providing functional or proliferative advantages to Tregs represent appealing approaches to overcome the inhibitory function of Tregs within the tumor microenvironment. However, IL-2 that is frequently used to sustain the *in vivo* proliferation and persistence of adoptively transferred CTLs is nonselective, stimulating both tumor-specific effector T cells and Tregs, as

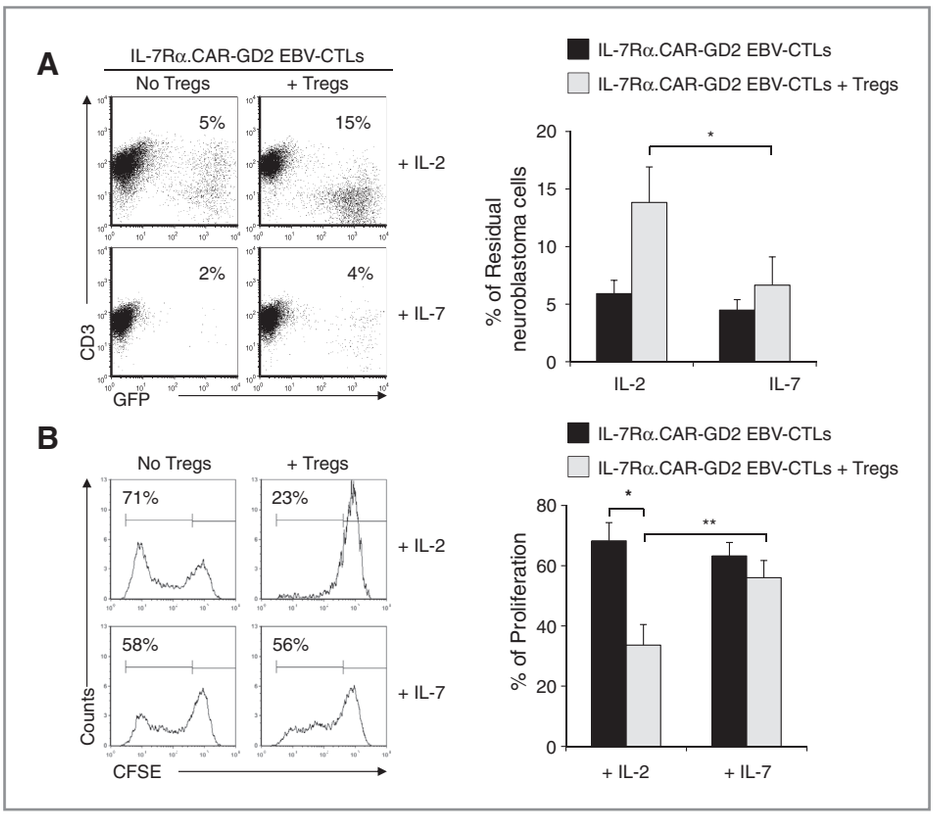

Figure 4. IL-7, unlike IL-2, supports *in vitro* the proliferation and function of IL-7Rα.CAR-GD2$^+$ EBV-CTLs in the presence of Tregs. A, IL-7Rα.CAR-GD2$^+$ EBV-CTLs were cocultured with CHLA-255 GFP-tagged cells (ratio 1:2) in the presence of IL-2 or IL-7, with or without Tregs. The percentage of residual tumor cells was measured by flow cytometry on day 7 of culture. The plots on the left show a representative experiment, whereas the graph on the right summarizes mean ± SD of five independent experiments. B, IL-7Rα.CAR-GD2$^+$ EBV-CTLs were labeled with CFSE and activated with autologous LCLs in the presence of IL-2 (top) or IL-7 (bottom) with or without Tregs. CFSE dilution was measured at day 7 of culture by flow cytometry. The plots on the left show a representative experiment, whereas the graph represents mean ± SD of five independent experiments. *, $P < 0.01$; **, $P = 0.005$.

both these cell subsets express the IL-2 high affinity receptor (CD25; refs. 19, 39). Thus, as illustrated in the current and prior studies, the net effect of IL-2 administration is to block the proliferation and antitumor effects of CAR-redirected CTLs both *in vitro* and *in vivo*.

Although IL-7 shares several functions with IL-2, it also has effects on specific T-cell subsets that depend on their expression of the private IL-7Rα subunit (23). Our experiments demonstrate both *in vitro* and *in vivo* that IL-7 can nonetheless support the survival, expansion, and effector function of CAR-redirected EBV-CTLs if these cells are engineered to reexpress the IL-7Rα and that it can thereby overcome the inhibitory effects of Tregs. Our approach has significant advantages over the use of IL-2 or cytotoxic drugs to eliminate Tregs in a nonselective manner (40) as it may promote the long-term persistence of CAR-redirected EBV-CTLs both in steady-state conditions and in a lymphopenic environment (23). In addition, the administration of recombinant IL-7 unlike recombinant IL-2 seems to be well tolerated even at high doses (20, 21, 41).

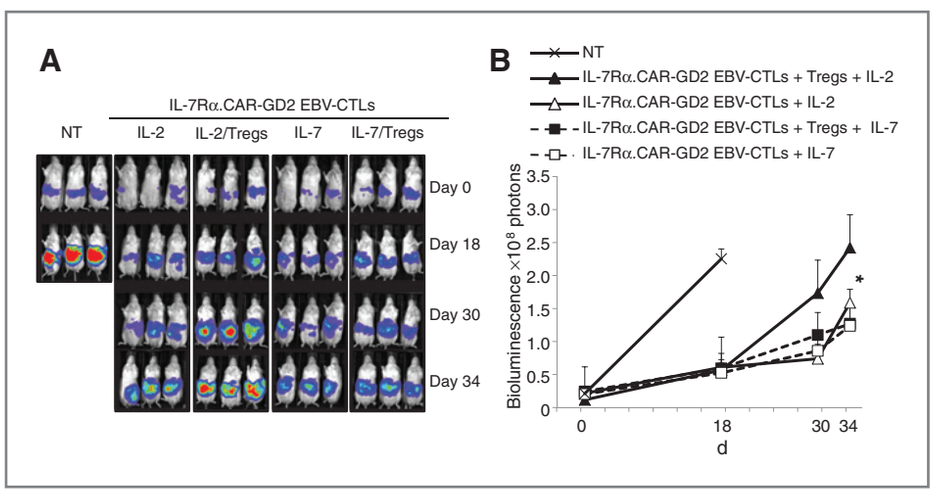

Figure 5. IL-7, but not IL-2, supports *in vivo* antitumor activity of IL-7Rα.CAR-GD2$^+$ EBV-CTLs in the presence of Tregs. NSG mice engrafted intraperitoneally with CHLA-255 cells tagged with FFLuc were infused with IL-7Rα.CAR-GD2$^+$ EBV-CTLs and received IL-2 ± Tregs or IL-7 ± Tregs. Tumor growth was monitored using an *in vivo* imaging system (Xenogen IVIS imaging system). A group of mice received control EBV-CTLs or tumor cells only (Control). A, images of different groups of mice. B, mean ± SD of photons for 8 mice/group in two independent experiments. *. $P < 0.05$.

Finally, as the infusion of virus-specific CTLs after allogeneic stem-cell transplant does not induce the occurrence of graft versus host disease (28), our proposed approach of infusing CAR-redirected CTLs with restored responsiveness to the homeostatic cytokine IL-7 may significantly increase the application of CAR technology in the allogeneic setting (42).

One potential concern associated with any genetic manipulation of T cells is that the cells will undergo malignant transformation, or grow in an antigen independent manner. This concern is particularly prominent when the genetic manipulation modifies a growth factor receptor or other portions of a signaling pathway. However, the experience of our own and other groups has been that the genetic manipulation of differentiated T cells to express cytokines or cytokine receptors does not affect the antigen specificity of these cells and does not elicit uncontrolled proliferation (24, 37, 43). These results were confirmed in the current study even if we cannot completely exclude the possibility of secondary paracrine effects due to the ectopic expression of IL-7Rα. If such a concern remains, however, incorporation of suicide or safety switches within the cells may provide a further level of reassurance (37, 44).

Our study suggests that restoring the responsiveness to IL-7 of virus-specific CTLs redirected with a CAR is a strategy that may allow enhanced T-effector cells without concomitant inhibition by Treg and may thereby further improve the clinical outcome of a promising therapeutic approach.

Disclosure of Potential Conflicts of Interest

M. Brenner is a consultant/advisory board member of Bluebird Bio. No potential conflicts of interest were disclosed by the other authors. Q10

Authors' Contributions

Conception and design: S.K. Perna, ~~M. Brenner,~~ B. Savoldo, G. Dotti Q11
Development of methodology: S.K. Perna, B. Savoldo, G. Dotti
Acquisition of data (provided animals, acquired and managed patients, provided facilities, etc.): S.K. Perna, D. Pagliara, B. Savoldo, G. Dotti
Analysis and interpretation of data (e.g., statistical analysis, biostatistics, computational analysis): S.K. Perna, D. Pagliara, H. Liu, B. Savoldo, G. Dotti
Writing, review, and/or revision of the manuscript: S.K. Perna, M. Brenner, B. Savoldo, G. Dotti
Administrative, technical, or material support (i.e., reporting or organizing data, constructing databases): ~~S.K. Perna, M. Brenner~~
Study supervision: B. Savoldo
Provided technical assistance for some of the *in vitro* and *in vivo* experiments: A. Mahendravada

Grant Support

This work was supported in part by R01 CA142636 NIH-NCI, W81XWH-10-10425 Department of Defense, Technology/Therapeutic Development Award.

The costs of publication of this article were defrayed in part by the payment of page charges. This article must therefore be hereby marked *advertisement* in accordance with 18 U.S.C. Section 1734 solely to indicate this fact.

Received April 12, 2013; revised September 20, 2013; accepted September 26, 2013; published OnlineFirst xx xx, xxxx.

References

1. Sadelain M, Brentjens R, Riviere I. The promise and potential pitfalls of chimeric antigen receptors. Curr Opin Immunol 2009;21:215–23.
2. Jena B, Dotti G, Cooper LJ. Redirecting T-cell specificity by introducing a tumor-specific chimeric antigen receptor. Blood 2010;116:1035–44.
3. Eshhar Z, Waks T, Gross G, Schindler DG. Specific activation and targeting of cytotoxic lymphocytes through chimeric single chains consisting of antibody-binding domains and the gamma or zeta subunits of the immunoglobulin and T-cell receptors. Proc Natl Acad Sci U S A 1993;90:720–4.
4. Imai C, Mihara K, Andreansky M, Nicholson IC, Pui CH, Geiger TL, et al. Chimeric receptors with 4-1BB signaling capacity provoke potent cytotoxicity against acute lymphoblastic leukemia. Leukemia 2004;18:676–84.
5. Savoldo B, Ramos CA, Liu E, Mims MP, Keating MJ, Carrum G, et al. CD28 costimulation improves expansion and persistence of chimeric antigen receptor-modified T cells in lymphoma patients. J Clin Invest 2011;121:1822–6.
6. Rossig C, Bollard CM, Nuchtern JG, Rooney CM, Brenner MK. Epstein-Barr virus-specific human T lymphocytes expressing antitumor chimeric T-cell receptors: potential for improved immunotherapy. Blood 2002;99:2009–16.
7. Savoldo B, Rooney CM, Di Stasi A, Abken H, Hombach A, Foster AE, et al. Epstein Barr virus specific cytotoxic T lymphocytes expressing the anti-CD30{zeta} artificial chimeric T-cell receptor for immunotherapy of Hodgkin disease. Blood 2007;110:2620–30.
8. Pule MA, Savoldo B, Myers GD, Rossig C, Russell HV, Dotti G, et al. Virus-specific T cells engineered to coexpress tumor-specific receptors: persistence and antitumor activity in individuals with neuroblastoma. Nat Med 2008;14:1264–70.
9. Louis CU, Savoldo B, Dotti G, Pule M, Yvon E, Myers GD, et al. Antitumor activity and long-term fate of chimeric antigen receptor-positive T cells in patients with neuroblastoma. Blood 2011;118:6050–6.
10. Zou W. Immunosuppressive networks in the tumour environment and their therapeutic relevance. Nat Rev Cancer 2005;5:263–74.
11. Baecher-Allan C, Hafler DA. Suppressor T cells in human diseases. J Exp Med 2004;200:273–6.
12. Johnson BD, Jing W, Orentas RJ. CD25+ regulatory T cell inhibition enhances vaccine-induced immunity to neuroblastoma. J Immunother 2007;30:203–14.
13. Wolf AM, Wolf D, Steurer M, Gastl G, Gunsilius E, Grubeck-Loebenstein B. Increase of regulatory T cells in the peripheral blood of cancer patients. Clin Cancer Res 2003;9:606–12.
14. Woo EY, Chu CS, Goletz TJ, Schlienger K, Yeh H, Coukos G, et al. Regulatory CD4(+)CD25(+) T cells in tumors from patients with early-stage non-small cell lung cancer and late-stage ovarian cancer. Cancer Res 2001;61:4766–72.
15. Curiel TJ, Coukos G, Zou L, Alvarez X, Cheng P, Mottram P, et al. Specific recruitment of regulatory T cells in ovarian carcinoma fosters immune privilege and predicts reduced survival. Nat Med 2004;10:942–9.
16. Marshall NA, Christie LE, Munro LR, Culligan DJ, Johnston PW, Barker RN, et al. Immunosuppressive regulatory T cells are abundant in the reactive lymphocytes of Hodgkin lymphoma. Blood 2004;103:1755–62.
17. Jing W, Yan X, Hallett WH, Gershan JA, Johnson BD. Depletion of CD25(+) T cells from hematopoietic stem cell grafts increases post-transplantation vaccine-induced immunity to neuroblastoma. Blood 2011;117:6952–62.
18. Rosenberg SA, Restifo NP, Yang JC, Morgan RA, Dudley ME. Adoptive cell transfer: a clinical path to effective cancer immunotherapy. Nat Rev Cancer 2008;8:299–308.
19. Ahmadzadeh M, Rosenberg SA. IL-2 administration increases CD4+ CD25(hi) Foxp3 +regulatory T cells in cancer patients. Blood 2006;107:2409–14.
20. Sportes C, Hakim FT, Memon SA, Zhang H, Chua KS, Brown MR, et al. Administration of rhIL-7 in humans increases *in vivo* TCR repertoire

diversity by preferential expansion of naive T cell subsets. J Exp Med 2008;205:1701–14.

21. Rosenberg SA, Sportes C, Ahmadzadeh M, Fry TJ, Ngo LT, Schwarz SL, et al. IL-7 administration to humans leads to expansion of CD8+ and CD4+ cells but a relative decrease of CD4+ T-regulatory cells. J Immunother 2006;29:313–9.
22. Liu W, Putnam AL, Xu-Yu Z, Szot GL, Lee MR, Zhu S, et al. CD127 expression inversely correlates with FoxP3 and suppressive function of human CD4+ T reg cells. J Exp Med 2006;203:1701–11.
23. Ma A, Koka R, Burkett P. Diverse functions of IL-2, IL-15, and IL-7 in lymphoid homeostasis. Annu Rev Immunol 2006;24:657–79.
24. Vera JF, Hoyos V, Savoldo B, Quintarelli C, Giordano Attianese GM, Leen AM, et al. Genetic manipulation of tumor-specific cytotoxic T lymphocytes to restore responsiveness to IL-7. Mol Ther 2009;17:880–8.
25. Pule MA, Straathof KC, Dotti G, Heslop HE, Rooney CM, Brenner MK. A chimeric T cell antigen receptor that augments cytokine release and supports clonal expansion of primary human T cells. Mol Ther 2005;12:933–41.
26. Vera J, Savoldo B, Vigouroux S, Biagi E, Pule M, Rossig C, et al. T lymphocytes redirected against the kappa light chain of human immunoglobulin efficiently kill mature B lymphocyte-derived malignant cells. Blood 2006;108:3890–7.
27. Song L, Ara T, Wu HW, Woo CW, Reynolds CP, Seeger RC, et al. Oncogene MYCN regulates localization of NKT cells to the site of disease in neuroblastoma. J Clin Invest 2007;117:2702–12.
28. Rooney CM, Smith CA, Ng CY, Loftin SK, Sixbey JW, Gan Y, et al. Infusion of cytotoxic T cells for the prevention and treatment of Epstein-Barr virus-induced lymphoma in allogeneic transplant recipients. Blood 1998;92:1549–55.
29. Chakraborty R, Mahendravada A, Perna SK, Rooney CM, Heslop HE, Vera JF, et al. Robust and cost effective expansion of human regulatory T cells highly functional in a xenograft model of graft-versus-host disease. Haematologica 2013;98:533–7.
30. Perna SK, De AB, Pagliara D, Hasan ST, Zhang L, Mahendravada A, et al. Interleukin 15 Provides Relief to CTLs from Regulatory T Cell-Mediated Inhibition: Implications for Adoptive T Cell-Based Therapies for Lymphoma. Clin Cancer Res 2013;19:106–17.
31. Battaglia M, Stabilini A, Migliavacca B, Horejs-Hoeck J, Kaupper T, Roncarolo MG. Rapamycin promotes expansion of functional CD4+CD25+FOXP3+ regulatory T cells of both healthy subjects and type 1 diabetic patients. J Immunol 2006;177:8338–47.
32. Heslop HE, Slobod KS, Pule MA, Hale GA, Rousseau A, Smith CA, et al. Long-term outcome of EBV-specific T-cell infusions to prevent or treat EBV-related lymphoproliferative disease in transplant recipients. Blood 2010;115:925–35.
33. Kalos M, Levine BL, Porter DL, Katz S, Grupp SA, Bagg A, et al. T cells with chimeric antigen receptors have potent antitumor effects and can establish memory in patients with advanced leukemia. Sci Transl Med 2011;3:95ra73.
34. Gattinoni L, Klebanoff CA, Palmer DC, Wrzesinski C, Kerstann K, Yu Z, et al. Acquisition of full effector function *in vitro* paradoxically impairs the *in vivo* antitumor efficacy of adoptively transferred CD8+ T cells. J Clin Invest 2005;115:1616–26.
35. Hoyos V, Savoldo B, Dotti G. Genetic modification of human T lymphocytes for the treatment of hematologic malignancies. Haematologica 2012;97:1622–31.
36. Dannull J, Su Z, Rizzieri D, Yang BK, Coleman D, Yancey D, et al. Enhancement of vaccine-mediated antitumor immunity in cancer patients after depletion of regulatory T cells. J Clin Invest 2005;115:3623–33.
37. Hoyos V, Savoldo B, Quintarelli C, Mahendravada A, Zhang M, Vera J, et al. Engineering CD19-specific T lymphocytes with interleukin-15 and a suicide gene to enhance their anti-lymphoma/leukemia effects and safety. Leukemia 2010;24:1160–70.
38. Liu K, Rosenberg SA. Transduction of an IL-2 gene into human melanoma-reactive lymphocytes results in their continued growth in the absence of exogenous IL-2 and maintenance of specific antitumor activity. J Immunol 2001;167:6356–65.
39. Terabe M, Berzofsky JA. Immunoregulatory T cells in tumor immunity. Curr Opin Immunol 2004;16:157–62.
40. Dudley ME, Yang JC, Sherry R, Hughes MS, Royal R, Kammula U, et al. Adoptive cell therapy for patients with metastatic melanoma: evaluation of intensive myeloablative chemoradiation preparative regimens. J Clin Oncol 2008;26:5233–9.
41. Rosenberg SA, Yannelli JR, Yang JC, Topalian SL, Schwartzentruber DJ, Weber JS, et al. Treatment of patients with metastatic melanoma with autologous tumor-infiltrating lymphocytes and interleukin 2. J Natl Cancer Inst 1994;86:1159–66.
42. Micklethwaite KP, Savoldo B, Hanley PJ, Leen AM, mmler-Harrison GJ, Cooper LJ, et al.Derivation of human T lymphocytes from cord blood and peripheral blood with antiviral and antileukemic specificity from a single culture as protection against infection and relapse after stem cell transplantation. Blood 2010;115:2695–703.
43. Quintarelli C, Vera JF, Savoldo B, Giordano Attianese GM, Pule M, Foster AE, et al. Co-expression of cytokine and suicide genes to enhance the activity and safety of tumor-specific cytotoxic T lymphocytes. Blood 2007;110:2793–802.
44. Di Stasi A, Tey SK, Dotti G, Fujita Y, Kennedy-Nasser A, Martinez C, et al. Inducible apoptosis as a safety switch for adoptive cell therapy. N Engl J Med 2011;365:1673–83.

AUTHOR QUERIES

AUTHOR PLEASE ANSWER ALL QUERIES

Q1: Page: 1: AU: Per journal style, genes, alleles, loci, and oncogenes are italicized; proteins are roman. Please check throughout to see that the words are styled correctly.

Q2: Page: 1: Author: Please verify the changes made in the article title.

Q3: Page: 1: Author: Units of measurement have been changed here and elsewhere in the text from "M" to "mol/L," and related units, such as "mmol/L" and μmol/L," in figures, legends, and tables in accordance with journal style, derived from the Council of Science Editors Manual for Authors, Editors, and Publishers and the Système international d'unités. Please note if these changes are not acceptable or appropriate in this instance.

Q4: Page: 1: Author: Please verify the drug names and their dosages used in the article.

Q5: Page: 2: Author: Please provide the institutional details of Dr. Leonid Metelitsa.

Q6: Page: 2: Author: Please verify the presentation of "FACSCalibur" for correctness.

Q7: Page: 3: Author: Please define "NSG."

Q8: Page: 4: Author: Author: Please confirm quality/labeling of all images included within this article. Thank you.

Q9: Page: 6: Author: Please define "TCR."

Q10: Page: 8: Author: AU/PE: The conflict-of-interest disclosure statement that appears in the proof incorporates the information from forms completed and signed off on by each individual author. No factual changes can be made to disclosure information at the proof stage. However, typographical errors or misspelling of author names should be noted on the proof and will be corrected before publication. Please note if any such errors need to be corrected. Is the disclosure statement correct?

Q11: Page: 8: Author: The contribution(s) of each author are listed in the proof under the heading "Authors' Contributions." These contributions are derived from forms completed and signed off on by each individual author. As the corresponding author, you are permitted to make changes to your own contributions. However, because all authors submit their contributions individually, you are not permitted to make changes in the contributions listed for any other authors. If you feel strongly that an error is being made, then you may ask the author or authors in question to contact us about making the changes. Please note, however, that the manuscript would be held from further processing until this issue is resolved.

AU: Below is a summary of the name segmentation for the authors according to our records. The First Name and the Surname data will be provided to PubMed when the article is indexed for searching. Please check each name carefully and verify that the First Name and Surname are correct. If a name is not segmented correctly, please write the correct First Name and Surname

on this page and return it with your proofs. If no changes are made to this list, we will assume that the names are segmented correctly, and the names will be indexed as is by PubMed and other indexing services.

First Name	Surname
Serena K.	Perna
Daria	Pagliara
Aruna	Mahendravada
Hao	Liu
Malcolm	Brenner
Barbara	Savoldo
Gianpietro	Dotti

Gene Therapy (2013), 1–5

www.nature.com/gt

SHORT COMMUNICATION

The immunogenicity of virus-derived 2A sequences in immunocompetent individuals

C Arber[1], H Abhyankar[1], HE Heslop[1,2,3], MK Brenner[1,2,3], H Liu[1,4], G Dotti[1,2,5] and B Savoldo[1,3]

Genetic engineering of T cells for adoptive immunotherapy in cancer patients has shown significant promise. To ensure optimal antitumor activity and safety, the simultaneous expression of multiple genes is frequently required, and short viral-derived 2A sequences are increasingly preferred for this purpose. Concerns exist, however, that these virus-derived sequences may induce unwanted immune responses, and thus diminish persistence of the gene-modified cells after adoptive transfer. Whereas such responses were absent in immunocompromised recipients, potential immunogenicity in immunocompetent individuals remains a concern. We now address whether *ex vivo* T cell responses can be elicited against the most widely used 2A sequences (2A-Thosea asigna virus (TAV) or 2A-equine rhinitis virus (ERAV), specifically) in immunocompetent individuals. We used a potent *ex vivo* culture system previously validated to induce T cell responses even against weakly immunogenic antigens. Of the sixteen donors tested, only five released very low levels of interferon-γ in response to 2A-TAV peptide mixtures (single peptide specificity in three donors, adjacent self-antigen peptide specificity in one donor and nonspecific reactivity in one donor). None of them produced cytotoxic activity or responded to 2A-ERAV. These results suggest that exposure to viral-derived 2A sequences is unlikely to produce unwanted T cell responses in immunocompetent individuals and further supports their continued use for studies of human gene therapy.

Gene Therapy advance online publication, 23 May 2013; doi:10.1038/gt.2013.25

Keywords: 2A sequences; polycistronic vectors; T cell gene transfer; immunogenicity

INTRODUCTION

Adoptive T cell-based immunotherapies and vaccines are promising approaches for cancer patients, and genetic engineering can significantly improve their potency.[1,2] Efficient expression of multiple genes in one single polycistronic vector can simultaneously coordinate the expression of multiple components of the immune system against cancer cells and counterbalance tumor immune evasion mechanisms,[3] and is often critical for the success of these therapies. For example, production of T lymphocytes that will safely and efficiently kill tumor cells after adoptive transfer may require simultaneous genetic modifications to increase their tumor specificity by forced expression of engineered T cell receptors;[2,4] enhance their trafficking by expression of chemokine receptors;[4,5] prolong their persistence by forced expression of cytokines or co-stimulatory molecules[6–11] and augment safety by the incorporation of a suicide switch to remove gene-modified cells on demand.[12,13]

Of the available strategies to generate polycistronic vectors, virus-derived 2A sequences are one of the most effective.[14] These sequences are *cis*-acting hydrolase elements that mediate a ribosomal skip between 2A-linked genes,[15] resulting in stoichiometric protein production[16] that can improve transgene expression and function, for example, of T cells engineered with transgenic αβT cell receptors.[17] Moreover, 2A sequences are quite short (54–60 nucleotides), and therefore have little impact on vector-packaging limits. However, as the 2A sequences are of viral origin, their expression in fusion proteins could lead to the expression of immunogenic epitopes and thereby diminish the *in vivo* persistence of corresponding gene-modified cells.

Recently, 2A sequences have been successfully incorporated in vectors used in human studies without eliciting discernible immune responses, although the recipients in these trials were significantly immunocompromised.[13,17] Thus, to discover whether virus-derived 2A sequences may cause troublesome immunogenicity in immunocompetent individuals, we assessed if T cell responses could be elicited to protein regions derived from two vectors containing either the 2A-TAV (Those asigna virus-derived)[13] or the 2A-ERAV (equine rhinitis virus-derived)[7] sequences. We used a potent *ex vivo* culture system that has been previously optimized to expand T cells with specificity for weak antigens, even from antigenically naive individuals,[18] such as umbilical cord blood T cells.[19] Our results support the continued exploration of 2A sequences even in immunocompetent human subjects.

RESULTS AND DISCUSSION

Using our optimized culture system,[18–20] we successfully generated T cell lines from normal adult donors that had robust interferon-γ (IFN-γ) production in response to the cytomegalovirus-derived pp65 peptide mixture (pepmix) (1274.6 ± 91.9 IFN-γ spot-forming cells (SFCs) per 10^5 cells) in

[1]Center for Cell and Gene Therapy, Baylor College of Medicine, The Methodist Hospital and Texas Children's Hospital, Houston, TX, USA; [2]Department of Medicine, The Methodist Hospital and Texas Children's Hospital, Houston, TX, USA; [3]Department of Pediatrics, The Methodist Hospital and Texas Children's Hospital, Houston, TX, USA; [4]Department of Biostatistics Shared Resource Dan L. Duncan Cancer Center, The Methodist Hospital and Texas Children's Hospital, Houston, TX, USA and [5]Department of Immunology, Baylor College of Medicine, The Methodist Hospital and Texas Children's Hospital, Houston, TX, USA. Correspondence: Professor B Savoldo, Center for Cell and Gene Therapy, Baylor College of Medicine, The Methodist Hospital and Texas Children's Hospital, 6621 Fannin St, MC 3-3320, Houston, TX 77030, USA.
E-mail: bsavoldo@bcm.edu
Received 10 November 2012; revised 21 March 2013; accepted 17 April 2013

7/7 donors (Figure 1a) and to the weak tumor-associated antigen, preferentially expressed antigen of melanoma (PRAME) pepmix[18] (409.1 ± 29.7 IFN-γ SFCs per 10^5 cells) in 8/9 donors (Figure 1b). By contrast, when we used the same culture conditions with peptide mixtures derived from the two 2A sequences, we found minimal reactivity against the 2A-TAV pepmix in only 5 of the 16 donors tested (59.6 ± 6.7 IFN-γ SFCs per 10^5 cells) (Figure 1c), and no discernible responses against the 2A-ERAV-pepmix in any of the 11 donors tested (Figure 1d). Phenotypically, all lines were a mixture of $CD4^+$ and $CD8^+$ cells, and contained some natural killer cells, with a trend ($P = 0.07$) for a lower proportion of $CD8^+$ cells in the 2A-TAV and 2A-ERAV lines (for 2A-TAV: $CD8^+ = 48.6 \pm 23.1\%$; for 2A-ERAV: $CD8^+ = 48.5 \pm 20.32\%$), as compared with pp65-specific T cell lines ($CD8^+ = 70.4 \pm 12.8\%$) or with PRAME-specific T cell lines ($CD8^+ = 58.8 \pm 19.7\%$, Figure 2).

To identify the weakly immunogenic peptides derived from the 2A-TAV sequence, we tested each of the 11 single 15-mer peptides against the five weakly reactive T cell lines. Three of these five lines (derived from donor nos. 13, 14 and 15, Figure 3a) released IFN-γ upon exposure to the RAEGRGSLLTCGDVE peptide (51.9 ± 6.9 IFN-γ SFCs per 10^5 cells, peptide no. 5 of the pool, Figure 4a). The line from donor no. 9 (Figure 3a) reacted against the CFNFLRKKLFFKTSA peptide (57.3 ± 10.3 IFN-γ SFCs per 10^5 cells, peptide no. 1 of the pool, Figure 4a) and simultaneously against the PRLLFFLLFLTPMEV peptide (21.0 ± 15.1 IFN-γ SFCs per 10^5 cells, peptide no. 11 of the pool, Figure 4a). These are junctional peptides between the 2A sequence, and the carboxy- and amino-terminal sequences of the expressed genes of interest (human inducible caspase9 and the signal peptide sequence of human CD19, respectively). The line derived from donor no. 8 was responsive against the 2A-TAV pepmix, but had no discernible reactivity to any of the individual peptides contained in the mixture and was thus classified as nonspecific.

To discover the associated biological consequences of the low-level IFN-γ responses seen in the four antigen-specific T cell lines, we measured their cytotoxic properties using the CD107a/b degranulation assay. All these lines responded appropriately to polyclonal stimulation with phorbol myristate acetate and ionomycin (66 ± 13% $CD107a/b^+$ $CD3^+$ cells), and therefore had functional potential, but no specific degranulation was detected upon stimulation with the 2A-TAV pepmix (2.5 ± 0.5% $CD107a/b^+$ $CD3^+$ cells) or the specific single peptide no. 5 (1.7 ± 0.5% $CD107a/b^+$ $CD3^+$ cells for lines from donor nos. 13–15), as compared with the negative control (2A-ERAV-pepmix, 2.2 ± 1% $CD107a/b^+$ $CD3^+$ cells) (Figures 3b and c, $P = NS$), consistent with the minimal reactivity shown in the IFN-γ ELISpot assay (Figures 1c and 3a). As expected, pp65-specific- and PRAME-reactive lines specifically degranulated on exposure to the corresponding pp65 or PRAME pepmixes (13.3 ± 12.2%

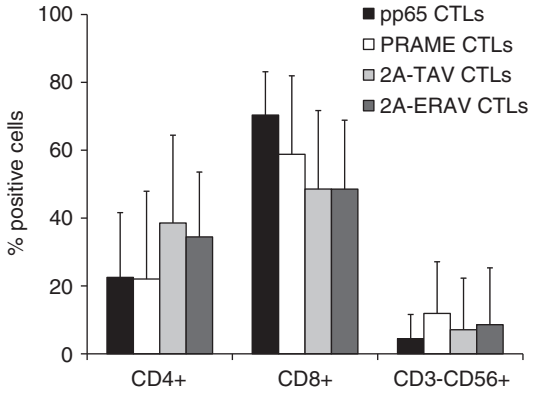

Figure 2. T cell lines contain a mixture of $CD4^+$ and $CD8^+$ T cells. The phenotypes of the T cell lines were analyzed by flow cytometry after three antigen-specific stimulations. All lines contained a mixture of $CD4^+$ and $CD8^+$ T cells, with some admixed $CD3^-CD56^+$ NK cells. Shown are mean ± s.d. of percentage of positive cells for CMV-pp65 lines ($n = 7$, black bars), for PRAME lines ($n = 7$, white bars), for 2A-TAV lines ($n = 14$, light gray bars) and for 2A-ERAV lines ($n = 9$, dark gray bars). We found a trend for a lower proportion of $CD8^+$ T cells in 2A-TAV and 2A-ERAV lines ($P = 0.07$) as compared with CMV-pp65 or PRAME lines.

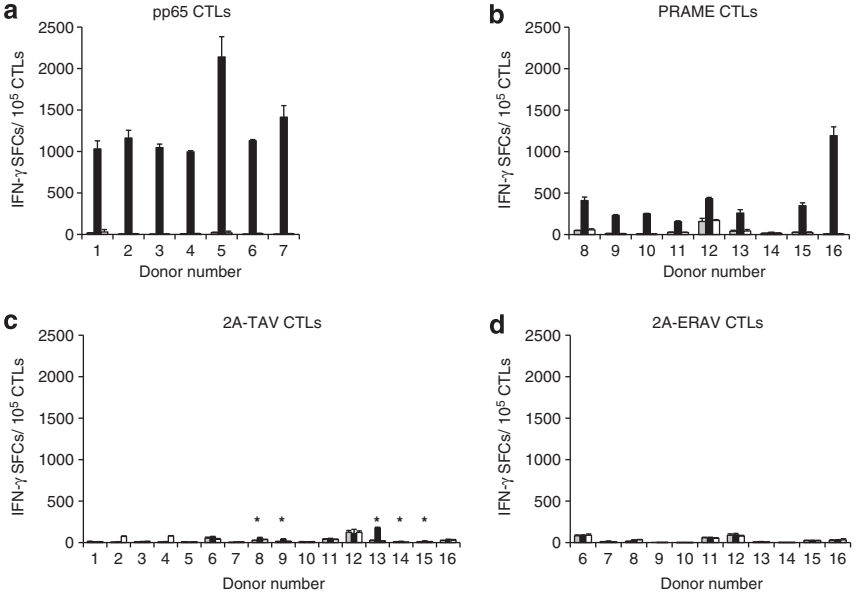

Figure 1. T cell lines produce IFN-γ upon antigenic stimulation. After three antigen-specific stimulations with pepmix-pulsed dendritic cells, T cell lines were analyzed for IFN-γ production by ELISpot in response to media (gray bars), relevant pepmix (black bars) or irrelevant pepmix (white bars). IFN-γ SFCs per 1×10^5 CTLs from (**a**) cytomegalovirus (CMV) pp65 lines, (**b**) PRAME lines, (**c**) 2A-TAV lines and (**d**) 2A-ERAV lines are shown (mean ± s.d. of triplicates). The 2A-TAV lines from donors nos. 8, 9, 13, 14 and 15 were reactive against the 2A-TAV pepmix with SFCs $\geqslant 2\times$ above media or irrelevant pepmix (*), and therefore selected for further analyses.

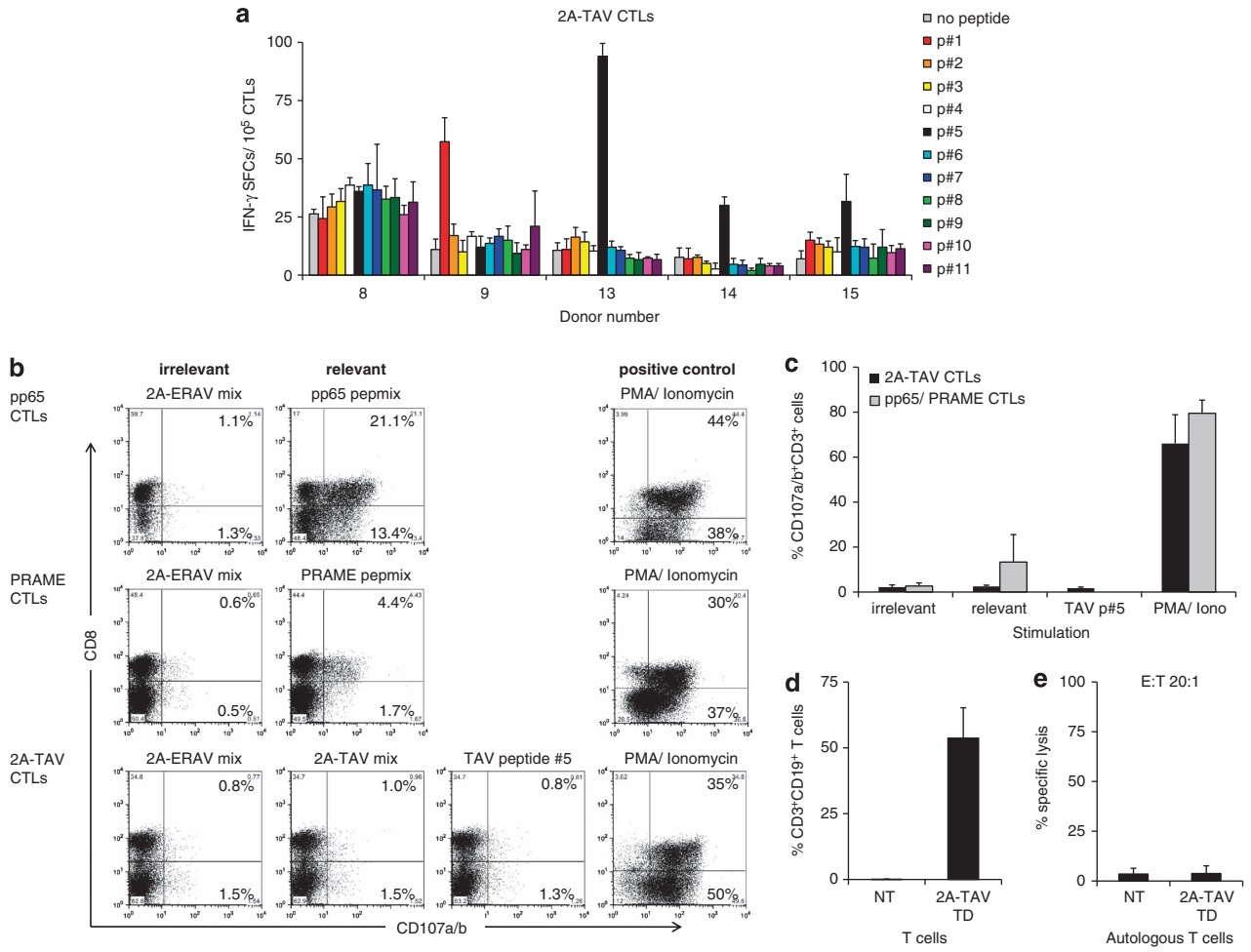

Figure 3. Lack of cytotoxic activity of 2A2A-TAV-specific T cells despite low levels of IFN-γ production. (**a**) The 2A-TAV pepmix-reactive T cell lines from donors nos. 8, 9, 13, 14 and 15 were analyzed by IFN-γ ELISpot against the single 15-mer peptides contained in the 2A-TAV pool (peptides p no. 1-p no. 11, colored bars) or no peptide (gray bar, mean ± s.d. of triplicates). Weak reactivity was found in 2A-TAV lines against the shown single peptides. Donor no. 8 only showed nonspecific reactivity. (**b**) Representative FACS plots of the CD107a/b degranulation assay (gated on $CD3^+$ cells) from a pp65-specific CTL line, a PRAME-specific CTL line and a 2A-TAV-specific CTL line stimulated with irrelevant (2A-ERAV) or relevant (pp65, PRAME or 2A-TAV) pepmixes, 2A-TAV peptide no. 5 (p no. 5) or phorbol myristate acetate (PMA)/ionomycin (positive control). (**c**) Summary of CD107a/b degranulation assay for 2A-TAV CTLs ($n = 4$) and pp65/PRAME CTLs ($n = 9$) (mean ± s.d. of % $CD107a/b^+CD3^+$ cells). (**d**) Summary of transduction efficiency of SFG.iCasp9.2A-TAV.ΔCD19-TD T cells from donors no. 9, and 13–15 (mean ± s.d. of % $CD19^+CD3^+$ cells). (**e**) Summary of ^{51}Cr-release assay of 2A-TAV-specific CTLs from donors no. 9, and 13–15 tested against non-transduced (NT) or 2A-TAV TD autologous T cells (mean ± s.d. of % specific lysis) at an E:T ratio of 20:1.

$CD107a/b^+$ $CD3^+$ cells, $n = 9$), but not to control peptides (2A-ERAV-pepmix, 2.7 ± 1.4% $CD107a/b^+$ $CD3^+$ cells) (Figures 3b and c, $P = 0.03$).

We next assessed whether T cells transduced with the 2A-TAV-containing retroviral vector, SFG.iCasp9.2A-TAV.ΔCD19, could present and process any of these epitopes. Autologous T cells from the reactive donor nos. 9, 13, 14 and 15 were transduced ($CD3^+CD19^+ = 53.7 \pm 11.5\%$) (Figure 3d) and then used as targets in a standard 6-h ^{51}Chromium (Cr)-release assay. No significant lysis of 2A-TAV transduced (TD) or non-transduced autologous target T cells was observed in any of the donors tested (3.5 ± 2.9% specific lysis against NT, 3.75 ± 3.9% specific lysis against TD T cells, effector to target ratio (E:T) 20:1) (Figure 3e).

Thus, our potent *ex vivo* culture system shows that the viral-derived 2A-TAV and 2A-ERAV ribosomal skip sequences, and adjacent fusion protein regions exhibit very low ($n = 5$) to absent ($n = 11$) immunogenicity in 16 healthy donors. That this paucity of response is genuine rather than a reflection of deficiencies in our detection system is demonstrated by the anticipated high level of reactivity against cytomegalovirus-derived antigens (7/7) or weak tumor antigens (8/9), and by our ability to generate an expected low frequency (1/16) of lines weakly reactive with peptides derived from the self-antigens linked by the 2A sequences (human caspase9 and CD19) that were also included in the peptide mixtures. Of note, the three donors with low-level reactivity to the peptide no. 5 of the 2A-TAV sequence (donors no. 13–15) shared the same class-I-restricted human leukocyte antigen (HLA) alleles (HLA-A*02 and HLA-B*44) and certain class-II haplotypes, including HLA-DRB1*04, HLA-DQB1*03 (Table 1). These findings suggest that the reactive peptide no. 5 of the SFG.iCasp9.2A-TAV.ΔCD19 retroviral vector could contain an HLA class-I or class-II epitope presented in the context of either of these HLA molecules. Given the overall low level of reactivity of these lines, we could not further dissect these reactivities, and precisely identify the epitope and its HLA context. The epitope prediction algorithms from SYFPEITHY (http://www.syfpeithi.de/) and the BioInformatics and Molecular Analysis Section, NIH, (http://www-bimas.cit.nih.gov/molbio/hla_bind/) failed to indicate a significantly high-scoring epitope within the 2A-TAV sequence in the context of

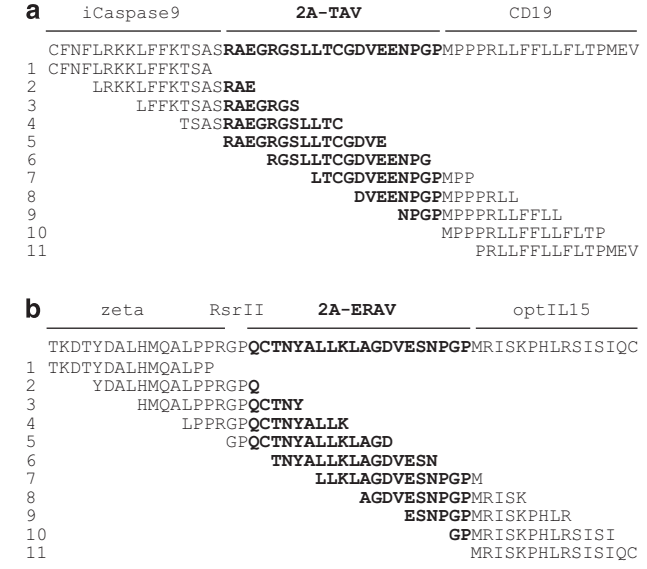

Figure 4. 2A sequences are contained in polycistronic retroviral vectors. (**a**) The 2A-TAV sequence and the single overlapping 15-mer peptides (no. 1–11) were derived from the SFG.iCasp9.2A-TAV.ΔCD19 retroviral vector.[13] (**b**) The 2A-ERAV sequence and the single overlapping 15-mer peptides (no. 1–11) were derived from the SFG.iCasp9.2A-TAV.CAR19-28ζ.2A-ERAV.optIL15 retroviral vector.[7]

Table 1. Donor HLA typing

HLA/ donor	*HLA-A2 FACS*	*HLA-A*	*HLA-B*	*HLA-DRB1*	*HLA-DQB1*
1	Pos	na	na	na	na
2	Pos	na	na	na	na
3	Neg	na	na	na	na
4	Pos	*02, —	*07,*15	*13, —	*03, *06
5	Pos	*02, *03	*51, —	*04, *07	*02, *03
6	Neg	na	na	na	na
7	Neg	na	na	na	na
8	Pos	*02, *03	*07, *35	*07, *09	*02, —
9	**Pos**	***02, *23**	***07, *18**	***11, *13**	***03, *06**
10	Pos	*02 *68	*07, *51	*04, *15	*03, *06
11	Pos	*02, —	*42, *53	*01, *08	*04, *05
12	Pos	*02, *33	*42, *58	*11, *13	*03, *06
13	**Pos**	***02, *03**	***14, *44**	***04, —**	***03, —**
14	**Pos**	***02, *23**	***44, *51**	***04, *14**	***03, *05**
15	**Pos**	***02, *29**	***44, —**	***03, *11**	***02, *03**
16	Pos	*02, —	*35, —	*04, *08	*03, *04

Abbreviations: HLA, human leukocyte antigen; na, not available; Neg, negative; Pos, positive. In bold, 2A-TAV-reactive donors.

HLA-A*0201, HLA-A*0205, HLA-B*4402, HLA-B*4403 or HLA-DRB1*0401 (data not shown, HLA-DQB1 epitopes are not available for prediction). Instead, the only epitope scoring significantly high in both prediction algorithms in the context of the HLA-A*0201 molecule was contained within the sequence of peptide no. 11 of the SFG.iCasp9.2A-TAV.ΔCD19 retroviral vector, which was recognized by the line derived from the HLA-A*02$^+$ donor no. 9, and corresponded to the signal peptide of the human CD19 self-antigen (Figures 3a and 4a). Nonetheless, 7 of the 11 HLA-A*02$^+$ donors failed to generate responses against such epitopes.

Adoptive T cell therapy in cancer patients aims to generate a long-term persistence of the transferred gene-modified T cells. This can be undermined if vectors contain potentially immunogenic sequences, and TD cells are infused in immunocompetent individuals or if multiple T cell administrations are performed. In these situations, *in vivo* sensitization against vector components can be induced and result in the immune-mediated elimination of the TD cells. No *ex vivo* system can fully reproduce the *in vivo* situation of a 'booster vaccination' effect, but we have attempted to answer immunogenicity concerns in our *in vitro* culture system by using three antigen-specific stimulations with professional antigen-presenting cells (dendritic cells) to amplify T cell responses from immunocompetent individuals. No significant cytotoxic activity was observed in the 16 donors tested, although this limited sample size means we cannot exclude a true positive rate of up to 0.17.

Only clinical trials that include these 2A sequences in immunocompetent individuals can definitely address the issue of their immunogenicity. However, the minimal reactivity we observed to the 2A-TAV sequence (in terms of IFN-γ production) associated with the lack of cytotoxic activity, as measured by the CD107a/b degranulation, seems unlikely to result in significant biological consequences, particularly as we found no evidence that these peptides could even be naturally processed and presented by T cells. In conclusion, our data suggest that the incorporation of 2A sequences in polycistronic vectors should not precipitate unwanted immune responses against the TD cells. Of the two 2A sequences studied, 2A-ERAV may be even less immunogenic than 2A-TAV. Careful monitoring for potential immunogenicity in future clinical trials with diverse patients and vectors will, however, still be required before we can be certain that there is no effective 2A-directed immune response against the TD T cells.

MATERIALS AND METHODS

Peptides and pepmixes

Fifteen-mer peptides overlapping by 11 amino acids spanning the 2A-TAV peptide sequence region of the SFG.iCasp9.2A-TAV.ΔCD19 retroviral vector[21] (Figure 4a) and the 2A-ERAV peptide sequence of the SFG.iCasp9.2A-TAV.CAR-CD19-28ζ.2A-ERAV.IL (interleukin)-15 retroviral vector[7] (Figure 4b) were synthesized by JPT Peptide Technologies (Berlin, Germany). Lyophilized peptides were reconstituted in dimethyl sulfoxide and then pooled into peptide mixtures (pepmixes) containing all the 11 peptides (2A-TAV mix or 2A-ERAV mix; 10 mg ml^{-1}) or stored as single peptides (10 mg ml^{-1}). The pepmixes or single peptides were used to pulse dendritic cells, as previously described.[18] Pepmixes spanning the cytomegalovirus pp65 protein or the cancer testes antigen PRAME (JPT Peptide Technologies) were used as controls.[18,20]

Generation and expansion of peptide-specific T cell lines

Buffy coats from healthy volunteer blood donors were obtained through the Gulf Coast Regional Blood Center, Houston, TX, USA. HLA typing of these samples was performed by the HLA, Flow and Diagnostic Immunology Laboratory of the Department of Laboratory Medicine at The Methodist Hospital, Houston, TX, USA, using PCR-SSO DNA-based procedures. Peripheral blood mononuclear cells were isolated by Lymphoprep (Accurate Chemical and Scientific Corp, Westbury, NY, USA) density gradient centrifugation. Dendritic cells were generated as previously described,[18] starting from CD14-selected cells and, after maturation, pulsed with 5 μM of the specific pepmix for 2 h at 37 °C and finally used to stimulate peripheral blood mononuclear cells at an E:T ratio of 20:1 in complete media, containing 45% Click's media (Irvine Scientific, Santa Ana, CA, USA), 45% RPMI 1640 (HyClone Laboratories, Logan, Utah), 5% heat-inactivated human AB serum (Valley Biomedical, Winchester, VA, USA), 1% L-glutamine and 1% penicillin/streptomycin (Invitrogen, Carlsbad, CA, USA) in the presence of a previously validated combination of cytokines (IL-7 (10 ng ml^{-1}), IL-12 (1 ng ml^{-1}) and IL-15 (2 ng ml^{-1}) (all from Peprotec, Rocky Hill, NJ, USA or R&D Systems, Minneapolis, MN, USA).[18] On days 9 and 16 of culture, T cells were re-stimulated with pepmix-pulsed dendritic cells at an E:T ratio of 10:1 in media containing IL-7, IL-12 and IL-15. IL-2 (50 U ml^{-1}) was added to the culture from day 16.

Retroviral transduction

The retroviral supernatant encoding the SFG.iCasp9.2A-TAV.ΔCD19 vector was prepared as previously described.[13] Peripheral blood mononuclear cells from donors 9, 13, 14 and 15 were activated with immobilized OKT3 and anti-CD28 (BD) antibodies, and IL-2 100 U ml^{-1}. After 72 h, cells were transduced on retronectin-coated plates (Takara Bio Inc, Shiga, Japan) as previously described.[7] Phenotype of TD cells was assessed by FACS 3 days after transduction, and used as targets in ^{51}Cr assays.

Immunophenotyping

T cell subset distribution was analyzed after the third stimulation by staining with fluorochrome-conjugated antibodies for CD3–APC, CD4–PE, CD8–PerCP and CD56–FITC. Transduction efficiency was analyzed by staining cells with CD3–FITC and CD19–APC antibodies. All antibodies were from BD Biosciences, San Jose, CA, USA, or Beckman Coulter, Brea, CA, USA; data acquisition was performed on a FACSCalibur (BD Biosciences) using CellQuest Software (BD Biosciences) and data analysis was performed using FlowJo Software (Treestar, Ashland, OR, USA). To evaluate CD107a/b degranulation, T cells at the end of the third antigen-specific stimulation were resuspended at 1×10^6 cells ml^{-1} in complete media with 10% fetal bovine serum (HyClone) without cytokines. After blocking protein transport (GolgiPlug and GolgiStop, both from BD), following the manufacturer's instruction, cells were stained with FITC-conjugated CD107a and CD107b (both from BD), and then stimulated with either relevant or irrelevant pepmixes or single peptides (5 μM) for 4–5 h at 37 °C at 5% CO_2. Phorbol myristate acetate (25 ng ml^{-1}, Sigma-Aldrich, St. Louis, MO, USA) and ionomycin (1 μg ml^{-1}, Sigma-Aldrich) were used as positive controls. Cells were then collected, fixed for 10 min in 1% Cytofix (BD), washed and then stained for 30 min with CD3–APC, CD4–PE and CD8–PerCP or appropriate isotype controls. After washing, cells were analyzed on the FACSCalibur.

ELISpot assay

The IFN-γ ELISpot assay was performed as previously described.[18] In brief, 1×10^5 T cells per well were plated in triplicates and then stimulated with 5 μM of the specific pepmixes of the single peptides or media alone. As positive control, T cells were stimulated with 25 ng ml^{-1} of phorbol myristate acetate and 1 μg ml^{-1} of ionomycin. The IFN-γ SFCs were enumerated (ZellNet, Fort Lee, NJ, USA). T cell lines were defined as being reactive when the number of SFCs was $\geqslant 2\times$ above background level (media control or irrelevant pepmix).

Chromium-release assay

The cytotoxic activity of T cells was evaluated using a standard 6-h ^{51}Cr-release assay, as previously described.[18] After labeling with ^{51}Cr, target cells were incubated with T cells at different E:T ratios in medium alone or in 1% Triton X-100 (Sigma-Aldrich) to determine spontaneous and maximum ^{51}Cr-release, respectively. The mean percentage of specific lysis of triplicate wells was calculated as follows: ((test counts − spontaneous counts)/(maximum counts − spontaneous counts)) × 100%.

Statistical analysis

Data were summarized by means and s.d. Student's *t*-test was used to determine the statistically significant differences between the samples, with *P*-value <0.05 indicating a significant difference. When multiple comparison analyses were required, statistical significance was evaluated by a repeated measures ANOVA, followed by a Newman–Keuls test for multiple comparisons. The exact binomial method was used to calculate the confidence interval.

CONFLICT OF INTEREST

The authors declare no conflict of interest.

ACKNOWLEDGEMENTS

CA is supported by Oncosuisse (BIL KFS 02506-08-2009), NIH-NHLBI T32 HL092332 (Trainee) and an American Society for Blood and Marrow Transplantation (ASBMT)/ Celgene New Investigator Award 2012; HEH is supported by a Dan L Duncan Chair, P50 CA126752, PO1 CA94237 and a SCOR from the Leukemia and Lymphoma Society; MKB is supported by a Fayez Sarofim Chair and a CPRIT award (RP110553); GD is supported by NIH R01 CA142636, a Leukemia and Lymphoma Society Translational Research grant and W81XWH-10-10425 Department of Defense, Technology/ Therapeutic Development Award; BS is supported by NIH R01 CA131027, a Leukemia and Lymphoma Society Translational Research grant and a CPRIT award (RP120298). We also appreciate the support of shared resources in the cancer center support grant P30CA125123.

REFERENCES

1 Restifo NP, Dudley ME, Rosenberg SA. Adoptive immunotherapy for cancer: harnessing the T cell response. *Nat Rev Immunol* 2012; **12**: 269–281.
2 Hoyos V, Savoldo B, Dotti G. Genetic modification of human T lymphocytes for the treatment of hematological malignancies. *Haematologica* 2012; **97**: 1622–1631.
3 Kerkar SP, Restifo NP. Cellular constituents of immune escape within the tumor microenvironment. *Cancer Res* 2012; **72**: 3125–3130.
4 Craddock JA, Lu A, Bear A, Pule M, Brenner MK, Rooney CM *et al.* Enhanced tumor trafficking of GD2 chimeric antigen receptor T cells by expression of the chemokine receptor CCR2b. *J Immunother* 2010; **33**: 780–788.
5 Di Stasi A, De Angelis B, Rooney CM, Zhang L, Mahendravada A, Foster AE *et al.* T lymphocytes coexpressing CCR4 and a chimeric antigen receptor targeting CD30 have improved homing and antitumor activity in a Hodgkin tumor model. *Blood* 2009; **113**: 6392–6402.
6 Quintarelli C, Vera JF, Savoldo B, Giordano Attianese GM, Pule M, Foster AE *et al.* Co-expression of cytokine and suicide genes to enhance the activity and safety of tumor-specific cytotoxic T lymphocytes. *Blood* 2007; **110**: 2793–2802.
7 Hoyos V, Savoldo B, Quintarelli C, Mahendravada A, Zhang M, Vera J *et al.* Engineering CD19-specific T lymphocytes with interleukin-15 and a suicide gene to enhance their anti-lymphoma/leukemia effects and safety. *Leukemia* 2010; **24**: 1160–1170.
8 Zhang L, Kerkar SP, Yu Z, Zheng Z, Yang S, Restifo NP *et al.* Improving adoptive T cell therapy by targeting and controlling IL-12 expression to the tumor environment. *Mol Ther* 2011; **19**: 751–759.
9 Liu D, Song L, Wei J, Courtney AN, Gao X, Marinova E *et al.* IL-15 protects NKT cells from inhibition by tumor-associated macrophages and enhances antimetastatic activity. *J Clin Invest* 2012; **122**: 2221–2233.
10 Milone MC, Fish JD, Carpenito C, Carroll RG, Binder GK, Teachey D *et al.* Chimeric receptors containing CD137 signal transduction domains mediate enhanced survival of T cells and increased antileukemic efficacy *in vivo*. *Mol Ther* 2009; **17**: 1453–1464.
11 Savoldo B, Ramos CA, Liu E, Mims MP, Keating MJ, Carrum G *et al.* CD28 costimulation improves expansion and persistence of chimeric antigen receptor-modified T cells in lymphoma patients. *J Clin Invest* 2011; **121**: 1822–1826.
12 Ciceri F, Bonini C, Stanghellini MT, Bondanza A, Traversari C, Salomoni M *et al.* Infusion of suicide-gene-engineered donor lymphocytes after family haploidentical haemopoietic stem-cell transplantation for leukaemia (the TK007 trial): a non-randomised phase I-II study. *Lancet Oncol* 2009; **10**: 489–500.
13 Di Stasi A, Tey SK, Dotti G, Fujita Y, Kennedy-Nasser A, Martinez C *et al.* Inducible apoptosis as a safety switch for adoptive cell therapy. *N Engl J Med* 2011; **365**: 1673–1683.
14 Szymczak-Workman AL, Vignali KM, Vignali DA. Design and construction of 2A peptide-linked multicistronic vectors. *Cold Spring Harb Protoc* 2012; **2012**: 199–204.
15 de Felipe P. Skipping the co-expression problem: the new 2A 'CHYSEL' technology. *Genet Vaccines Ther* 2004; **2**: 13.
16 Szymczak AL, Workman CJ, Wang Y, Vignali KM, Dilioglou S, Vanin EF *et al.* Correction of multi-gene deficiency *in vivo* using a single 'self-cleaving' 2A peptide-based retroviral vector. *Nat Biotechnol* 2004; **22**: 589–594.
17 Johnson LA, Morgan RA, Dudley ME, Cassard L, Yang JC, Hughes MS *et al.* Gene therapy with human and mouse T-cell receptors mediates cancer regression and targets normal tissues expressing cognate antigen. *Blood* 2009; **114**: 535–546.
18 Quintarelli C, Dotti G, De Angelis B, Hoyos V, Mims M, Luciano L *et al.* Cytotoxic T lymphocytes directed to the preferentially expressed antigen of melanoma (PRAME) target chronic myeloid leukemia. *Blood* 2008; **112**: 1876–1885.
19 Hanley PJ, Cruz CR, Savoldo B, Leen AM, Stanojevic M, Khalil M *et al.* Functionally active virus-specific T cells that target CMV, adenovirus, and EBV can be expanded from naive T-cell populations in cord blood and will target a range of viral epitopes. *Blood* 2009; **114**: 1958–1967.
20 Quintarelli C, Dotti G, Hasan ST, De Angelis B, Hoyos V, Errichiello S *et al.* High-avidity cytotoxic T lymphocytes specific for a new PRAME-derived peptide can target leukemic and leukemic-precursor cells. *Blood* 2011; **117**: 3353–3362.
21 Tey SK, Dotti G, Rooney CM, Heslop HE, Brenner MK. Inducible caspase 9 suicide gene to improve the safety of allodepleted T cells after haploidentical stem cell transplantation. *Biol Blood Marrow Transplant* 2007; **13**: 913–924.